

THE ELECTROMAGNETIC TRANSIENT IN
MULTIPLE CONDUCTOR STRUCTURES ABOVE AN EARTH

A Thesis Presented to

The Department of Electrical Engineering
The Faculty of Engineering
The University of Manitoba

In Partial Fulfillment
of the Requirements for the Degree
Master of Science in Electrical Engineering

by

Gregory Ernest John Bridges

Winnipeg, Manitoba, 1984

© Gregory Ernest John Bridges, 1984

THE UNIVERSITY OF MANITOBA
FACULTY OF GRADUATE STUDIES

The undersigned certify that they have read, and recommend to
the Faculty of Graduate Studies for acceptance, a Master's thesis
entitled: ".THE..ELECTROMAGNETIC..TRANSIENT..IN
MULTIPLE..CONDUCTOR..STRUCTURES..ABOVE..AN.
EARTH.".....

submitted by ..Gregory..E..J..Bridges.....

in partial fulfilment of the requirements for the degree of
..MASTER..OF..SCIENCE.....

Sama Abdul Atta
.....
Advisor

.....
M. Hamid
.....

Edward Tomchuk
.....
External Examiner

Date *April..10, 1984*

.....

Oral Examination is:

Satisfactory Not Required

[Unless otherwise specified by the major Department, thesis students
must pass an oral examination on the subject of the thesis and matters
relating thereto.]

THE ELECTROMAGNETIC TRANSIENT IN
MULTIPLE CONDUCTOR STRUCTURES ABOVE AN EARTH

by

Gregory Ernest John Bridges

A thesis submitted to the Faculty of Graduate Studies of
the University of Manitoba in partial fulfillment of the requirements
of the degree of

MASTER OF SCIENCE

© 1984

Permission has been granted to the LIBRARY OF THE UNIVER-
SITY OF MANITOBA to lend or sell copies of this thesis. to
the NATIONAL LIBRARY OF CANADA to microfilm this
thesis and to lend or sell copies of the film, and UNIVERSITY
MICROFILMS to publish an abstract of this thesis.

The author reserves other publication rights, and neither the
thesis nor extensive extracts from it may be printed or other-
wise reproduced without the author's written permission.

I hereby declare that I am the sole author of this publication.

I authorize the University of Manitoba to lend this publication to other institutions or individuals for the purpose of scholarly research.

Gregory Bridges

Gregory Ernest John Bridges

I further authorize the University of Manitoba to reproduce this publication by photocopying or by other means, in total or in part, at the request of other institutions or individuals for the purpose of scholarly research.

Gregory Bridges

Gregory Ernest John Bridges

The University of Manitoba requires the signatures of all persons using or photocopying this publication. Please sign below, and give address and date.

ABSTRACT

The propagation of a transient current along a multiple conductor structure above a lossy earth is studied. A frequency domain technique is proposed to determine the time domain current quantity at any point along the structure due to an injected current waveform. The formulation requires a knowledge of the electromagnetic fields at a specific frequency, for which an exact solution in integral form is derived. Difficulties in the accurate evaluation of the integral solution are discussed and various methods for its approximation are described. Then, a numerical method for extracting the structure's characteristics, the propagation constants and the eigen-current transformation matrix, is developed and employed in a computer program. A comparison of calculated results is made with those of other researchers to verify the solution technique, and finally, the current impulse response of a specified transmission line structure is given.

ACKNOWLEDGMENTS

The author is indebted to his advisor Dr. O. Aboul-Atta for his supervision and enlightening discussions of the subject. The assistance of Prof. E. Bridges and Muriel Aboul-Atta in preparation of the manuscript is appreciated. The author is grateful to his colleagues and parents for their help and tolerance during the course of this work. Financial assistance from the Natural Sciences and Engineering Research Council of Canada is gratefully acknowledged.

CONTENTS

ABSTRACT	iv
ACKNOWLEDGMENTS	v
<u>Chapter</u>	<u>page</u>
I. INTRODUCTION	1
II. FORMULATION OF PROBLEM	7
Transient Solution Method	7
Calculation Of Natural Modes	13
Internal Impedance Matrix Formulation	16
External Impedance Matrix Formulation	20
Mode Equation And Transformation Matrix	26
III. SOLUTION TECHNIQUE	29
Numerical Evaluation	29
Determinant Solution	32
Convergence Of Roots	34
Evaluation Of The Transformation Matrices	36
Evaluation Of The Complex Integrals	37
J Integral Evaluation	40
G Integral Evaluation	42
G Integrand Pole Extraction	43
Reduction To Carson's Formulation	45
IV. NUMERICAL RESULTS	48
Preliminary Results	50
Effect Of The G Function	54
Examination Of The Transformation Matrix	60
Impulse Response Characteristics	65
V. CONCLUSIONS	74
REFERENCES	79

Appendix

page

A.	POLYNOMIAL COEFFICIENT FORMULATION	83
B.	MULTI-CONDUCTOR CHARACTERISTIC EXTRACTION COMPUTER PROGRAM	86

LIST OF TABLES

<u>Table</u>		<u>page</u>
4.1	Comparison of k_z/k_e to the results of Grinberg. . .	51
4.2	Comparison of k_z/k_e and [P] to the results of Perel'man.	52
4.3	Parameters for the four cases presented by Perel'man.	53
4.4	Percent effect of the G integral.	53

LIST OF FIGURES

<u>Figure</u>		<u>page</u>
2.1	General transmission line structure.	8
2.2	Single mode transmission line equivalent.	10
2.3	Space transformation diagram.	13
2.4	N conductor structure geometry.	15
2.5	Single conductor internal impedance geometry.	17
2.6	Single conductor external impedance geometry.	20
3.1	Calculation of roots for the iteration technique.	35
3.2	Location of k_e , k_g , and k_z in the complex k plane.	39
3.3	Branch point and pole locations in the complex k_x plane.	39
4.1	Percent effect of the G integral.	55
4.2	Propagation constant of a single wire at various heights.	57
4.3	Propagation constant for two wires of varying seperation.	59
4.4	Frequency variation of k_z^m for the unbalanced case.	62
4.5	Frequency variation of k_z^m for case C of table 4.3.	62
4.6	Frequency dependence of [P] for the unbalanced case.	63
4.7	Frequency dependence of [P] for case C of table 4.3.	64
4.8	Frequency response for the [D] matrix.	69
4.9	Frequency response for the element $S_{11}(z, \omega)$	70

4.10	Impulse response for the [D] matrix elements. . .	71
4.11	Impulse response for the [S] matrix.	72
4.12	Frequency dependence of the [P] matrix.	73

Chapter I

INTRODUCTION

The problem of determining the propagation of a transient current along a multi-wire transmission line is examined. The problem has received much attention by researchers since its solution is required in many power system and antenna applications. The disturbing current at any point along the structure is calculated from the characteristics of the transmission line in the frequency domain, the transient signals then being obtained through the Fourier transform. Therefore, it is of great importance to determine at given frequencies, the behavior of an electromagnetic wave propagating along a system of conductors above a lossy earth.

In the limit, where the conductors as well as the earth are assumed to be perfectly conducting, the situation reduces to a planar electrostatic problem, the wave velocity along the structure being equal to the wave velocity in air and propagating with no attenuation. However, when a finite conductivity for either the conductors or the earth is taken into account, the problem complexity increases drastically. The classical solution to the problem of wave propagation along multi-conductor lines was formulated via the

Telegrapher's equations. Results are obtained from a set of differential equations which, for an $\exp(-j\omega t)$ dependence, are of the form

$$\frac{\partial}{\partial z^2} [I] = [Y][Z][I] , \quad (1.1)$$

$$[Y] = ([G] - j\omega[C]) , \quad (1.2)$$

$$[Z] = ([R] - j\omega[M]) . \quad (1.3)$$

where [R], [M], [G], and [C] are, respectively, the self resistance, mutual inductance, shunt conductance, and shunt capacitance matrices describing the system. This formulation leads to a circuit description of the system where the components of the admittance [Y] and impedance [Z] matrices are calculated under the assumption that the electromagnetic fields in both air and ground are static. A theory to include the influence of the earth was developed by Carson [1] and its effect was incorporated into the self and mutual impedances of the structure. This theory has been successfully applied to many power engineering problems, but due to the circuit analogy used, it is valid only at lower frequencies.

Since Carson's early work much research has been done to study the effect of the earth at higher frequencies. The problem was first tackled from the standpoint of a single wire above a lossy earth where an exact solution for the electromagnetic fields was derived using Maxwell's equations

and treating the situation as a boundary value problem. Wait [2] obtained an integral modal equation determining the propagation constants for currents which decreased exponentially along the wire. The exact solution to the problem is formed in terms of complicated functions as

$$z^{int} = K_1 + K_2 + J + G . \quad (1.4)$$

Here the function z^{int} is the self impedance term for the conductor. K_1 and K_2 are, respectively, functions representing the conductor primary field and its image for a perfectly conducting earth. The J and G functions are complicated integrals that account for the earth losses due to the longitudinal and transverse circulating currents, respectively.

Difficulty has been encountered in arriving at a proper solution of the J and G integrals to accurately determine the transmission line characteristics and permit further understanding of the contribution of each integral to the modal equation. In Carson's formulation the J integral was evaluated under the assumption of quasi-static fields in the air medium which means that the current on the line propagates with the free space velocity. The earth's permittivity was also assumed zero in the J evaluation (the longitudinal displacement current was neglected) and the G integral was assumed negligible (the transverse currents were neglected). Wise [3] later refined Carson's equations

to take into account the longitudinal displacement currents in the earth. Other early developments that attempted to take into account the earth conduction effects are summarized by Sunde [4].

The extension of the theory to multi-conductor systems was made by Perel'man [5] where the existence of N distinct propagating modes for an N -wire structure was firmly established. The wave nature of these discrete modes was first analysed by Pistol'kors [6] and later by Grinberg and Bonshtedt [7]. They did not neglect the G integral, which was formulated under the assumption of a highly conductive earth. Further improvements to the evaluation of the J integral through the use of a Struve function representation have been established by Wait [8] and Bannister [9], also under the restriction of a highly conductive earth.

Attempts to study the higher frequency behavior of a wire above a lossy earth were made by Kikuchi [10] who pointed out that as frequency increases, the wave propagating along the conductor becomes a surface wave bound to the conductor. Recent work by Olsen and Chang [11,12] and others [13,14] suggests the inclusion of an added "fast wave" mode which also propagates on the structure as well as the previously established transmission line mode. This degenerate mode is generated through a singularity in the G integral. At high frequencies the singularity is assumed to produce a significant enough contribution so as to create an extra

root to the mode equation (1.4) which describes the structure. Under this assumption, conventional transmission line theory breaks down entirely since more than N modes are allowed to propagate on an N -wire system. In comment, the proper evaluation of the G integral is still under active investigation and the incorporation of the degenerate mode remains a highly debatable topic [15,16].

Chapter two of the thesis presents the theory to solve for the propagation of a transient current on an N -wire transmission line structure. The general solution methodology, where the problem is solved in terms of modal currents in the frequency domain and later transformed to the time domain, is given. An integral expression for the exact fields due to a single wire above a lossy earth and satisfying all boundary conditions is derived using Maxwell's equations. The integral expression is used in the formation of the elements of an impedance matrix whose solution yields the transmission line characteristics.

Chapter three of the thesis describes the numerical evaluation technique used to extract the transmission line characteristics from the impedance matrix. The method of solving the J and G integrals is also discussed here. Aboul-Atta [17] has derived an exact analytical solution for the J integral with no assumed restrictions and an asymptotic expression for the G integral is given [18]. A brief account of how Carson's equations can be formed by

imposing various assumptions that are valid at low frequencies is included.

The results produced by a computer program which yields the transmission line characteristics of an N-wire structure using the numerical techniques described in chapter three is presented in chapter four. A comparison with previously published results of other workers is made. To complete the examination of the problem, the time domain impulse response for a specific transmission line structure is determined.

An exact solution for the electromagnetic fields in integral form for a transmission line structure is given in the thesis. Concentration will be in the accurate evaluation of the integral solution for the lower portion of the frequency spectrum so as to improve existing power transmission line transient calculations.

Chapter II
FORMULATION OF PROBLEM

2.1 TRANSIENT SOLUTION METHOD

The fundamental problem of determining the propagation of a transient current along a multi-wire transmission line will be examined. The commonly used Telegrapher's equations, which rely on circuit concepts, will be set aside and instead, a more fundamental equivalent theory will be presented which utilizes Maxwell's equations as the sole solution basis. In this section it will be demonstrated that a unique decomposition of the currents induced on the wires into discrete modes is possible. The solution of the transient problem will be formulated in terms of these modes. Later sections will then solve for the properties of the discrete modes.

The general transmission line problem consisting of a system of N conductors located above a homogeneous lossy earth is considered as shown in figure 2.1. The conductors are parallel to the z -axis and are each assumed to carry a current which is injected at $z = 0$ of value $I_n^s(0,t)$, $n=1,2,\dots,N$. In general, the current at any point, z , along the transmission line can be determined from the transformed Fourier components of the injected current, which written in vector matrix form is

$$[I(z,t)] = \mathcal{F}^{-1} [S(z,\omega)] \mathcal{F} [I^S(0,t)] \quad (2.1)$$

where

$$\mathcal{F} = \frac{1}{2\pi} \int_{-\infty}^{\infty} dt e^{j\omega t} \quad , \quad \mathcal{F}^{-1} = \int_{-\infty}^{\infty} d\omega e^{-j\omega t} \quad (2.2)$$

Here \mathcal{F} and \mathcal{F}^{-1} are the standard Fourier transform and its inverse, respectively. The system matrix, $[S]$, can be considered as the current transfer function characteristic of the N-wire system. $[S]$ is dependent on the geometry of the structure, the electrical properties of the supporting mediums, as well as any boundary (load) conditions imposed at the terminating ends of the system.

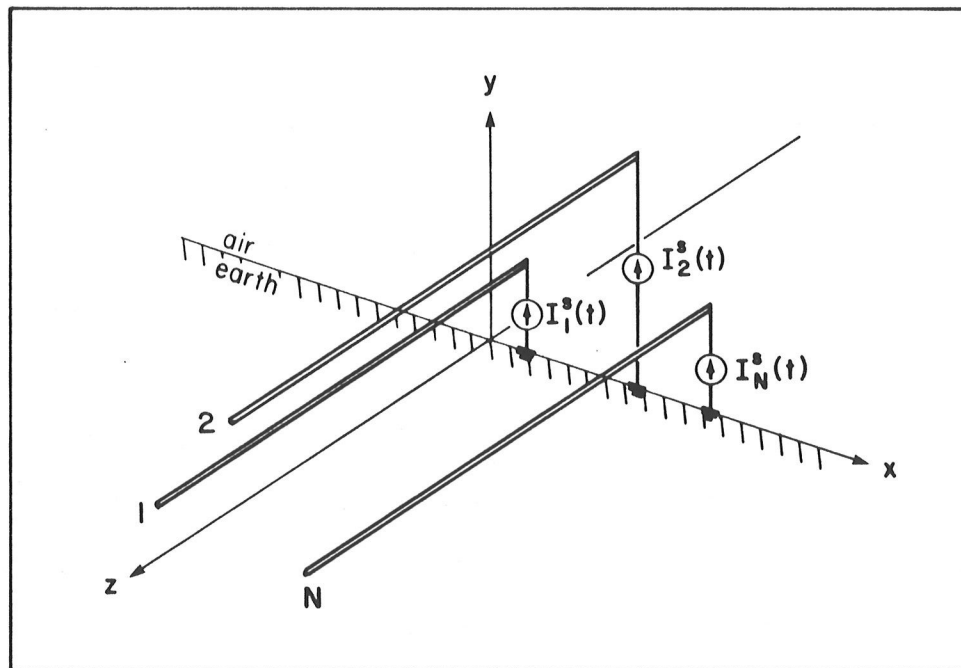


Figure 2.1: General transmission line structure.

In the frequency domain solution of the problem, the harmonic currents, assuming an $\exp(-j\omega t)$ dependence, can be constructed as a linear superposition of eigen-current modes. Thus, for an N-wire structure, there will be N characteristic propagating modes taking the form: $\exp(-j\omega t + jk_z^m z)$, $m=1,2,\dots,N$, where k_z^m is the propagation constant of the m^{th} mode. The components of the eigen-currents for each propagating mode is determined by a modal transformation matrix, which yields the total current distribution in the multi-conductor system as

$$[P(\omega)][i(z,\omega)] = [I(z,\omega)] \quad (2.3)$$

with $[I]$ as the conductor current column vector and $[i]$ as the modal current column vector. Here $[P]$, yet to be defined, is the non-singular linear transformation whose utilization allows computations involving each propagating mode to be handled independently. The physical interpretation of the transformation can be examined by considering the fields in a plane perpendicular to the conductors. The field configuration changes if any one of the wire currents I_n is varied. However, using the transformation $[P]$ creates an alternate orthogonal current system $[i]$, for which the field configuration remains unchanged when any individual mode current i_n is varied.

Once the conductor currents are decomposed using (2.3), the individual propagating modes can be considered as a sum

of forward and reverse travelling waves whose magnitudes depend on the boundary (load) conditions imposed on the transmission line. For each mode, the general transmission line system considered will consist of a transmitting structure of infinite length in the positive z direction and a source $i_m^s(0)$ with an associated source impedance Z_s^m at $z=0$ as shown in figure 2.2.

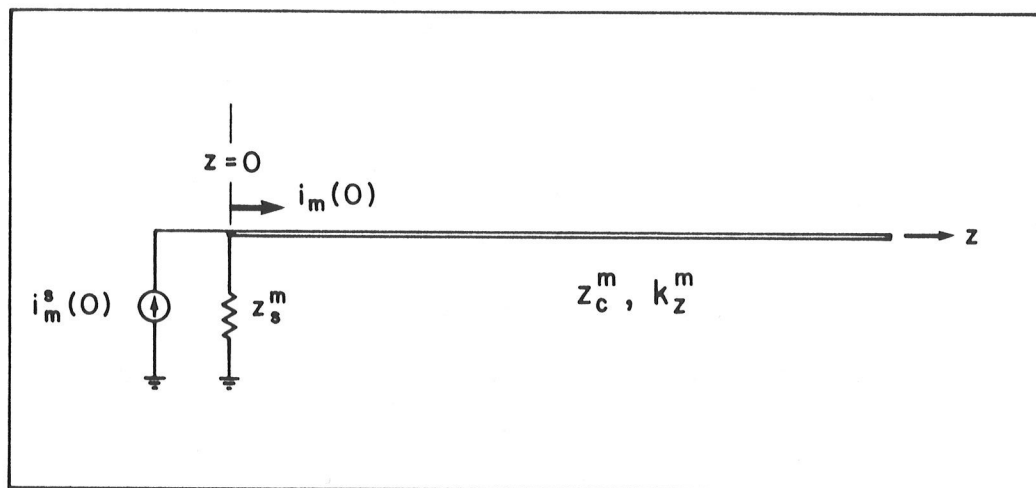


Figure 2.2: Single mode transmission line equivalent.

For the m^{th} mode, the transmitting structure will have a single propagation constant k_z^m and characteristic impedance Z_c^m associated with it. Thus, the eigen-currents for this mode will take the form

$$i_m(z) = a_m e^{+jk_z^m z} + b_m e^{-jk_z^m z} \quad (2.4)$$

The unknown coefficients, a_m and b_m , are the forward and reverse traveling wave components, respectively. Since the transmission line is infinite in the positive z direction, $b_m=0$. At $z=0$ we have

$$i_m(0) = a_m = \left(\frac{1 + R_s^m}{2}\right) i_m^s(0) \quad (2.5)$$

where

$$R_s^m = \frac{z_s^m - z_c^m}{z_s^m + z_c^m} \quad (2.6)$$

Thus, replacing a_m with (2.5) we can determine the unknown eigen-current at a point z on the transmission line to be

$$i_m(z) = \left(\frac{1 + R_s^m}{2}\right) (e^{jk_z^m z}) i_m^s(0) \quad (2.7)$$

Applying an appropriate transformation matrix $[P]$ the system matrix $[S]$ in (2.1) can be replaced by

$$[S(z, \omega)] = [P(\omega)][D(z, \omega)][P(\omega)]^{-1} \quad (2.8)$$

where $[D]$ is a diagonal matrix composed of the propagation functions given by (2.7) for the N propagating modes characteristic to the system, written as

$$[D(z, \omega)] = \begin{bmatrix} d_1 & & \dots & 0 \\ & \ddots & & \\ & & d_m & \dots \\ 0 & & & \dots & d_N \end{bmatrix} \quad (2.9)$$

with

$$d_m = \left(\frac{1 + R_s^m}{2}\right) e^{jk_z^m z} \quad (2.10)$$

Note that the modal form of the injected current source vector $[i^S(0,\omega)]$ is defined in terms of the transformation matrix as

$$[i^S(0,\omega)] = [P(\omega)]^{-1} [I^S(0,\omega)] \quad (2.11)$$

Combining these results, the generalized transmission line current propagation equation in the frequency domain can be formed as

$$[I(z,\omega)] = [P(\omega)][D(z,\omega)][P(\omega)]^{-1} [I^S(0,\omega)] \quad (2.12)$$

or alternatively in the time domain as

$$[I(z,t)] = \mathcal{F}^{-1} [P(\omega)][D(z,\omega)][P(\omega)]^{-1} \mathcal{F} [I^S(0,t)] \quad (2.13)$$

The time domain formulation is more easily seen to be a convolution of the known current $[I^S(0,t)]$ with the system impulse response function $[S(z,t)]$, i.e.,

$$[I(z,t)] = [S(z,t)] * [I^S(0,t)] \quad (2.14)$$

where

$$[S(z,t)] = \mathcal{F}^{-1} [P(\omega)][D(z,\omega)][P(\omega)]^{-1} \quad (2.15)$$

The development of the system matrix $[S(z,t)]$ in terms of the transfer matrices, $[P]$ and $[D]$, can be better understood by the space diagram shown in figure 2.3. At this point, the problem is now reduced to one of having to accurately determine the mode propagation constants k_z^m , the

transformation matrix $[P]$, and the modal characteristic impedances Z_C^m for the transmission line structure.

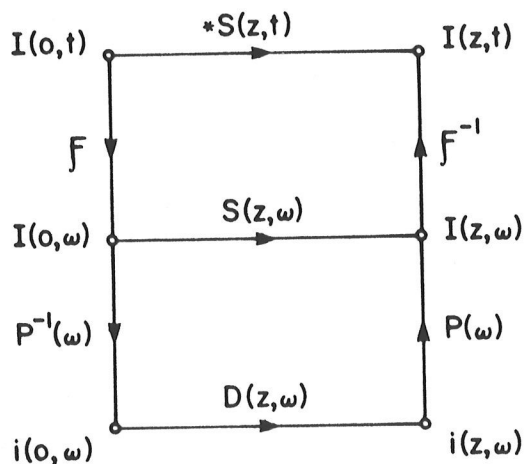


Figure 2.3: Space transformation diagram.

2.2 CALCULATION OF NATURAL MODES

The following sections describe the theory used to derive the propagation constants k_z^m and the transformation matrix $[P]$ necessary for the solution of the generalized propagation transformation equation (2.13). In 1926, Carson [1] formulated the problem by applying Maxwell's equations as well as some circuit concepts. The propagating modes were derived from the eigenvalues of the system matrix, $[S]=[Y][Z]$, which characterizes the N-wire structure, where the shunt matrix $[Y]$ and the impedance matrix $[Z]$ are dependent on the geometry of the structure [19]. The theory has been successfully applied to many power engineering

problems; however, due to its circuit analogies it is a quasi-static theory valid only for the lower frequency portion of the spectrum. In the exact formulation of the problem, all fields are solutions of Maxwell's equations and is an exact theory to the extent that all boundary conditions are satisfied [20,p.486]. The method used to solve for the propagating modes will follow that of Perel'man [5] and is as formulated below. The unknown propagating modes are found by matching the tangential electric field at the N conductor surfaces, together with satisfying the continuity of fields at the air-earth interface.

Consider an N-wire transmission line structure of infinite extent in the z direction and parallel to the interface between two homogeneous half-spaces, as shown in figure 2.4. The upper half-space ($y > 0$) is characterized by the electrical constants $\mu_e, \epsilon_e, \sigma_e$, and the lower half-space ($y < 0$) is characterized by the electrical constants $\mu_g, \epsilon_g, \sigma_g$. The N conductors are assigned the electrical constants $\mu_n, \epsilon_n, \sigma_n$, and are positioned at the point (x_n, y_n) in the x-y plane, $n=1,2,\dots,N$, respectively.

For a specified angular frequency ω and as described in section 2.1, the currents along the conductors can be constructed as a linear superposition of eigen-current modes that take the form $I_n(\exp(-j\omega t + jk_z^m z))$ where k_z^m is the propagation constant in the z direction of the m^{th}

propagating mode. Note that for an N-wire structure there will be N propagating modes. The determination of the propagation constants is forced by satisfying the boundary conditions at the N wire surfaces. Thus, matching the tangential electric field components at the m^{th} wire surface yields

$$E_{mm}^{\text{int}} = E_{mm}^{\text{ext}} + \sum_{\substack{n=1 \\ n \neq m}}^N E_{mn}^{\text{ext}}, \quad (2.16)$$

where E_{mn}^{ext} is the external field due to the n^{th} wire, and E_{mm}^{int} , E_{mm}^{ext} are the internal and external fields of the m^{th} wire, respectively.

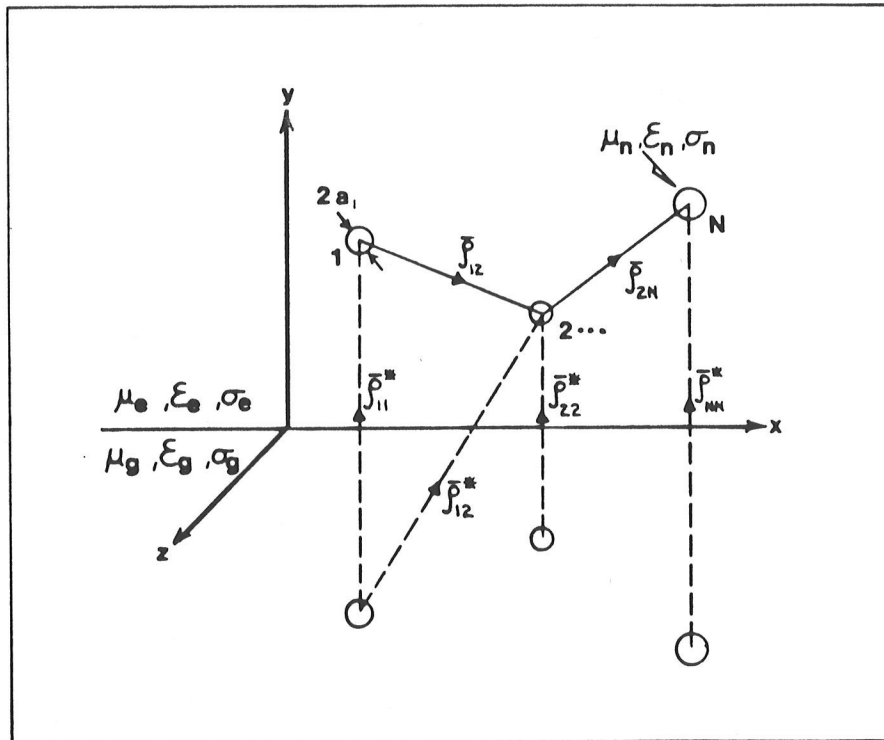


Figure 2.4: N conductor structure geometry.

We can also write (2.16) in terms of currents as

$$Z_{mm}^{int} I_m = Z_{mm}^{ext} I_m + \sum_{\substack{n=1 \\ n \neq m}}^N Z_{mn}^{ext} I_n \quad (2.17)$$

Similarly, this boundary condition must hold for all conductors in the structure, $m=1,2,\dots,N$, giving the result

$$[Z_{mn}^{int} - Z_{mn}^{ext}] [I_n] = 0 \quad (2.18)$$

where

$$Z^{int} = \begin{bmatrix} Z_{11}^{int} & \dots & 0 \\ \vdots & \ddots & \vdots \\ 0 & \dots & Z_{NN}^{int} \end{bmatrix}; \quad (2.19)$$

$$Z^{ext} = \begin{bmatrix} Z_{11}^{ext} & \dots & Z_{1N}^{ext} \\ \vdots & \ddots & \vdots \\ Z_{N1}^{ext} & \dots & Z_{NN}^{ext} \end{bmatrix}.$$

2.3 INTERNAL IMPEDANCE MATRIX FORMULATION

The internal impedance matrix Z^{int} is derived by examining a conducting cylinder of infinite length in the z direction, of radius a , and embedded in an infinite homogeneous medium, as shown in figure 2.5. The propagation constant internal to the cylinder is k_i^z and that of the external medium is k_e . Stratton [20, pp.524-533], separates

the differential wave equations describing the system into elementary cylindrical waves of the form

$$\psi_n = \begin{cases} e^{jn\phi} J_n(j\tau_i \rho) e^{\pm jk_z^n z - j\omega t}, & \rho \leq a \\ e^{jn\phi} H_n^{(1)}(j\tau_e \rho) e^{\pm jk_z^n z - j\omega t}, & \rho \geq a \end{cases} \quad (2.20)$$

where

$$\tau_i = \sqrt{k_z^{n2} - k_i^2} \quad (2.21)$$

$$\tau_e = \sqrt{k_z^{n2} - k_e^2}$$

and

$$k_i^2 = \omega^2 \mu_i \epsilon_i + j\omega \mu_i \sigma_i$$

$$k_e^2 = \omega^2 \mu_e \epsilon_e + j\omega \mu_e \sigma_e \quad (2.22)$$

Here an $\exp(-j\omega t + jk_z^n z)$ dependence is assumed with k_z^n being the propagation constant in the positive z direction.

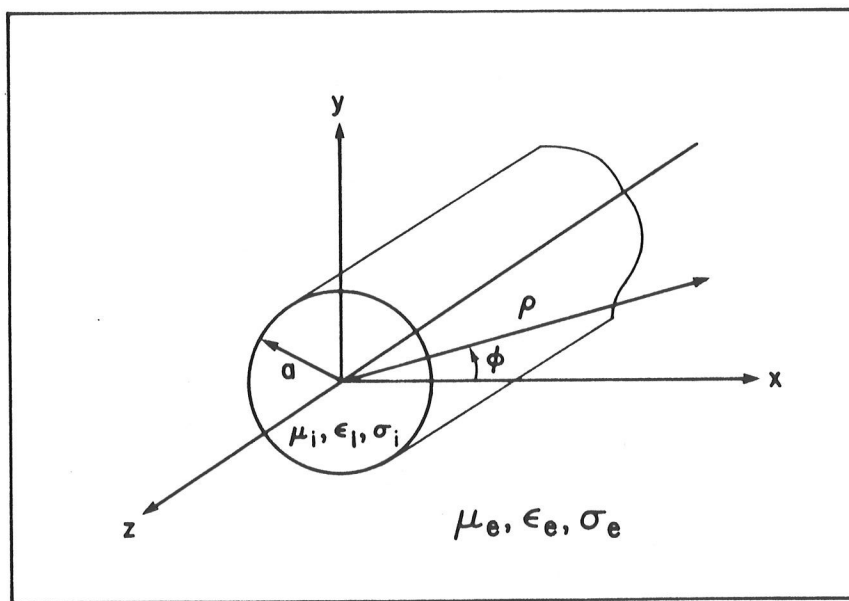


Figure 2.5: Single conductor internal impedance geometry.

The general solution to the problem can be constructed as a linear superposition of fields taking this elementary form for both the transverse electric and transverse magnetic cases. However, for the case of an axially directed current in the conductor the waves will be predominantly transverse magnetic [20,p.527], physically taking the form of concentric magnetic field rings inside the cylinder. Also, all asymmetric modes, $n \neq 0$, attenuate rapidly and do not play a significant role in the propagation of current along the conductor. We then can assume expressions for the required fields as follows: Internal to the conductor ($\rho < a$)

$$E_z^{\text{int}} = a_i I_i J_0(j\tau_i \rho) \quad (2.23)$$

$$H_z^{\text{int}} = 0 \quad (2.24)$$

$$H_\phi^{\text{int}} = a_i I_i \frac{k_i^2}{\mu_i \omega \tau_i} J_1(j\tau_i \rho) \quad (2.25)$$

External to the conductor ($\rho > a$)

$$E_z^{\text{ext}} = b_e I_i H_0^{(1)}(j\tau_e \rho) \quad (2.26)$$

$$H_z^{\text{ext}} = 0 \quad (2.27)$$

$$H_\phi^{\text{ext}} = b_e I_i \frac{k_e^2}{\mu_e \omega \tau_e} H_1^{(1)}(j\tau_e \rho) \quad (2.28)$$

The unknown integration coefficients, a_i and b_e , will be expressed in terms of the total conduction current inside the cylinder. Having assumed the current to take the form $I_i \exp(-j\omega t + jk_z z)$ we have

$$I_i = \int_0^a \int_0^{2\pi} J_z \rho \partial \phi \partial \rho \quad (2.29)$$

where $J_z = \sigma_i E_z^{int}$ is the current density parallel to the axis at a point inside the cylinder. Thus, integrating (2.29) and equating it with (2.23) we obtain

$$a_i = \frac{j\tau_i}{2\pi a \sigma_i J_1(j\tau_i a)} \quad (2.30)$$

Likewise, by matching the tangential fields at the conductor surface ($\rho = a$) gives

$$a_i J_0(j\tau_i a) = b_e H_0^{(1)}(j\tau_e a) \quad ; \quad (2.31)$$

$$a_i \frac{k_i^2}{\mu_i \tau_i} J_1(j\tau_i a) = b_e \frac{k_e^2}{\mu_e \tau_e} H_1^{(1)}(j\tau_e a) \quad (2.32)$$

from which we get

$$b_e = \frac{j\tau_e}{2\pi a \sigma_i} \cdot \frac{\mu_e k_i^2}{\mu_i k_e^2} \cdot \frac{1}{H_1^{(1)}(j\tau_e a)} \quad (2.33)$$

Replacing the Bessel's functions by their equivalent modified Bessel's function representations [21,p.375], the internal impedance matrix elements of (2.19) are given from (2.23) and (2.30) as

$$z_{mn}^{int} = \delta_{mn} \frac{j\omega \mu_e}{2\pi k_e^2} \left[\frac{\mu_n k_e^2}{\mu_e k_n^2} \cdot \frac{\tau_n^2 I_0(\tau_n a_n)}{(\tau_n a_n) I_1(\tau_n a_n)} \right] \quad (2.34)$$

with

$$\delta_{mn} = \begin{cases} 0, & m \neq n \\ 1, & m = n \end{cases} \quad .$$

2.4 EXTERNAL IMPEDANCE MATRIX FORMULATION

The calculation of the external impedance matrix Z^{ext} is obtained from the electric field due to a single line source above a conducting half-space. The formulation, is the two dimensional equivalent of the three dimensional case treated by Sommerfeld [22], and has been examined by many authors [2,23,24]. Consider a single line source, of infinite extent in the z direction and of radius a , situated at a height $y=h$ above the air-earth interface at $y=0$ as shown in figure 2.6.

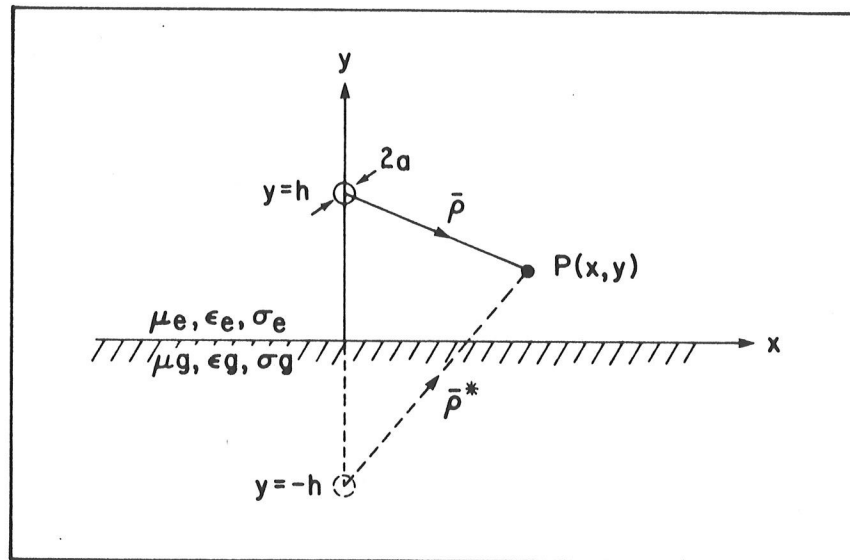


Figure 2.6: Single conductor external impedance geometry.

The total electromagnetic field will be expressed in terms of the Hertz vector potentials $\vec{\pi}^e$ and $\vec{\pi}^g$ for the regions $y \geq 0$ and $y \leq 0$, respectively. The electric and magnetic

fields in each region will be derived from the vector potentials using

$$\bar{\mathbf{E}} = \nabla(\nabla \cdot \bar{\boldsymbol{\pi}}) + k^2 \bar{\boldsymbol{\pi}} \quad , \quad (2.35)$$

$$\bar{\mathbf{H}} = -j\omega\epsilon'(\nabla \times \bar{\boldsymbol{\pi}}) \quad . \quad (2.36)$$

As explained in section 2.3, for an axially directed current, only the symmetric transverse magnetic case will be considered. Again we will assume the current to take a space and time dependence of the form $I_n \exp(-j\omega t + jk_z z)$. The following two dimensional differential expressions satisfying Maxwell's equations can then be used to describe the system:

$$\left[\frac{\partial^2}{\partial x^2} + \frac{\partial^2}{\partial y^2} + (k_e^2 - k_z^2) \right] \bar{\boldsymbol{\pi}}^e = -\bar{\mathbf{J}} \quad ; \quad y \geq 0 \quad , \quad \rho > a \quad (2.37)$$

$$\left[\frac{\partial^2}{\partial x^2} + \frac{\partial^2}{\partial y^2} + (k_g^2 - k_z^2) \right] \bar{\boldsymbol{\pi}}^g = 0 \quad ; \quad y \leq 0 \quad (2.38)$$

where

$$\bar{\mathbf{J}} = \hat{\mathbf{z}} C I_n e^{-j\omega t + jk_z z} \delta(x) \delta(y-h) \quad (2.39)$$

$$k_e^2 = \omega^2 \mu_e \epsilon'_e \quad , \quad \epsilon'_e = \epsilon_e + j\sigma_e/\omega \quad , \quad (2.40)$$

$$k_g^2 = \omega^2 \mu_g \epsilon'_g \quad , \quad \epsilon'_g = \epsilon_g + j\sigma_g/\omega \quad .$$

The source term $\bar{\mathbf{J}}$ is formed in terms of the total conduction current I_n inside the conductor, as in section 2.3, with C

being the integration constant. It is required that all fields and their first derivatives be continuous (except at the source) in the domain of the solution. The constants k_e and k_g are the propagation constants in the regions $y > 0$ and $y < 0$, respectively.

The solution to the system must also satisfy the boundary conditions at the interface ($y = 0$); namely, $E_x^e = E_x^g$, $E_z^e = E_z^g$, $H_x^e = H_x^g$, $H_z^e = H_z^g$, $\epsilon_e' E_y^e = \epsilon_g' E_y^g$, and $\mu_e H_y^e = \mu_g H_y^g$. Thus, using (2.35) and (2.36) to form the field components the following set of conditions must be enforced on the vector potentials $\bar{\pi}^e$ and $\bar{\pi}^g$ at the interface:

$$\pi_x^e = \pi_x^g = 0 \quad (2.41)$$

$$k_e^2 \pi_z^e = k_g^2 \pi_z^g \quad (2.42)$$

$$\epsilon_e' \frac{\partial}{\partial y} \pi_z^e = \epsilon_g' \frac{\partial}{\partial y} \pi_z^g \quad (2.43)$$

$$\epsilon_e' \pi_y^e = \epsilon_g' \pi_y^g \quad (2.44)$$

$$\nabla \cdot \bar{\pi}^e = \nabla \cdot \bar{\pi}^g \quad (2.45)$$

The solution to (2.37) can be formed from the appropriate two dimensional Green's function for the region $y \geq 0$; the integral equivalent to (2.26), for the symmetric case $n = 0$, being [21,p.376]

$$\bar{\pi}_p = \hat{z} \frac{CI}{2\pi} K_0(\tau_e \rho) = \hat{z} \frac{CI}{4\pi} \int_{-\infty}^{\infty} \frac{e^{-jk_x x - U_e |y-h|}}{U_e} dk_x \quad (2.46)$$

As in section 2.3, the integration coefficient C is expressed in terms of the total conduction current inside the wire and is obtained by applying the boundary conditions at the wire surface ($\rho = a$). Replacing the Bessel's functions of equation (2.33) by their equivalent modified Bessel's function representations we get

$$C = \frac{j\omega\mu_e}{k_e^2} \cdot \frac{1}{(\tau_e a)K_1(\tau_e a)} \quad (2.47)$$

Now, using the boundary condition (2.41) we can write $\bar{\pi}^e$ and $\bar{\pi}^g$ in terms of their components as

$$\bar{\pi}^e = \pi_y^e \hat{y} + \pi_z^e \hat{z} \quad (2.48)$$

$$\bar{\pi}^g = \pi_y^g \hat{y} + \pi_z^g \hat{z} \quad (2.49)$$

Using the integral representation of (2.46) the components of the vector potentials can be expanded as

$$\pi_z^e = A \int_{-\infty}^{\infty} \frac{e^{-jk_x x - U_e |y-h|}}{U_e} + \frac{R}{U_e} e^{-jk_x x - U_e (y+h)} dk_x \quad (2.50)$$

, $y \geq 0$

$$\pi_z^g = A \int_{-\infty}^{\infty} \frac{T}{U_e} e^{-jk_x x - U_e h + U_g y} dk_x \quad (2.51)$$

, $y \leq 0$

$$\pi_y^e = A \int_{-\infty}^{\infty} \frac{M}{U_e} e^{-jk_x x - U_e (y+h)} dk_x \quad (2.52)$$

, $y \geq 0$

$$\pi_y^g = A \int_{-\infty}^{\infty} \frac{N}{U_e} e^{-jk_x x - U_e h + U_g y} dk_x \quad (2.53)$$

, $y \leq 0$

where

$$A = \frac{C}{4\pi} I_n e^{-j\omega t + jk_z z} \quad , \quad (2.54)$$

$$U_e = \sqrt{k_x^2 + \tau_e^2} \quad , \quad \tau_e^2 = k_z^2 - k_e^2 \quad , \quad (2.55)$$

$$U_g = \sqrt{k_x^2 + \tau_g^2} \quad , \quad \tau_g^2 = k_z^2 - k_g^2 \quad . \quad (2.56)$$

Here the z component of $\bar{\pi}^e$ has been formed as a sum of the primary potential (2.46) and a secondary potential. The unknown coefficients R , T , M , and N are determined by applying the remaining boundary conditions at $y=0$. Thus, using (2.42 - 2.45) we get

$$(1 + R) = n^2 m^2 T \quad , \quad (2.57)$$

$$T = \frac{1}{n^2} \frac{U_e}{U_g} (1 - R) \quad , \quad (2.58)$$

$$M = n^2 N \quad , \quad (2.59)$$

$$-U_e M + jk_z (1 + R) = U_g N + jk_z T \quad (2.60)$$

where

$$n^2 = \frac{\epsilon'_g}{\epsilon'_e} \quad , \quad m^2 = \frac{\mu_g}{\mu_e} \quad . \quad (2.61)$$

Solving for the $\bar{\pi}^e$ potential requires the values R and M , which are derived as

$$\frac{R}{U_e} = -\frac{1}{U_e} + \frac{2m^2}{(m^2 U_e + U_g)} \quad , \quad (2.62)$$

$$\frac{M}{U_e} = jk_z \frac{2}{U_e} \frac{(n^2 m^2 - 1)}{(n^2 - m^2)} \left[\frac{1}{(m^2 U_e + U_g)} - \frac{1}{(n^2 U_e + U_g)} \right] \quad . \quad (2.63)$$

The z component of the electric field at any point in the upper half-space ($y \geq 0$) can now be derived using (2.35) as

$$E_z = \frac{\partial}{\partial z} (\nabla \cdot \bar{\pi}^e) + k_e^2 \pi_z^e \quad (2.64)$$

or

$$E_z = A \left\{ jk_z \frac{\partial}{\partial y} \int_{-\infty}^{\infty} \frac{M}{U_e} e^{\bar{\tau}_e \cdot \bar{\rho}^*} dk_x \right. \\ \left. + \left[jk_z \frac{\partial}{\partial z} + k_e^2 \right] \int_{-\infty}^{\infty} \frac{e^{\bar{\tau}_e \cdot \bar{\rho}}}{U_e} + \frac{R}{U_e} e^{\bar{\tau}_e \cdot \bar{\rho}^*} dk_x \right\} \quad (2.65)$$

where

$$\bar{\tau}_e \cdot \bar{\rho} = -jk_x x - U_e |y - h| \quad , \quad (2.66)$$

$$\bar{\tau}_e \cdot \bar{\rho}^* = -jk_x x - U_e (y + h) \quad . \quad (2.67)$$

We will now only consider the special case $\mu_e = \mu_g = \mu_0$ for which $m^2=1$. Thus after replacing R and M in (2.65) we get

$$E_z = -2A \left\{ \tau_e^2 [K_0(\tau_e \rho) - K_0(\tau_e \rho^*)] \right. \\ \left. - \int_{-\infty}^{\infty} \left[\frac{\tau_e^2}{n^2 U_e + U_g} + k_e^2 \left(\frac{1}{U_e + U_g} - \frac{1}{n^2 U_e + U_g} \right) \right] e^{\bar{\tau}_e \cdot \bar{\rho}^*} dk_x \right\} . \quad (2.68)$$

Note that two terms of (2.65) are the integral representations of the modified Bessel's function $K_0(z)$ and have been replaced in (2.68) as such.

The required external impedance matrix elements Z_{mn}^{ext} can now be obtained from (2.68) by dividing by the wire currents I_n . When (x_n, y_n) is the source location and (x_m, y_m) is the field observation point the elements of the external impedance matrix of (2.19) are given by

$$z_{mn}^{ext} = \frac{-j\omega\mu_e}{2\pi k_e^2 (\tau_e a_n) K_1(\tau_e a_n)} \left\{ \tau_e^2 [K_0(\tau_e \rho_{mn}) - K_0(\tau_e \rho_{mn}^*) + G(\bar{\rho}_{mn}^*)] - k_e^2 [J(\bar{\rho}_{mn}^*) - G(\bar{\rho}_{mn}^*)] \right\} \quad (2.69)$$

where

$$J(\bar{\rho}_{mn}^*) = \int_{-\infty}^{\infty} \frac{1}{U_e + U_g} e^{\bar{\tau}_e \cdot \bar{\rho}_{mn}^*} dk_x \quad , \quad (2.70)$$

$$G(\bar{\rho}_{mn}^*) = \int_{-\infty}^{\infty} \frac{k_e^2}{k_g^2 U_e + k_e^2 U_g} e^{\bar{\tau}_e \cdot \bar{\rho}_{mn}^*} dk_x \quad (2.71)$$

and

$$\rho_{mn} = \sqrt{(x_m - x_n)^2 + (y_m - y_n)^2}$$

$$\rho_{mn}^* = \sqrt{(x_m - x_n)^2 + (y_m + y_n)^2}$$

$$\bar{\tau}_e \cdot \bar{\rho}_{mn}^* = -jk_x |x_m - x_n| - U_e (y_m + y_n) \quad .$$

2.5 MODE EQUATION AND TRANSFORMATION MATRIX

As formulated in section 2.1, the general problem of solving for the propagation of an injected current on a transmission line can be solved in terms of the eigen-current modes propagating on the system. The equation giving the values of the N eigen-currents, (2.18), is

$$[z_{mn}^{int} - z_{mn}^{ext}] [I_n] = 0 \quad (2.72)$$

where z_{mn}^{int} and z_{mn}^{ext} were formed using (2.34) and (2.69), respectively. z^{int} and z^{ext} , however, are functions of the

unknown propagation constant k_z^m and thus will have N forms corresponding to the N propagating modes of the system. The problem can be recognized as an eigenvalue problem, whose solution requires that the determinant of the impedance matrix be zero. This brings about the "mode equation",

$$\det[Z^{\text{int}}(k_z^m) - Z^{\text{ext}}(k_z^m)] = 0 \quad (2.73)$$

whose solution will yield N eigenvalues, which are the N propagating modes characteristic to the transmission line structure.

Substitution of each eigenvalue k_z^m into the impedance matrix of equation (2.72) will yield a corresponding current eigenvector defining the proportionality between currents in the N wires for that particular mode. The normalized eigenvectors are then used as the column vectors of the transformation matrix [P] in (2.3) which appropriately adds the eigen-currents to form the total current quantity for each conductor. The elements of the [P] matrix can be deduced from the impedance matrix by

$$[P_{mn}] = [V(k_z^1), V(k_z^2), \dots, V(k_z^N)] \quad (2.74)$$

where

$$V_j(k_z^m) = (-1)^{j+1} \Delta_{1j}(k_z^m), \quad (2.75)$$

$$j = 1, 2, \dots, N, \quad m = 1, 2, \dots, N$$

and

$$\Delta_{1j} = \det \begin{bmatrix} z_{21} \cdots z_{j-1,1} & z_{j+1,1} & \cdots & z_{N1} \\ \vdots & \vdots & & \vdots \\ z_{N1} \cdots & & & \cdots & z_{NN} \end{bmatrix} \quad (2.76)$$

N-1 x N-1

For each k_z^m , the elements of the column vector $V_j(k_z^m)$ are given by the complement of the j^{th} element in the first row of the impedance matrix of equation (2.72). Thus, N column vectors can be formed corresponding to the N values of k_z^m substituted into the impedance matrix.

Chapter III

SOLUTION TECHNIQUE

As discussed in section 2.1, the N modal propagation constants k_z^m and the system transformation matrix $[P]$ must first be determined so that the system transfer matrix $[S(z, \omega)]$ can be found. This chapter describes the numerical technique used to evaluate k_z^m and $[P]$ for a specified transmission line structure. The solution of the Sommerfeld integrals $J(\bar{p}_{mn}^*)$ and $G(\bar{p}_{mn}^*)$ will be discussed and an exact solution for the J function will be presented as well as an asymptotic expression for the G function. Also, the frequently used approximations for the functions J and G will be made to develop Carson's equations, which are commonly used to solve many power system problems.

3.1 NUMERICAL EVALUATION

As developed in section 2.2, the propagation constants k_z^m and the transformation matrix $[P]$ can be extracted by solving the linear system of equations

$$[z_{mn}^{int} - z_{mn}^{ext}] [I_n] = 0 \quad (3.1)$$

where z_{mn}^{int} and z_{mn}^{ext} were formed using (2.34) and (2.69), respectively. The mode equation (2.73), whose solution

yields the N propagating modes characteristic to the system, will be modified to make its numerical evaluation more practical. The constant $j\omega\mu_e/2\pi k_e^2$ is cancelled from all terms in the impedance matrix and all current terms I_n are divided by the factor $(\mathcal{Y}_e a_n)K_1(\mathcal{Y}_e a_n)$. After rearrangement, (3.1) can then be written in the form

$$[A_{mn} + \chi B_{mn}][I_n/(\tau_e a_n)K_1(\tau_e a_n)] = 0 \quad (3.2)$$

where the elements of the new impedance matrix are given by

$$A_{mn} = \left\{ \delta_{mn} \cdot \frac{\mu_n}{\mu_e k_n^2} \cdot \frac{\tau_n^2 I_0(\tau_n a_n)}{(\tau_n a_n) I_1(\tau_n a_n)} (\tau_e a_n) K_1(\tau_e a_n) - [J(\bar{\rho}_{mn}^*) - G(\bar{\rho}_{mn}^*)] \right\}, \quad (3.3)$$

$$B_{mn} = [K_0(\tau_e \rho_{mn}) - K_0(\tau_e \rho_{mn}^*) + G(\bar{\rho}_{mn}^*)], \quad (3.4)$$

with $\rho_{nn} = a_n$,

$$\chi = \frac{\tau_e^2}{k_e^2}. \quad (3.5)$$

The solution of (3.2) requires that the determinant of the impedance matrix be zero, bringing about a new mode equation which is in the form of a generalized eigenvalue problem. The solution of the mode equation will yield N eigenvalues χ_m from which the propagating modes can be found, as

$$k_z^m = \sqrt{\tau_e^{m^2} + k_e^2} = k_e \sqrt{\chi_m + 1} \quad (3.6)$$

where

$$\det[A + \chi_m B] = 0, \quad m = 1, 2, \dots, N. \quad (3.7)$$

Difficulty arises in evaluating the mode equation by the usual eigenvalue techniques since the defining matrices A and B are non-linear functions of χ_m . However, since χ_m is incorporated in the matrices only through the modified Bessel's functions K_0 , K_1 , I_0 , and I_1 and the integrals $J(\bar{p}_{mn}^*)$ and $G(\bar{p}_{mn}^*)$, which all vary slowly as compared to χ_m itself, an iterative technique can be employed to solve (3.2). The matrices A and B will be formed using previously calculated estimates of the eigenvalues χ_m^{j-1} . Convergence to the exact eigenvalues of the system can then be found by iteratively evaluating

$$\det[A(\chi_m^{j-1}) + \chi_m^j B(\chi_m^{j-1})] = 0, \quad m = 1, 2, \dots, N \quad (3.8)$$

where A and B are now constant matrices at each iteration step j , $j=1, 2, \dots, \infty$. At each iteration j , the error is given by $\mathcal{E} = \chi_m^j - \chi_m^{j-1}$. The initial assignments for the eigenvalues χ_m^0 are assumed to be zero, which is the case when all modes propagate with the value k_e . For this initial case the function $G(\bar{p}_{mn}^*)$ and the modified Bessel's functions of equations (3.3) and (3.4) will take, in the limit as $\tau_e \rightarrow 0$, the values [21, p.375]

$$k_z^m \xrightarrow{\tau_e \rightarrow 0} k_e \quad (3.9)$$

$$K_0(\tau_e \rho_{mn}) - K_0(\tau_e \rho_{mn}^*) \xrightarrow{\tau_e \rightarrow 0} \ln \left(\frac{\rho_{mn}^*}{\rho_{mn}} \right) \quad (3.10)$$

$$(\tau_e a_n) K_1(\tau_e a_n) \xrightarrow{\tau_e \rightarrow 0} 1 \quad (3.11)$$

Since the value of the G function is small compared to the other functions, it will be assumed for the initial case that

$$G(\bar{\rho}_{mn}^*) \approx 0 \Big|_{j=1} \quad (3.12)$$

Thus, at each iteration step it is required to find the N values χ_m^j satisfying (3.8) where $A(\chi_m^{j-1})$ and $B(\chi_m^{j-1})$ are constant. Various methods can be employed to solve this problem.

3.1.1 Determinant Solution

One method of solving the problem described in the previous section is to break (3.8) down into a polynomial in terms of χ_m^j as follows:

$$a_N \chi^N + a_{N-1} \chi^{N-1} + \dots + a_1 \chi^1 + a_0 = 0 \quad (3.13)$$

where χ_m^j has been replaced by χ for clarity. The complex coefficients a_j are derived from the matrices $A(\chi_m^{j-1})$ and $B(\chi_m^{j-1})$ using

$$a_j = \sum_{k=1}^{M_j} \det[A_k^j] \quad ; \quad j = 0, 1, 2, \dots, N \quad (3.14)$$

$$M_j = \binom{N}{j} = \frac{N!}{(N-j)!j!} \quad (3.15)$$

Here A_k^j is the matrix A with j of its rows replaced by the k^{th} possible combination of j rows of the matrix B. Thus, for the coefficient a_j there are j rows of A replaced by the corresponding rows of B and for the coefficient a_j there are M_j possible substitution combinations. An example illustrating the expansion of (3.13) using (3.14) for the case $N=3$ is given in appendix A.

The problem has now been reduced to one of finding the complex roots of the polynomial (3.13), for which an exact solution exists for orders up to $n = 4$. For orders $n > 4$ various methods can be used to determine the roots, the one used being a combination of Lehmer's method and Newton's iteration method [25]. In summary, the described technique of evaluating (3.8) is very accurate for low orders where the number of conductors in the transmission line system is small. However, as the order increases the accuracy with which the polynomial coefficients a_j are formed decreases rapidly since the number of determinants required to be evaluated increases drastically as given by (3.15). For higher order systems, alternate techniques can be employed to solve the eigenvalue problem [26].

Another method of solving (3.8) would be to use a two variable non-linear optimization technique to search for the eigenvalues [27]. In this case the minimizing function is defined by $ABS(\det(A - \chi_m^j B))$. The major advantage of this method is that only the search for the minimum due to

the m^{th} root would be necessary for each χ_m^{j-1} . The previously discussed polynomial method resulted in the determination of N roots for each χ_m^{j-1} , with only the m^{th} root being the desired result. Also, by using an optimization technique, the number of search steps can be reduced by utilizing the fact that the desired root χ_m^j is in the neighbourhood of the last calculated χ_m^{j-1} . However, this method may be unstable for the first few iteration steps since difficulty occurs in identifying the m^{th} root when the roots are in close proximity to each other. This problem will be discussed next. In general, the method is well suited to this problem once the proximity of all roots are firmly established.

3.1.2 Convergence Of Roots

The iterative process described in the previous sections must be carried out for all roots χ_m^j , $j=1,2,\dots,\infty$, $m=1,2,\dots,N$. At each search step j , however, the solution of the polynomial (3.13) will yield N roots, with only the m^{th} one being the desired root as shown in figure 3.1. The remaining $N-1$ calculated roots are "false" roots in the sense that they only add extraneous information as to how the roots converge. If two or more roots are near each other, the use of a non-linear optimization search method to locate the m^{th} root may result in the convergence to one of the false roots. Thus, only when the proximity of all the

roots is determined by the iterative solution of (3.8) can an optimization technique be used to converge to the desired eigenvalues with greater accuracy. Note here also that the the solution of the general eigenvalue equation (3.2) directly through the use of an optimization technique from the initial phase would be very time consuming since the matrices A and B would need to be evaluated at every search step. In the thesis, the propagation constants k_z^m are evaluated numerically using the iterative technique and by employing the polynomial expansion method to calculate the roots.

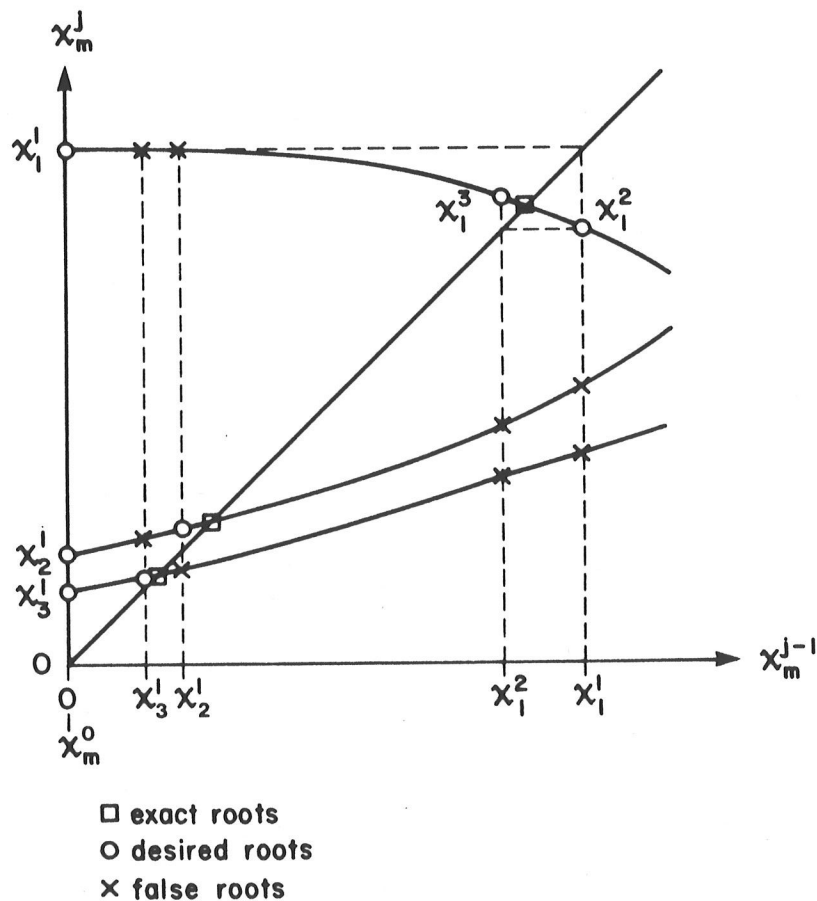


Figure 3.1: Calculation of roots for the iteration technique.

3.2 EVALUATION OF THE TRANSFORMATION MATRICES

Once the roots χ_m and the resulting propagation constants k_z^m are determined by the iteration technique described in the last section, the eigenvectors of the system can be derived using (2.74). It should be remembered, however, that the mode equation had been modified in section 3.1 to the form of (3.2) by dividing the currents I_n by the factor $(\gamma_e a_n) K_1(\gamma_e a_n)$. To take this into account the eigenvectors are found using

$$[V_j(k_z^m)] = [(-1)^{j+1} \Delta_{1j}(k_z^m)] \cdot (\tau_e^m a_j) K_1(\tau_e^m a_j), \quad (3.16)$$

$$j = 1, 2, \dots, N, \quad m = 1, 2, \dots, N$$

where Δ_{1j} is now the complement of the j^{th} element in the first row of the modified impedance matrix (3.2), evaluated at k_z^m . The eigenvectors, which are derived using (3.16), are all normalized in phase with respect to the first element in the column vector using

$$[V_j(k_z^m)] = \frac{V_j}{V_1}, \quad j = 1, 2, \dots, N \quad (3.17)$$

and in magnitude using

$$[V_j(k_z^m)] = \frac{V_j}{\sqrt{\sum_{k=1}^N V_k V_k^*}}, \quad j = 1, 2, \dots, N \quad (3.18)$$

The transformation matrix $[P]$ is then formed using (2.74). The inverse transformation matrix $[P]^{-1}$ is calculated by inverting $[P]$ using the simple method of Gauss elimination which is an adequate method for matrices of low order.

3.3 EVALUATION OF THE COMPLEX INTEGRALS

In this section the evaluation of the complex integrals $J(\bar{\rho}_{mn}^*)$ and $G(\bar{\rho}_{mn}^*)$ will be discussed. Their solution is required in the calculation of the elements of the impedance matrix (2.18) which is used to extract the characteristics of the transmission line structure. The two integrals were defined by (2.70) and (2.71) as

$$J(\bar{\rho}_{mn}^*) = \int_{-\infty}^{\infty} \frac{1}{U_e + U_g} e^{-jk_x x - U_e y} dk_x \quad (3.19)$$

$$G(\bar{\rho}_{mn}^*) = \int_{-\infty}^{\infty} \frac{1}{n^2 U_e + U_g} e^{-jk_x x - U_e y} dk_x \quad (3.20)$$

where

$$U_e = \sqrt{k_x^2 + \tau_e^2}, \quad \tau_e^2 = k_z^2 - k_e^2 \quad (3.21)$$

$$U_g = \sqrt{k_x^2 + \tau_g^2}, \quad \tau_g^2 = k_z^2 - k_g^2 \quad (3.22)$$

and

$$x = |x_m - x_n|, \quad y = (y_m + y_n)$$

$$\rho_{mn}^* = \sqrt{(x_m - x_n)^2 + (y_m + y_n)^2}$$

$$n^2 = \frac{k_g^2}{k_e^2}$$

The contour of integration is the total real axis of the complex k_x plane.

Exact solutions of the two integrals in terms of analytical expressions that are valid throughout the possible argument range are not available except when various assumptions are made to simplify their integrands.

Also, their direct numerical integration along the real axis is inaccurate and time consuming since the integrands' behaviors are significant over the entire range of the real axis. Thus, a solution is usually determined in terms of analytical expressions which are valid in either the large argument or small argument range and later linked together appropriately.

The integrands of (3.19) and (3.20) are both doubly irrational and thus, for convergence of the two integrals $\text{Real}\{U_e\} \geq 0$ and $\text{Real}\{U_g\} \geq 0$ must be ensured over the entire complex k_x plane. Using (3.21) and (3.22), the locations of the branch points of the two radicals are given by

$$U_e = \sqrt{k_x^2 + \tau_e^2} = 0 \rightarrow k_x = \pm j\tau_e \quad (3.23)$$

and

$$U_g = \sqrt{k_x^2 + \tau_g^2} = 0 \rightarrow k_x = \pm j\tau_g \quad (3.24)$$

Knowledge of the behavior of k_e , k_g , and k_z in the complex k plane yields the locations of the branch points as well as aids in the general understanding of the problem. Figure 3.2 gives the regions for the possible values of k_e , k_g , and k_z in the complex k plane. The propagation constant k_e will always be located on the real axis for a non-lossy air medium and the propagation constant in the earth k_g is located in the region $0^\circ < \angle k_g < 45^\circ$.

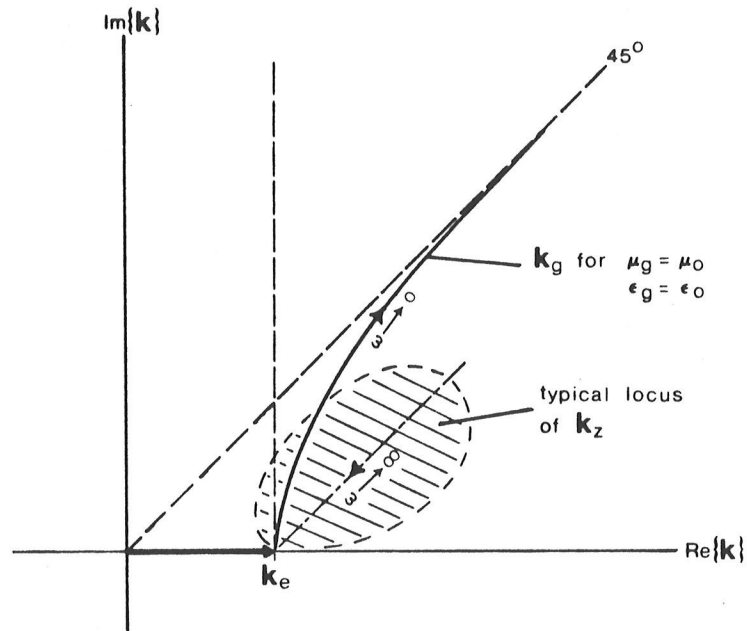


Figure 3.2: Location of k_e , k_g , and k_z in the complex k plane.

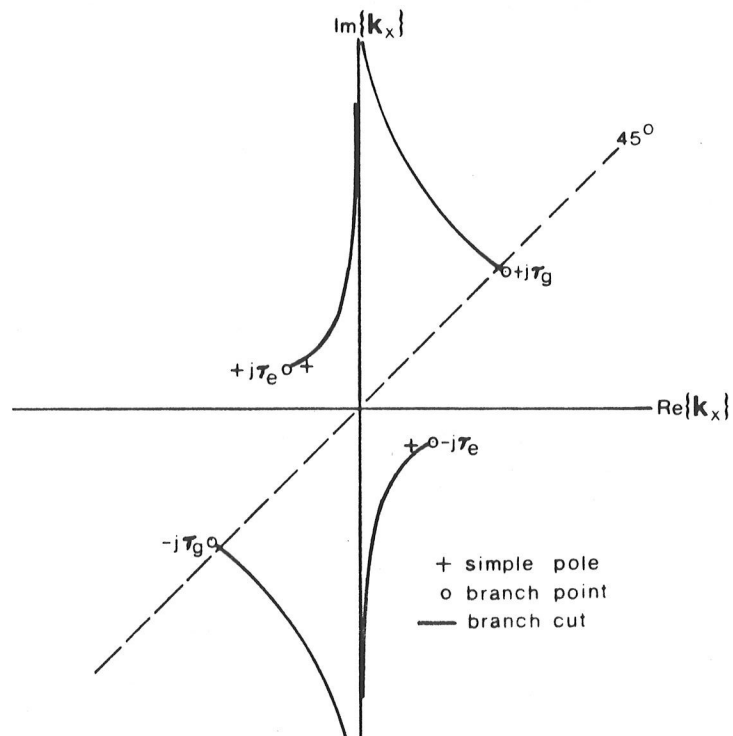


Figure 3.3: Branch point and pole locations in the complex k_x plane.

The constant k_g will approach the 45° limit as frequency decreases or for high earth conductivities. The possible locus of k_z , whose exact value is to be determined, will fall in the upper half plane and is best considered as a perturbation of the propagation constant k_e .

From the probable values of k_e , k_g , and k_z shown in figure 3.2 the corresponding locations of the branch points and their associated branch cuts can be deduced as shown in figure 3.3 where

$$\begin{aligned} 0^\circ \leq \angle j\tau_e \leq 180^\circ \\ 0^\circ \leq \angle j\tau_g \leq 180^\circ \end{aligned} \quad (3.25)$$

The $+j\tau_g$ branch point will lie near the 45° axis in most cases since k_g is near 45° and much larger than k_e . The $+j\tau_e$ branch point will always be located in the second quadrant near the origin and is the unknown value that is evaluated in section 3.1 to obtain the values of the propagation constants of the transmission line structure.

3.3.1 J Integral Evaluation

Accurate analytical formulations for the $J(\bar{J}_{mn}^*)$ integral express it in terms of Struve functions under the assumption that the propagation constant k_z is the free space value k_e in the exponent term [8,9]. The J integral (3.19) can be separated into two integral forms by multiplying by $(U_e - U_g)/(U_e - U_g)$ as

$$\begin{aligned}
 J(\bar{\rho}_{mn}^*) &= J_1 + J_2 \\
 &= \frac{1}{(n^2-1)k_e^2} \int_{-\infty}^{\infty} U_e e^{-jk_x x - U_e y} dk_x - \frac{1}{(n^2-1)k_e^2} \int_{-\infty}^{\infty} U_g e^{-jk_x x - U_e y} dk_x \quad (3.26)
 \end{aligned}$$

The first integral J_1 has a single irrationality U_e and is known in terms of modified Bessel's functions [21,p.376] as

$$J_1 = \frac{2}{(n^2-1)k_e^2} \frac{\partial^2}{\partial y^2} K_0(\tau_e \rho_{mn}^*) \quad (3.27)$$

or

$$J_1 = -2 \left[\frac{(\tau_e \rho) K_1(\tau_e \rho) - \left(\frac{y}{\rho}\right)^2 (\tau_e \rho) K_2(\tau_e \rho)}{(n^2-1)k_e^2} \right] \quad (3.28)$$

where $\rho = \rho_{mn}^*$. The second integral J_2 is not as easily identified since it retains the double irrationality U_e and U_g . It can, however, be expressed in terms of known functions in the limit of $k_z \rightarrow k_e$ in the exponent. For this condition J_2 becomes

$$J_2 = \frac{1}{(n^2-1)k_e^2} \left[\int_{-\infty}^0 U_g e^{k_x(y-jx)} dk_x + \int_0^{\infty} U_g e^{-k_x(y+jx)} dk_x \right] \quad (3.29)$$

The limits of integration for the first integral can be changed from $(-\infty, 0)$ to $(0, \infty)$ by setting $k_x = -k_x$. Also, for the case $-\pi/2 < \angle \gamma_g(y \pm jx) < \pi/2$, the integration paths for the two integrals can be altered from the real k_x axis to $\gamma_g w$ through the following:

$$\begin{aligned}
 k_x &= \tau_g w \\
 dk_x &= \tau_g dw \\
 U_g &= \sqrt{w^2 + 1} \quad .
 \end{aligned} \quad (3.30)$$

Thus, the J_2 integral of (3.29) becomes

$$J_2 = \frac{\tau_g^2}{(n^2-1)k_e^2} \left[\int_0^\infty \sqrt{w^2+1} e^{-z_1 w} dw + \int_0^\infty \sqrt{w^2+1} e^{-z_2 w} dw \right] \quad (3.31)$$

where

$$z_1 = \tau_g(y-jx) \quad , \quad z_2 = \tau_g(y+jx)$$

which can be expressed in terms of Struve functions [21,p.496] as

$$J_2 = \frac{\tau_g^2}{(n^2-1)k_e^2} \frac{\pi}{2} \left[\frac{H_1(z_1) - Y(z_1)}{z_1} + \frac{H_1(z_2) - Y(z_2)}{z_2} \right] \quad (3.32)$$

The formulation of the J integral just presented using (3.28) and (3.32) is equivalent to the expression used by Perel'man [5] and Olsen et al. [28]. The formulation is adequate for small argument evaluation ($\mathcal{V}_e \bar{\rho}_{mn}^*$ small). An exact solution for the $J(\bar{\rho}_{mn}^*)$ integral under no assumptions can be deduced from the formulation presented by Aboul-Atta [17].

3.3.2 G Integral Evaluation

Unlike the J integral solution method, the G integral can not be separated into easily identified forms. Instead, the asymptotic behavior of the integrand as $k_x \rightarrow \infty$ will be used to determine the small argument behavior of the $G(\bar{\rho}_{mn}^*)$ function as $\mathcal{V}_g \bar{\rho}_{mn}^* \rightarrow 0$ by applying the final value theorem [29]. The G function integrand of (3.20) can be written in the form

$$\frac{1}{n^2 U_e + U_g} = \left(\frac{2}{n^2+1} \right) \frac{1}{2U_e} \left[\frac{1+R}{1 + \left(\frac{n^2-1}{n^2+1} \right) R} \right] \quad (3.33)$$

where

$$R = \frac{U_e - U_g}{U_e + U_g} \quad (3.34)$$

Since $|R| < 1$ and $|(n^2-1)/(n^2+1)| < 1$, the denominator of (3.33) can be expressed in terms of a binomial expansion as

$$\left[1 + \left(\frac{n^2-1}{n^2+1}\right)R\right]^{-1} = \left[1 - \left(\frac{n^2-1}{n^2+1}\right)R + \left(\frac{n^2-1}{n^2+1}\right)^2 R^2 - \dots\right] \quad (3.35)$$

Replacing (3.35) into (3.33), the integrand of the G integral can be written as

$$\frac{1}{n^2 U_e + U_g} = \left(\frac{2}{n^2+1}\right) \frac{1}{2U_e} \left\{1 + \left[1 - \left(\frac{n^2-1}{n^2+1}\right)R\right] + \left[\left(\frac{n^2-1}{n^2+1}\right)^2 - \left(\frac{n^2-1}{n^2+1}\right)\right]R^2 + \dots\right\} \quad (3.36)$$

The first order approximation, which was employed by Perel'man [5], can be recognized as the modified Bessel's function K_0 as

$$G(\bar{\rho}_{mn}^*) \approx \frac{2k_e^2}{k_g^2} K_0(\tau_e \rho_{mn}^*) \quad (3.37)$$

In the evaluation used in the thesis the second order approximation is used to express the G integral as

$$G_{MOD}(\bar{\rho}_{mn}^*) = \frac{2k_e^2}{k_e^2 + k_g^2} \left[\frac{k_g^2 - k_e^2}{k_g^2 + k_e^2} K_0(\tau_e \rho_{mn}^*) + \frac{2k_e^2}{k_g^2 + k_e^2} J(\bar{\rho}_{mn}^*) \right] \quad (3.38)$$

3.3.3 G Integrand Pole Extraction

Recently, much attention has been paid to the effect of the singularity in the G integral. Early work by Olsen, Chang, and Kuester [11,30,28] and Carpentier and dos Santos

[13] suggest that at high frequencies the contribution of the simple pole singularity dominates the remaining contribution due to the two branch cuts. Thus, an examination of the significance of the singularity is of importance to the proper evaluation of the G integral. The location of the poles of the G integrand (3.33) in the complex k_x plane are extracted for the condition

$$n^2 U_e + U_g = 0 \quad (3.39)$$

Using (3.21) and (3.22), the pole locations are given as

$$k_x = \pm j \sqrt{\tau_e^2 + \frac{k_e^2}{n^2+1}} \quad (3.40)$$

in the complex k_x plane and are shown in figure 3.3. The poles are located near the branch points $\pm j \tau_e$ for values of large n^2 , which is usually the case unless extremely high frequencies are considered.

The contribution of the poles to the G integral can be determined by calculating the residue term at a pole location. By multiplying the integrand of (3.20) by $(n^2 U_e - U_g)/(n^2 U_e - U_g)$ the G integral can be written as

$$G(\bar{\rho}_{mn}^*) = \frac{1}{n^4 - 1} \int_{-\infty}^{\infty} \frac{(n^2 U_e - U_g) e^{-jk_x x - U_e y}}{\left[k_x - j \sqrt{\tau_e^2 + \frac{k_e^2}{n^2+1}} \right] \left[k_x + j \sqrt{\tau_e^2 + \frac{k_e^2}{n^2+1}} \right]} dk_x \quad (3.41)$$

Thus, using (3.40) the pole contribution is given by

$$G_{\text{pole}} = 2\pi j \frac{n^2 k_e^2}{n^4 - 1} \frac{e^{-\left(x \sqrt{\tau_e^2 + \frac{k_e^2}{n^2+1}} - jy \frac{k_e}{\sqrt{n^2+1}}\right)}}{\sqrt{n^2+1} \sqrt{\tau_e^2 + \frac{k_e^2}{n^2+1}}} \quad (3.42)$$

Examination of (3.42) shows that, except for the case at extremely high frequencies, the contribution due to the poles is small compared to the previously derived expression for the G integral (3.38) since n^2 is large.

In accordance, Sorbello's experimental results [31] for a horizontal wire antenna above a dissipative half-space show only one mode of propagation on the structure for frequencies where $n^2 \gg 1$. Recently, however, Degauge et al. [16] have studied the current distribution on a long line parallel to a ground at high frequencies. Their experimental results indicate that the current distribution on the transmission line can not be considered as an exponential function beyond a given distance of propagation. The existence of an extra mode is suggested as an explanation. In the thesis, only currents due to the common transmission line modes will be considered and the existence and incorporation of the degenerate mode will be left for later research.

3.3.4 Reduction To Carson's Formulation

In this section the relationship between Carson's theory and the exact theory as presented in chapter two of the thesis will be discussed. Carson's formulation has been used in many power engineering applications and the degree to which it is correct can be determined by observing the approximations necessary for its derivation from the exact equations.

Olsen and Pankaskie [32] derive Carson's equations by applying approximations which are valid at low frequencies and for high earth conductivities. At low frequencies all significant distances will be small compared to the free space wavelegnth and under the quasi-static approximation it can be assumed

$$|\tau_e \rho_{mn}|, |\tau_e \rho_{mn}^*| \ll 1 \quad (3.43)$$

$$k_z \approx k_e.$$

Under these conditions [21,p.375]

$$K_0(\tau_e \rho_{mn}) - K_0(\tau_e \rho_{mn}^*) \approx \ln \left(\frac{\rho_{mn}^*}{\rho_{mn}} \right) \quad (3.44)$$

$$(\tau_e a_n) K_1(\tau_e a_n) \approx 1 \quad (3.45)$$

$$U_e \approx |k_x| \quad (3.46)$$

Further, for high earth conductivities $|k_g/k_e| \gg 1$ and thus

$$U_g \approx \sqrt{k_x^2 - k_g^2} \quad (3.47)$$

Using the approximations (3.46) and (3.47), the $G(\bar{J}_{mn}^*)$ integral (3.20) can be neglected since n^2 is large and the $J(\bar{J}_{mn}^*)$ integral (3.19) can be simplified to the form

$$J_c(\bar{J}_{mn}^*) = -2 \int_0^\infty \frac{(U_g - k_x)}{k_g^2} e^{-jk_x(|x_m - x_n| + j(y_m + y_n))} dk_x \quad (3.48)$$

Equation (3.48) is the term derived by Carson [1] to take into account the earth's effect and is usually expressed in terms of an infinite series. Thus, under the low frequency

approximation, the elements of the external impedance matrix (2.69) become

$$z_{mn}^{\text{ext}} = - \frac{j\omega\mu_e}{2\pi k_e^2} \left[\tau_e^2 \ln \left(\frac{\rho_{mn}^*}{\rho_{mn}} \right) - k_e^2 J_c(\bar{\rho}_{mn}^*) \right]. \quad (3.49)$$

In summary, the required conditions for a transmission line approach are that the wavenumber of the ground be large compared with that of the air, and all relevant distances be a small fraction of a wavelegnth. These conditions are almost always met for power engineering applications when the system is evaluated at 60Hz.

Chapter IV

NUMERICAL RESULTS

In this chapter the calculated results will be presented for the propagation constants k_z^m and the transformation matrix [P] as evaluated using the numerical technique presented in chapter 3. Also, the system transfer matrix [S(z,ω)] and the system impulse response matrix [S(z,t)] will be determined.

A program has been written which yields k_z^m and [P] for a specified transmission line structure and is listed in appendix B. The number, location, radius, and electrical properties of the conductors as well as the electrical properties of the air and earth media are all arbitrary. Assumptions made in deriving the mode equation are that the earth is considered homogeneous, the conductors are assumed to be thin relative to their structural spacing (i.e. field matching done at a conductor location assumes the field due to the other conductors is constant over its surface), and only the symmetric transverse magnetic case is considered since the wire currents are taken to be predominantly axially symmetric. Also, an asymptotic expression for the $G(\bar{f}_{mn}^*)$ function is employed as explained in chapter 3. Other errors will occur due to the inaccuracy of finite

digit arithmetic and any inaccuracy in the numerical evaluation technique. An exact expression for the $J(\bar{f}_{mn}^*)$ is used in the evaluation as explained in chapter three.

A comparison of calculated results with previously published values will be made for various cases. The results obtained when often used assumptions are made to ease the evaluation of the $J(\bar{f}_{mn}^*)$ and $G(\bar{f}_{mn}^*)$ functions will be examined. It will be shown that many of these assumptions are valid only when all relevant distances are small compared to the free space wavelength and the factor $k_g/k_e \gg 1$, as is the case at low frequencies and for large earth conductivities. Concentration will be mainly on the effect of the G function since it is usually assumed to be zero in these cases. Then, k_z^m and [P] will be calculated over a large spectral range for a specific transmission line example and compared to the results produced by the Electromagnetic Transient Program EMTP [33,34], a commonly used program in power systems applications. Finally, the system transfer matrix $[S(z,\omega)]$ will be evaluated for the example and from this, the system impulse response matrix $[S(z,t)]$ will be determined by employing the inverse Fourier transform.

4.1 PRELIMINARY RESULTS

Initial comparisons will be made to the results of Grinberg and Bonshtedt [7] and Perel'man [5] to determine the validity of the analytical and numerical technique used. As explained in chapter 3, Grinberg and Perel'man have used a Struve function series to evaluate the J function and have assumed an asymptotic expression for the G function as

$$G(\bar{\rho}_{mn}^*) = \frac{2k_e^2}{k_g^2} K_0(\tau_e \rho_{mn}^*) \quad (4.1)$$

The expression for the modified G function that has been incorporated in our evaluation was given by (3.38) as

$$G_{\text{MOD}}(\bar{\rho}_{mn}^*) = \frac{2k_e^2}{k_e^2 + k_g^2} \left[\frac{k_g^2 - k_e^2}{k_g^2 + k_e^2} K_0(\tau_e \rho_{mn}^*) + \frac{2k_e^2}{k_g^2 + k_e^2} J(\bar{\rho}_{mn}^*) \right] \quad (4.2)$$

Since at the frequencies and earth conductivities they have chosen $k_g/k_e \gg 1$ and all relevant distances are small compared to the free space wavelength, the differences in the determination of the J and G functions will be minimal and the evaluated results should be comparable.

Grinberg and Bonshtedt calculate the propagation constant k_z for the case of a single wire above a lossy earth. Table 4.1 presents a comparison of the normalized propagation constant k_z/k_e for frequencies ranging from 300 rad/sec to 10^6 rad/sec. The wire, of radius 1cm and conductivity $5.7 \times 10^7 \text{ } \Omega/\text{m}$, is located in an air medium at a height of 10m. The earth's electrical parameters are $\mu_g = \mu_o$, $\epsilon_g = \epsilon_o$, and

$\sigma_g = 1.0 \times 10^{-2} \text{ } \nu/\text{m}$. For the results presented $|k_g/k_e|$ ranges from 1.9×10^3 to 33.6 and thus the effect of differences in the G function evaluation should be minimal, as verified by the results in table 4.1 where

$$\% \text{ Effect of G} = \frac{|k_z| \Big|_{G=G_{\text{MOD}}}}{|k_z| \Big|_{G=0}} \cdot \quad (4.3)$$

Further examination shows that the effect of the G function tends to be directly proportional to the frequency.

TABLE 4.1: Comparison of k_z/k_e to the results of Grinberg and Bonshtedt and the percent effect of the G function.				
(rad/sec)	$ k_g/k_e $	PROPAGATION CONSTANT (k_z/k_e)		% EFFECT OF G ON $\text{Im}(k_z)$
		G (Modified)	Grinberg	
300.0	1941.6	1.2456+j0.0908	1.246-j0.0907	0.0006
1.0×10^3	1063.5	1.2110+j0.0595	1.211-j0.0594	0.002
1.0×10^4	336.3	1.1419+j0.0455	1.143-j0.0453	0.02
1.0×10^5	106.3	1.0815+j0.0363	1.081-j0.0363	0.21
1.0×10^6	33.6	1.0367+j0.0238	1.037-j0.0236	2.09

Perel'man calculates k_z^m and [P] for one, two, and three wire systems at a single frequency. A comparison of results for four of his cases are shown in table 4.2. Calculations are made at a frequency of 10^6 rad/sec, with an air medium and earth electrical parameters $\mu_g = \mu_o$, $\epsilon_g = \epsilon_o$, and $\sigma_g = 1.0 \times 10^{-2} \text{ } \nu/\text{m}$, which corresponds to a value $|k_g/k_e| = 33.6$. Conductor dimensions and electrical parameters for the four cases are given in table 4.3.

TABLE 4.2: Comparison of kz/ke and $[P]$ for G(MOD) and G=0 to the results of Perel'man.

CASE	METHOD	RELETIVE PROPAGATION CONSTANT (kz/ke) AND $[P]$
A	G(Modified) Perel'man G=0	MODE 1 1.036689+j0.023808 1.0368 +j0.0239 1.036666+j0.023321
B	G(Modified) Perel'man G=0 [P] (Modified) [P] Perel'man	MODE 1 MODE 2 1.060825+j0.040176 1.006375+j0.002380 1.061 +j0.0404 1.0064 +j0.0024 1.060791+j0.039345 1.006375+j0.002366 [0.7071+j0.0 0.7071+j0.0] [0.7071+j0.0 -0.7071+j0.0] [0.7071+j0.0 0.7071+j0.0] [0.7071+j0.0 -0.7071+j0.0]
C	G(Modified) Perel'man G=0 [P] (Modified) [P] Perel'man	MODE 1 MODE 2 1.067450+j0.046544 1.012997+j0.008660 -- -- 1.013 +j0.0088 1.067413+j0.045736 1.013002+j0.008628 [0.5920+j0.0 0.7885+j0.0] [0.8050+j0.0402 -0.6146+j0.0242] [-- 0.788 +j0.0] [-- -0.615 -j0.024]
D	G(Modified) Perel'man G=0 [P] (Modified) [P] (Modified)	MODE 1 MODE 2 MODE 3 1.078112+j0.053063 1.015886+j0.006080 1.002665+j0.000990 1.081 +j0.0528 1.016 +j0.0062 1.0026 +j0.0009 1.078071+j0.051933 1.015886+j0.006038 1.002663+j0.000984 [0.5679+j0.0 0.7071+j0.0 0.4315+j0.0] [0.5955-j0.0180 0.0 +j0.0 -0.7920-j0.0180] [0.5680+j0.0 -0.7071+j0.0 0.4315+j0.0] [0.568 +j0.0 0.7071+j0.0 0.432 +j0.0] [0.596 +j0.017 0.0 +j0.0 -0.791 +j0.017] [0.568 +j0.0 -0.7071+j0.0 0.432 +j0.0]

The effect of the G function is also calculated and compared to Perel'mans results as shown in table 4.4. The effect is small as expected since k_g/k_e is still considerably large in all cases.

TABLE 4.3: Parameters for the four test cases presented by Perel'man.

CASE	NUMBER OF CONDUCTORS	RAD	ELECTRICAL PARAMETERS			POSITION IN (x,y) PLANE
			μ	ϵ	σ	
A	1	1cm	$\mu_1 = \mu_0$	$\epsilon_1 = \epsilon_0$	$\sigma_1 = 5.7 \times 10^7 \text{ U/m}$	(0m, 10m)
B	2	1cm	$\mu_1 = \mu_0$	$\epsilon_1 = \epsilon_0$	$\sigma_1 = 5.7 \times 10^7 \text{ U/m}$	(0m, 10m)
		1cm	$\mu_2 = \mu_0$	$\epsilon_2 = \epsilon_0$	$\sigma_2 = 5.7 \times 10^7 \text{ U/m}$	(10m, 10m)
C	2	1cm	$\mu_1 = \mu_0$	$\epsilon_1 = \epsilon_0$	$\sigma_1 = 5.7 \times 10^7 \text{ U/m}$	(0m, 10m)
		1cm	$\mu_2 = 100\mu_0$	$\epsilon_2 = \epsilon_0$	$\sigma_2 = 9.0 \times 10^6 \text{ U/m}$	(10m, 10m)
D	3	1cm	$\mu_1 = \mu_0$	$\epsilon_1 = \epsilon_0$	$\sigma_1 = 5.7 \times 10^7 \text{ U/m}$	(0m, 10m)
		1cm	$\mu_2 = \mu_0$	$\epsilon_2 = \epsilon_0$	$\sigma_2 = 5.7 \times 10^7 \text{ U/m}$	(10m, 10m)
		1cm	$\mu_3 = \mu_0$	$\epsilon_3 = \epsilon_0$	$\sigma_3 = 5.7 \times 10^7 \text{ U/m}$	(20m, 10m)

TABLE 4.4: Influence of the G function on Imaginary(kz) compared to Perel'mans results.

CASE	G TYPE	% EFFECT OF G ON Im(kz)		
A	G (Modified) Perel'man	MODE 1		
		+2.09		
B	G (Modified) Perel'man	MODE 1	MODE 2	
		+2.11	+0.62	
C	G (Modified) Perel'man	MODE 1	MODE 2	
		+1.77	+0.37	
D	G (Modified) Perel'man	MODE 1	MODE 2	MODE 3
		+2.18	+0.71	+0.66
		+1.8	+1.0	+0.7

For the multi-conductor cases just presented note the existence of two distinct classes of modes. As indicated by examining the column eigen-vectors of the [P] matrix, one mode has all currents flowing predominantly in the same direction in all N conductors. The return current path for this mode is mainly through the earth and is thus known as the "ground mode". All other modes tend to have currents flowing out of phase in one or more of the conductors. For these modes the currents are mainly concentrated to the conductors and are thus known as "metallic modes". Since a dependence of the form $\exp(-j\omega t + jk_z^m z)$ has been assumed for all modes, the propagation constant k_z^m can be written as $k_z^m = \beta^m + j\alpha^m$ where β^m is the propagation phase velocity and α^m is the attenuation for mode m. In general, the ground mode will have the highest attenuation since the return current path is through the lossy earth. Note that the normalized propagation constant k_z/k_e will usually be presented in the results.

4.2 EFFECT OF THE G FUNCTION

To examine the effect of the G function on k_z^m when $k_g/k_e \gg 1$, the two wire case of Perel'man will be evaluated over a large frequency range. As discussed in chapter one, the G function represents the earth losses due to the transverse induced currents and in many previous solutions to the problem it has been neglected entirely. Thus, a

thorough study of its effect is warranted. For the parameters listed for case B in table 4.2 the propagation constant was calculated for $G=0$ and for $G=G_{MOD}$ as given by (4.2). The real and imaginary parts of k_z^m/k_e as a function of frequency were found for the two cases, and using (4.3) the percent effect of the function G was determined as shown in figure 4.1. For the presented frequency range $|k_g/k_e|$ varies from 134.1 to 4.24. The results shown reveal that in the higher frequency portion of the spectrum the G function can not be neglected. Also, note that the effect of the G function is more prominent for the ground mode.

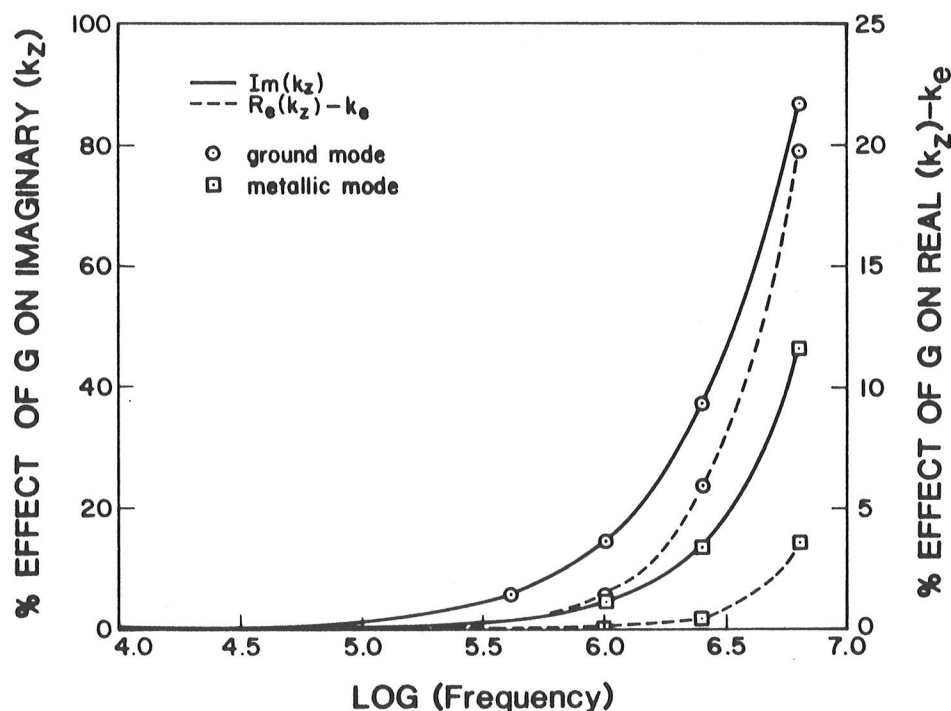


Figure 4.1: Percent effect of the G integral.

A comparison of calculated k_z^m values will now be made to the results of other workers for frequencies where $k_g/k_e \gg 1$ or relevant distances are not small compared to the free space wavelength. Olsen and Chang [11] present results for the case of a single wire above a lossy earth. In their evaluation, the J function is calculated using only the dominant term of its Struve function representation and the value of the G function is obtained by considering only its pole contribution. As discussed in chapter 3, they have assumed that the singularity in the G function integrand produces a significant enough contribution so as to create an added root which they have called a "fast wave" mode. Our interest in this section is for the excited currents on the structure that are due only to the transmission line modes and thus only they are compared here.

A comparison with Olsen and Chang's results for k_z in the complex k_z/k_e plane is shown in figure 4.2, where the height of the conductor above the earth is varied. Here the wire radius is 0.3m with ground constants of $\mu_g = \mu_o$, $\epsilon_g = 10\epsilon_o$, and $\sigma_g = 5.55 \times 10^{-2}$ ν/m . For a frequency of 10MHz, $|k_g/k_e| = 10.0$ and the free space wavelength is 30m. Discrepancies in the results are due to the evaluation of the G integral, where Olsen and Chang have assumed that the only significant contribution to the G integral is the residue term extracted from its singularity and thus have neglected the remaining terms due to the branch cuts.

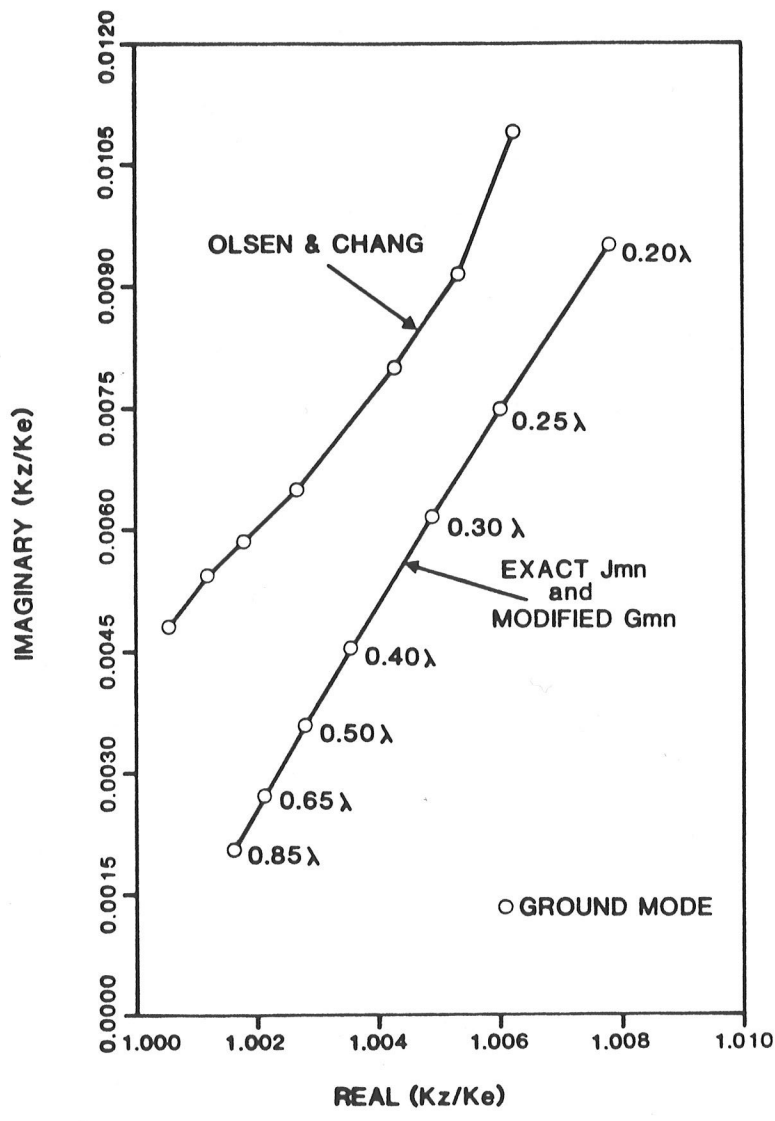


Figure 4.2: Propagation constant of a single wire at various heights.

Olsen and Chang [35] also present results for a two conductor transmission line structure. In this case the spacing between the conductors is varied while their heights remain constant and equal. In their formulation, the wire impedance has been neglected and a simplified modal equation form is used where only the dominant term is used to express the J function and only the pole contribution is considered in the G function evaluation. Again their results also include a fast wave mode contribution, but only the values for the transmission line modes are presented here. A comparison of results is shown in figure 4.3, where the wires, of radius 0.75cm and infinite conductivity, are both located at a height of 3.0m above the earth. For ground parameters of $\mu_g = \mu_o$, $\epsilon_g = 10\epsilon_o$, and $\sigma_g = 5.55 \times 10^{-2}$ ν/m and at a frequency of 10MHz, $|k_g/k_e| = 10.0$. Again discrepancies in the results are due the evaluation of the G integral.

A comparison with the results produced by a frequency dependent version of the EMTP is also shown in figure 4.3. In the EMTP evaluation, Carson's equations are used to calculate the transmission line characteristics. As explained in chapter 3, Carson's formulation assumes that at low frequencies and for high earth conductivities the "quasi-static" approximation can be made. Under these conditions, the J function is expressed as a finite series where ϵ_g is assumed zero and the G function is assumed negligible.

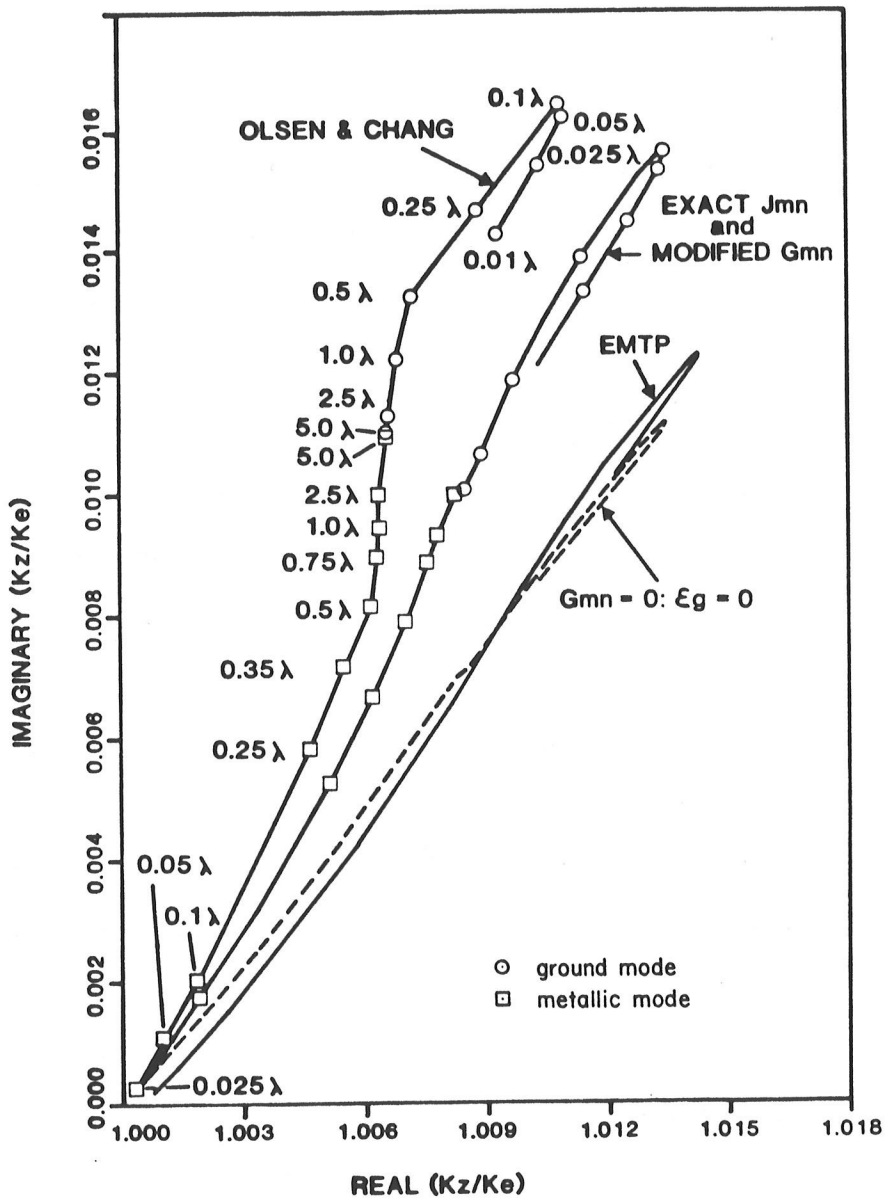


Figure 4.3: Propagation constant for two wires of varying separation.

This corresponds to neglecting effects due to the longitudinal displacement currents and the transverse induced currents in the earth.

Figure 4.3 shows the results produced by EMTTP alongside the values calculated by our method when the G function and ϵ_g were intentionally set to zero. The inaccuracy of the results when these assumptions are made is clear.

4.3 EXAMINATION OF THE TRANSFORMATION MATRIX

In this section the propagation constants k_z^m and the transformation matrix [P] will be examined over a wide frequency range (10Hz to 10MHz). A comparison with the results produced by the EMTTP, which uses Carson's equations to obtain a solution, will be made and the assumption by authors [36] that the transformation matrix can be assumed constant will be examined. Two cases will be considered.

For the balanced case of two identical conductors located at the same height above the earth, as presented by Perel'man (case B of table 4.3), all diagonal elements of the impedance matrix (2.18) will be equal and thus, the elements of the transformation matrix will be independent of frequency. To examine the effect of a deviation in the conductor position on this balanced structure, a two wire transmission line is considered where the wire locations are (0m,10m) and (10m,20m) in the (x,y) plane, respectively. The conductors remain identical with a radius 1cm and

conductivity $5.7 \times 10^7 \text{ } \nu/\text{m}$. The earth's electrical properties are $\mu_g = \mu_o$, $\epsilon_g = \epsilon_o$, and $\sigma_g = 1.0 \times 10^{-2} \text{ } \nu/\text{m}$. A comparison of the imaginary parts of the relative propagation constant k_z^m/k_e as determined using an exact J function evaluation and G_{MOD} of (4.2) with the EMTP results is given in figure 4.4. The values of the real and imaginary parts of transformation matrix elements P_{ij} over the frequency range are shown in figure 4.6. Note that since the column vectors forming the [P] matrix have been normalized in phase with respect to the first element using (3.17), the imaginary parts of P_{11} and P_{12} are zero. Figure 4.6 indicates that the effect of conductor position does not cause the elements of the transformation matrix to vary considerably.

The second case considered examines the effect of a deviation in the conductor properties on the balanced structure. The example presented by Perel'man (case C of table 4.3) is used where one conductor is copper with $\mu_1 = \mu_o$ and $\sigma_1 = 5.7 \times 10^7 \text{ } \nu/\text{m}$ and the other is steel with $\mu_2 = 100\mu_o$ and $\sigma_2 = 9.0 \times 10^6 \text{ } \nu/\text{m}$. Both conductors are at equal heights and the earth's electrical parameters are as in the previous case. A comparison of the imaginary parts of the relative propagation constant is given in figure 4.5. The values of the real and imaginary parts of the transformation matrix elements are given in figure 4.7. In contradiction to the results of the previously examined case, figure 4.7 indicates a strong dependence on frequency.

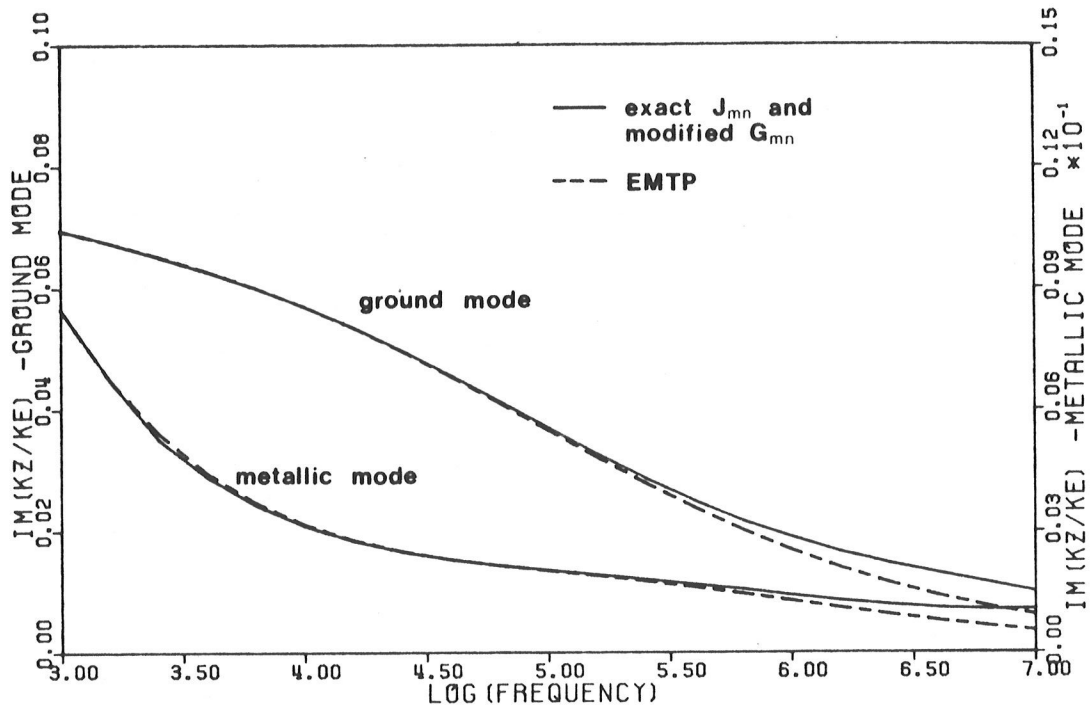


Figure 4.4: Frequency variation of k_z^m for the unbalanced case.

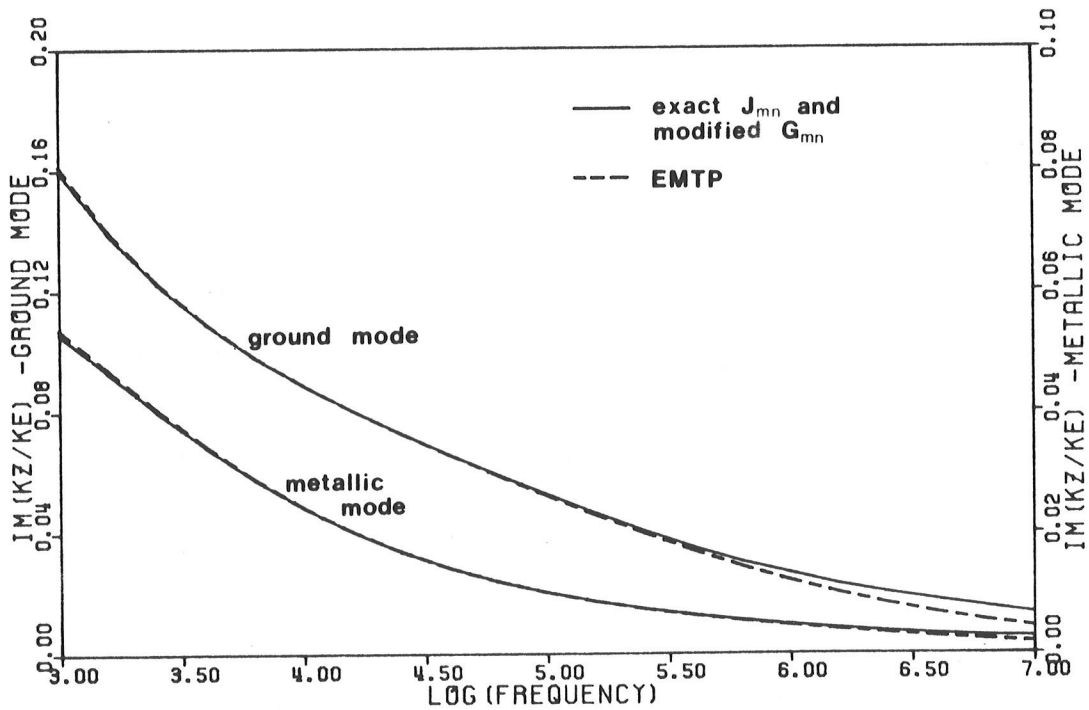


Figure 4.5: Frequency variation of k_z^m for case C of table 4.3.

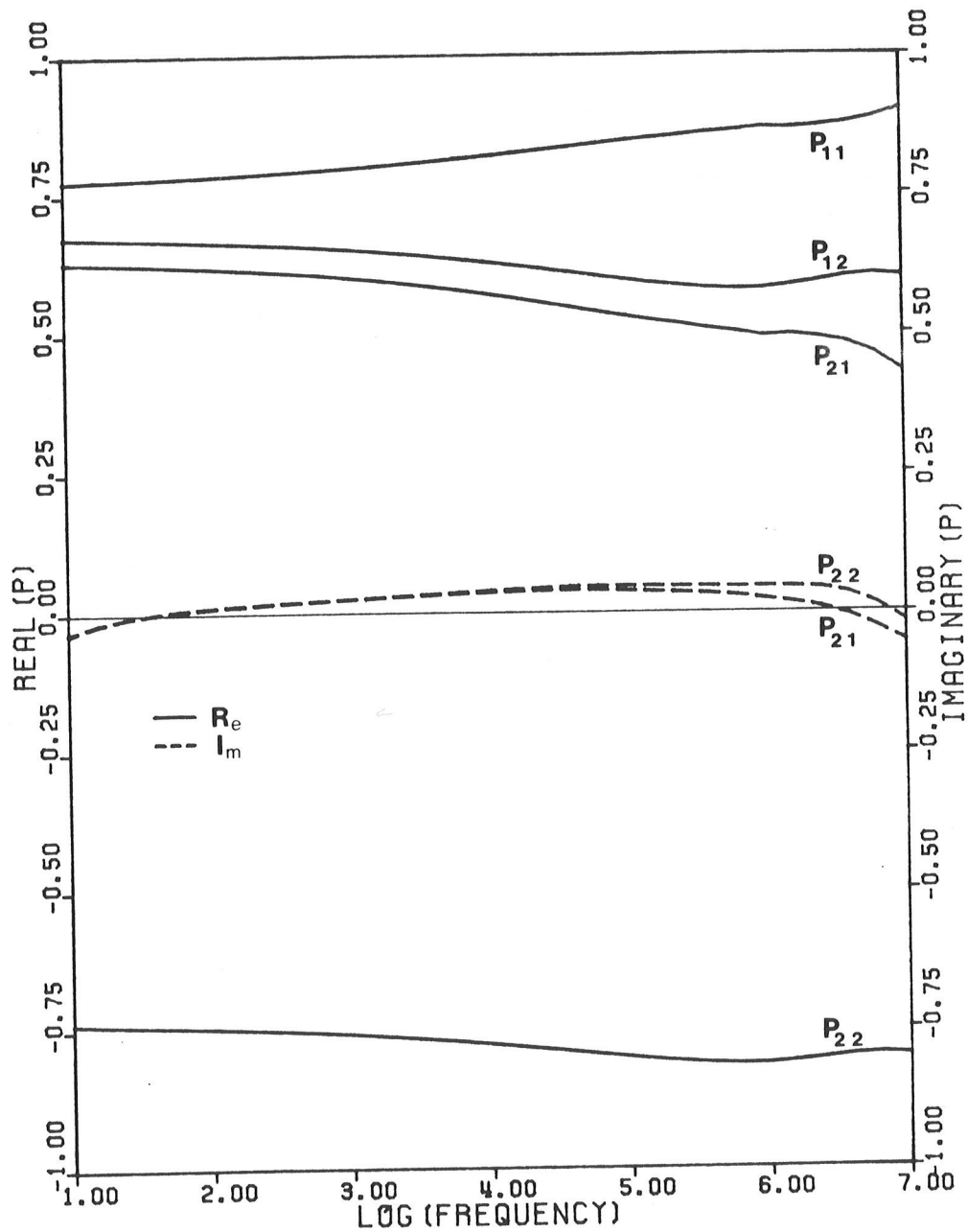


Figure 4.6: Frequency dependence of $[P]$ for the unbalanced case.

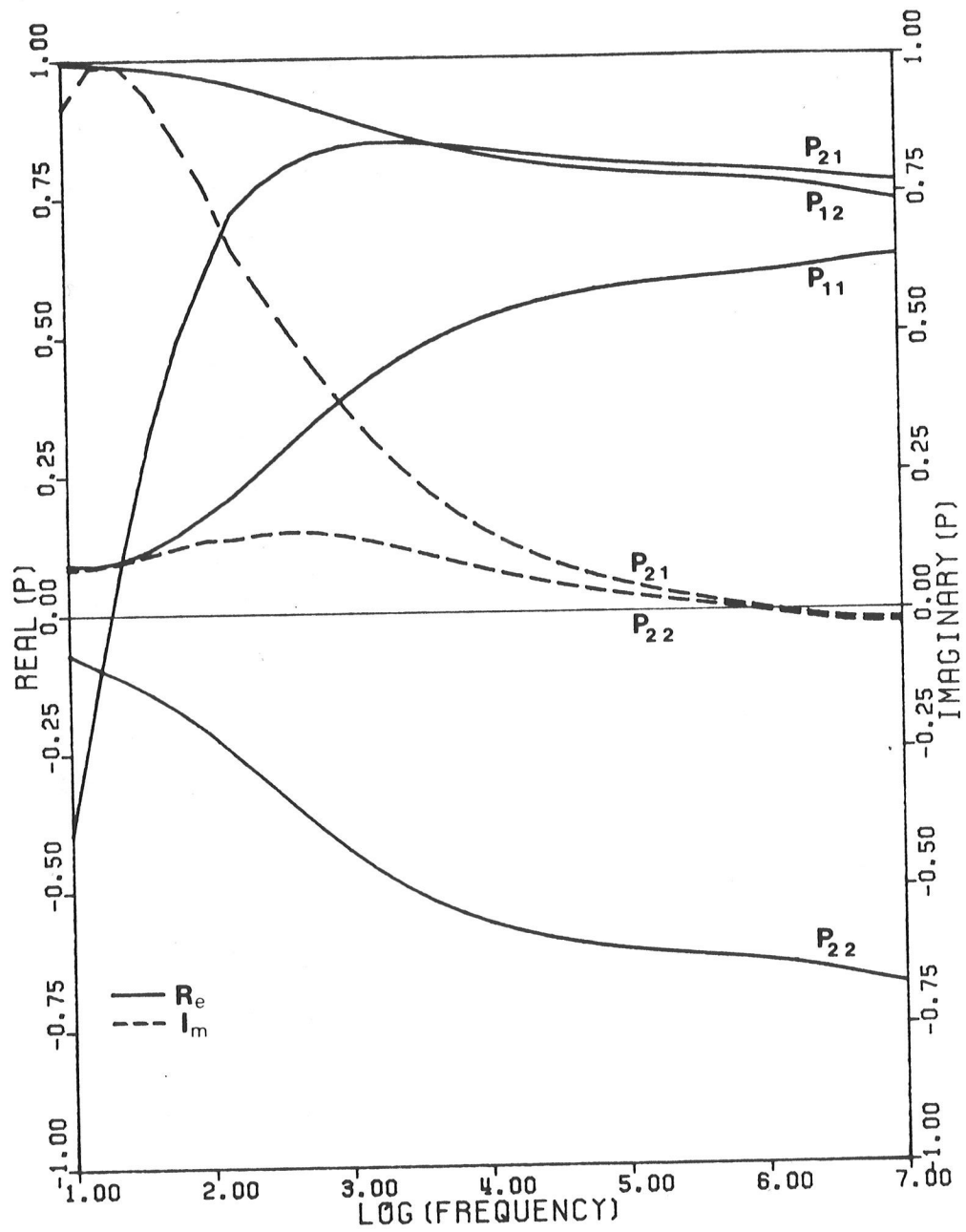


Figure 4.7: Frequency dependence of $[P]$ for case C of table 4.3.

Thus, it is not sufficient to assume that the elements of the [P] matrix can be taken as constant in the frequency domain for all cases. Also, the comparisons of k_z^m/k_e in figures 4.4 and 4.5 show that the error in Carson's formulation becomes significant for frequencies greater than 1MHz.

4.4 IMPULSE RESPONSE CHARACTERISTICS

In this section, the impulse response of a specified transmission line structure will be determined. Using the theory developed in chapter two, the system impulse response matrix [S(z,t)] was defined as the inverse Fourier transform of the system transfer function [S(z, ω)], which was formed through the transformation matrix [P] and the diagonal matrix [D] using (2.15) as

$$[S(z,t)] = \mathcal{F}^{-1}[S(z,\omega)] = \mathcal{F}^{-1}[P(\omega)][D(z,\omega)][P(\omega)]^{-1}. \quad (4.4)$$

The current at any point, z, along the transmission line can then be determined by

$$[I(z,t)] = [S(z,t)] * [I^S(0,t)] \quad (4.5)$$

or, in the frequency domain by

$$[I(z,t)] = \mathcal{F}^{-1}[S(z,\omega)] \mathcal{F}[I^S(0,t)]. \quad (4.6)$$

Thus, once the transmission line characteristics k_z^m and [P] have been calculated, as by the numerical technique

described in chapter three, the impulse response of the system can then be found through the inverse Fourier transform.

The inverse Fourier transform used to obtain the system impulse response was defined by (2.2) as

$$[f(t)] = \int_{-\infty}^{\infty} [f(\omega)] e^{-j\omega t} d\omega \quad (4.7)$$

Since an analytical solution to (4.7) is not available, $f(t)$ must be calculated numerically. This requires the infinite integral to be truncated to some finite limits $\pm\Omega$. Also, since $f(t)$ is a real function, $f(\omega) = f^*(-\omega)$, and (4.7) need only be integrated from 0 to $+\Omega$. Thus, the Fourier transform can be set up for numerical integration in the form

$$[f(t)] = 2 \operatorname{Re} \left\{ \sum_{n=0}^N [f(n\Delta\omega)] e^{-jn\Delta\omega t} \Delta\omega \right\} \quad (4.8)$$

where $\Delta\omega$ is the step width and $N = \Omega/\Delta\omega$ is the number of sample points in the frequency domain.

The case considered in this section is the unbalanced two wire transmission line structure presented by Perel'man (case C of table 4.3) which was examined in section 4.3 of the thesis. The transmission line is taken to be of infinite length in the positive z direction with sources that are matched to the structure. For the two conductor case, the system impulse response matrix (4.4) can be decomposed to take the form

$$[S(z,t)] = \mathcal{F}^{-1} [P] [D] [P]^{-1} \quad (4.9)$$

$$= \mathcal{F}^{-1} \begin{bmatrix} P_{11} P'_{11} d_1 + P_{12} P'_{21} d_2 & P_{11} P'_{12} d_1 + P_{12} P'_{22} d_2 \\ P_{21} P'_{11} d_1 + P_{22} P'_{21} d_2 & P_{21} P'_{12} d_1 + P_{22} P'_{22} d_2 \end{bmatrix}$$

where P_{ij} and P'_{ij} are the elements of the $[P]$ and $[P]^{-1}$ matrices, respectively, and d_i are the diagonal elements of the $[D]$ matrix. For a matched source $R_S^m = 0$ and using (2.10) we have

$$d_m = \frac{1}{2} e^{jk_z^m z} \quad (4.10)$$

The variation of the propagation constants k_z^m and the transformation matrix elements P_{ij} over the frequency spectrum for this case was shown previously in figures 4.5 and 4.7 of section 4.3.

The elements of the impulse response matrix (4.9) are defined by the current response to a delta function input. Thus, to obtain the value of the impulse response matrix element $S_{11}(z,t)$ an input source signal

$$[I^S(0,t)] = \begin{bmatrix} 2\pi\delta(t) \\ 0 \end{bmatrix} \quad (4.11)$$

is used where

$$\mathcal{F} [I^S(0,t)] = \begin{bmatrix} 1 \\ 0 \end{bmatrix} \quad (4.12)$$

Thus, the current impulse response determining the element $S_{11}(z,t)$ is given by

$$S_{11}(z,t) = I_1(z,t) = \mathcal{F}^{-1} \{P_{11} P'_{11} d_1 + P_{12} P'_{21} d_2\}. \quad (4.13)$$

Similarly, the remaining elements of the impulse response matrix are the inverse Fourier transforms of their corresponding system transfer function elements.

Also in this section, the effect on the impulse response matrix of assuming the transformation matrix $[P]$ to be constant over the frequency spectrum will be examined. The assumption that $[P]$, and implicitly $[P]^{-1}$, are constant allows (4.4) to be written in the form

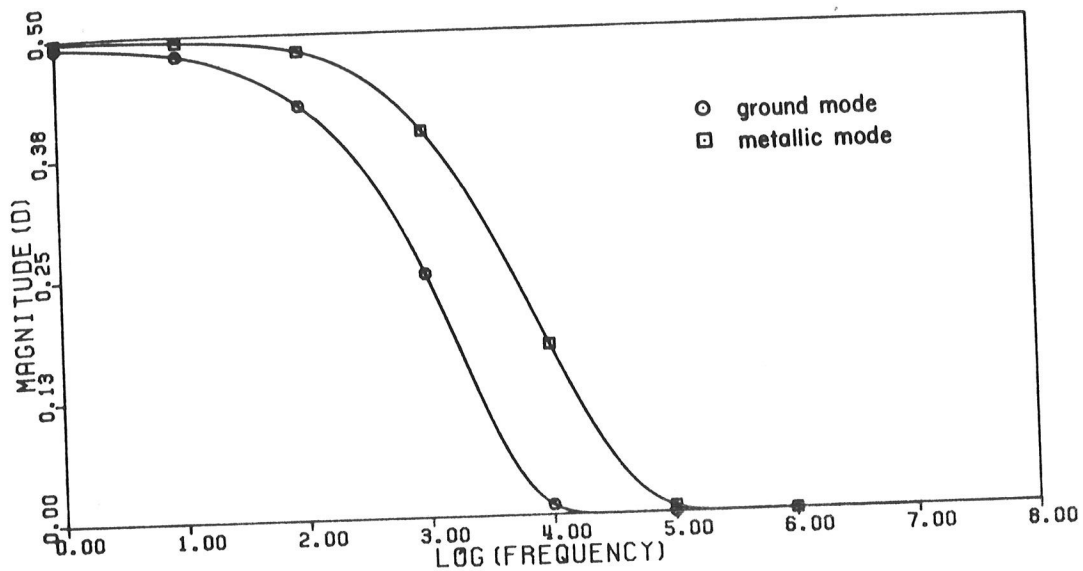
$$[S(z,t)] = [P] \{ \mathcal{F}^{-1} [D] \} [P]^{-1}. \quad (4.14)$$

This reduces the required number of inverse Fourier transforms that must be calculated to determine $[S(z,t)]$ from N^2 to N since $[D]$ is diagonal. Using this form, the impulse response matrix element $S_{11}(z,t)$ of (4.13) is now

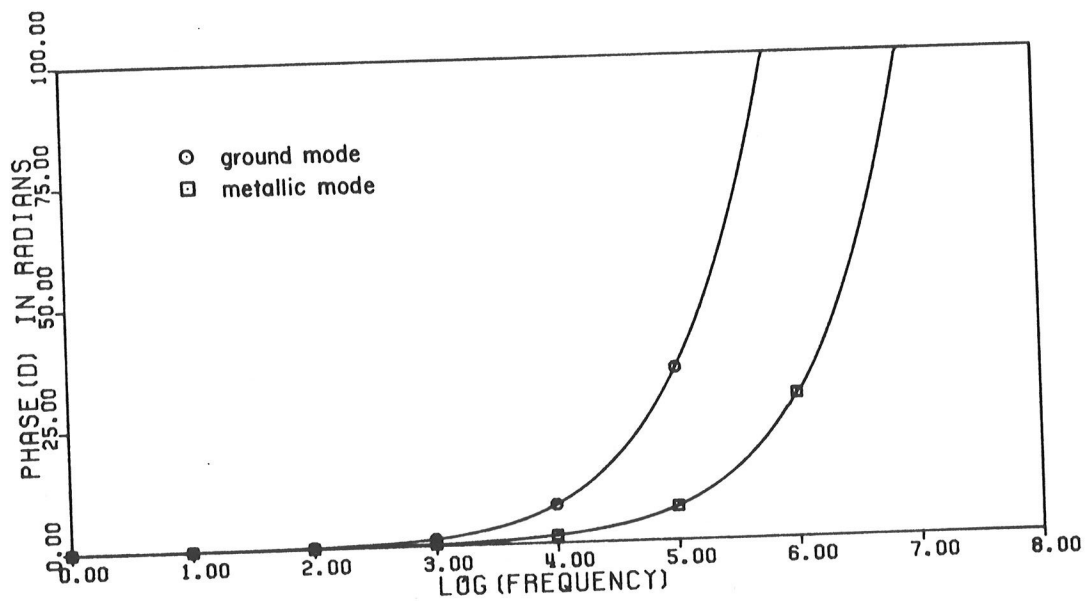
$$S_{11}(z,t) = P_{11} P'_{11} \mathcal{F}^{-1} \{d_1\} + P_{12} P'_{21} \mathcal{F}^{-1} \{d_2\} \quad (4.15)$$

where $\mathcal{F}^{-1} \{d_1\}$ and $\mathcal{F}^{-1} \{d_2\}$ are the impulse responses of the individual propagating modes on the system.

The calculated frequency domain response for the two modes d_1 and d_2 at a point $z = 200\text{km}$ along the transmission line structure as given by (4.10) is shown in figure 4.8. Figure 4.9 gives the frequency response for the system transfer matrix element $S_{11}(z,\omega)$ which incorporates the effect of both modes in the proper proportion, as determined by (4.13).

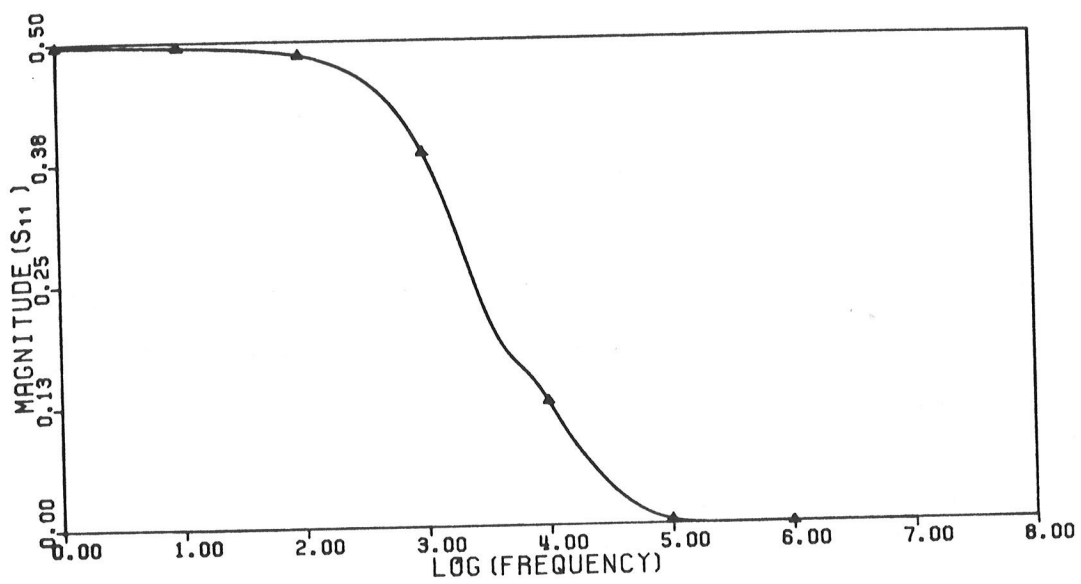


(a) Magnitude

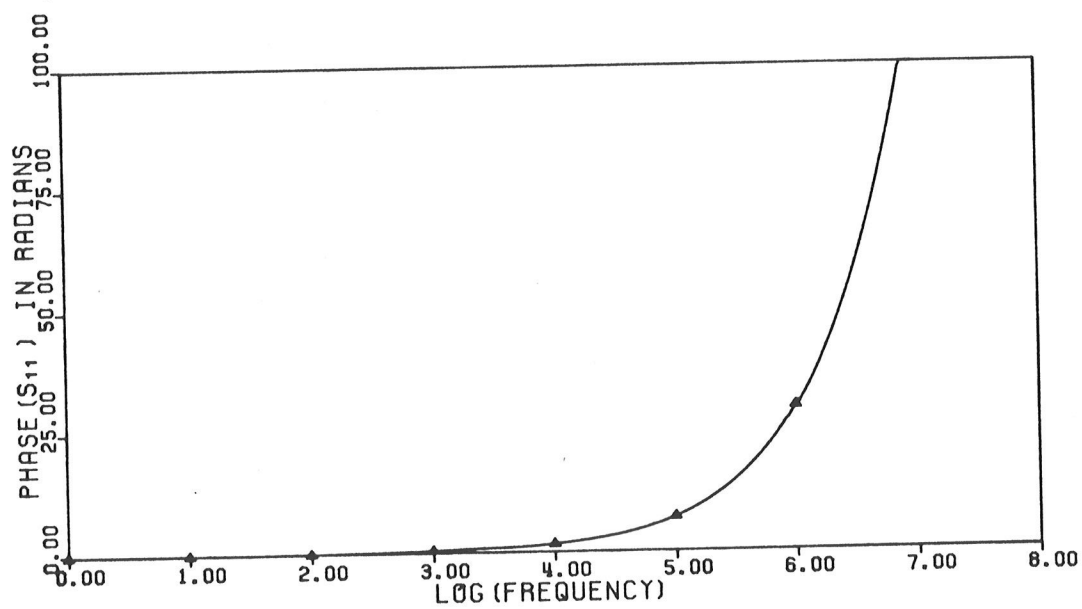


(b) Phase

Figure 4.8: Frequency response for the [D] matrix.



(a) Magnitude



(b) Phase

Figure 4.9: Frequency response for the element $S_{11}(z, \omega)$.

The corresponding time domain response of the two propagating modes $\mathcal{F}^{-1}\{d_1\}$ and $\mathcal{F}^{-1}\{d_2\}$ at the points $z = 200\text{km}$, 300km , 400km , and 500km along the transmission line is shown in figure 4.10. The attenuation and dispersion of the two modes, as they travel along the structure, is demonstrated as well as the relationship between the two modes; the ground mode being attenuated to a greater extent than the metallic mode as expected. Note that the time reference frame for the time domain response is set so that the input impulse is injected at $t=0$, $z=0$. Similarly, the time domain response of all the elements of the impulse response matrix $[S(z,t)]$, as given by (4.9), are shown in figure 4.11 also for points $z = 200\text{km}$, 300km , 400km , and 500km along the structure.

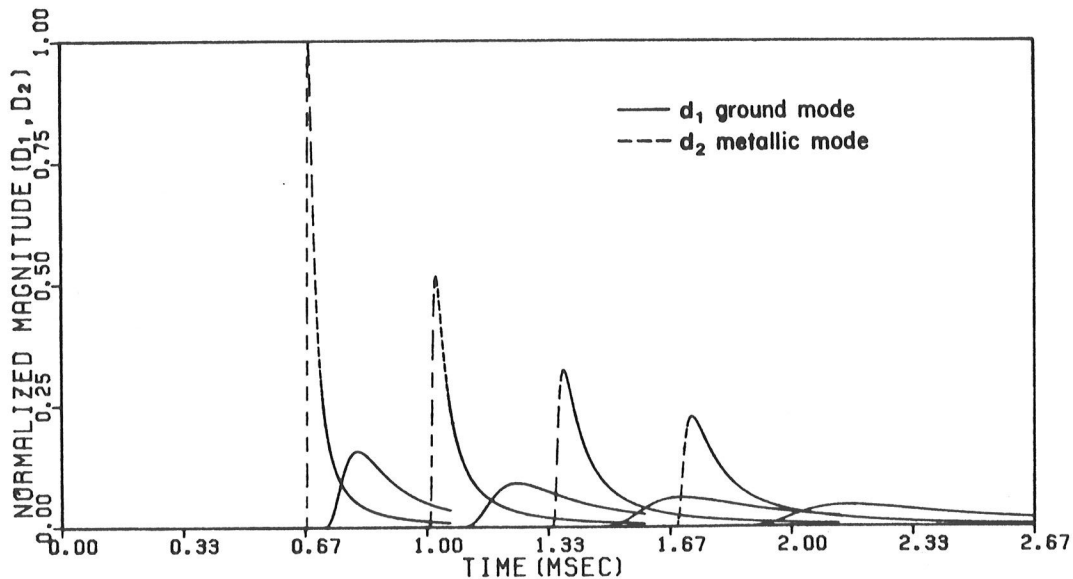


Figure 4.10: Impulse response for the $[D]$ matrix elements.

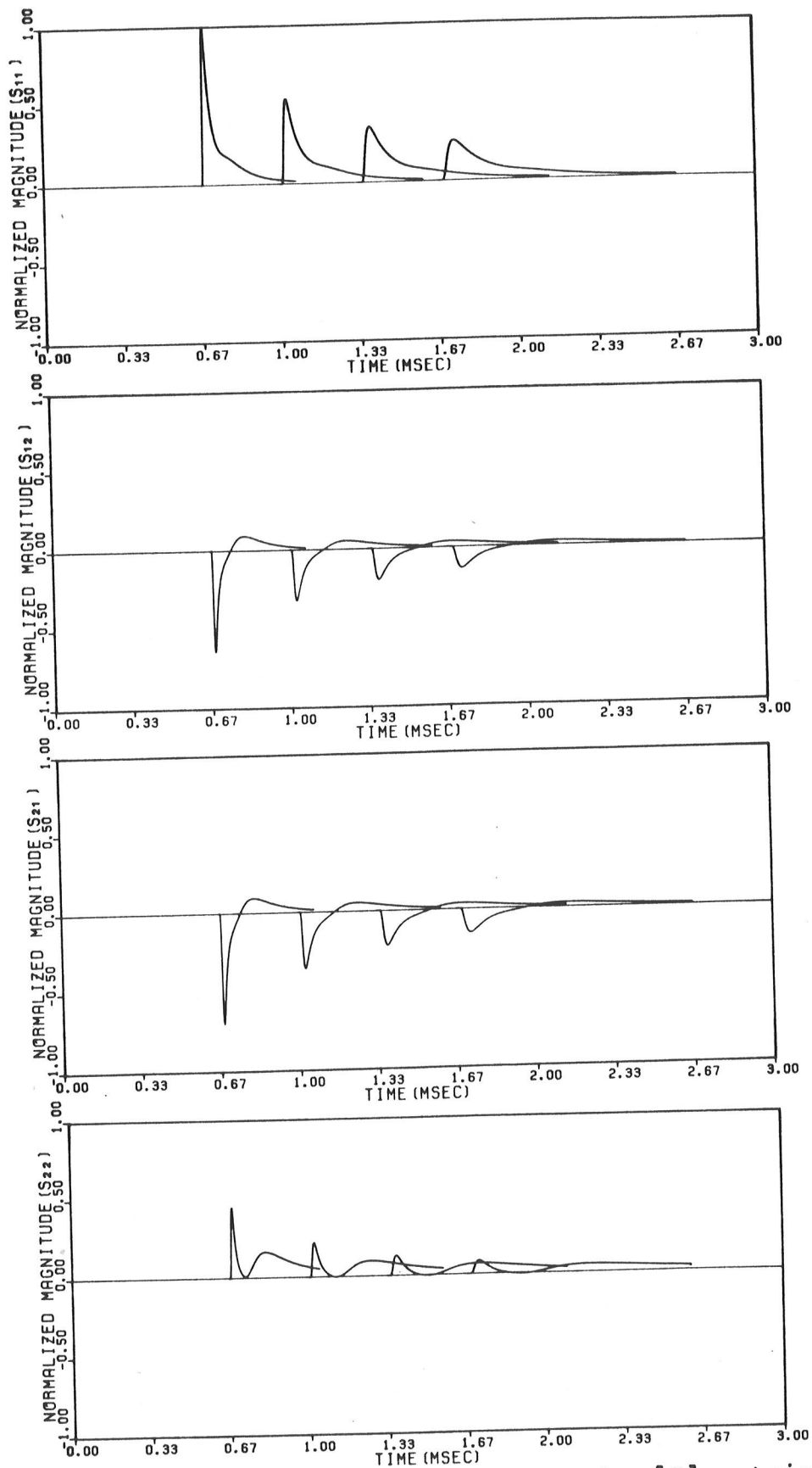


Figure 4.11: Impulse response for the $[S]$ matrix.

A comparison of the calculated impulse response $[S(z,t)]$ with that obtained when the transformation matrix $[P]$ is assumed constant is shown in figure 4.12. Here the element $S_{11}(z,t)$ as evaluated using (4.13) and as evaluated using (4.15) is compared for $[P]$ determined at frequencies of 1kHz and 100kHz. The comparison shows a significant difference in the calculated impulse response and thus the $[P]$ matrix can not be assumed constant in all cases.

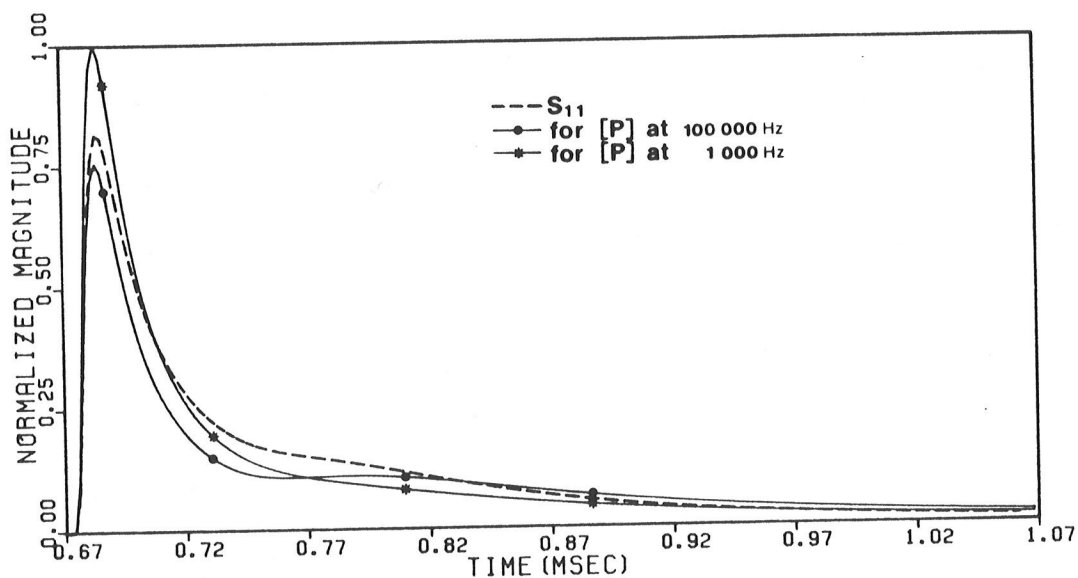


Figure 4.12: Frequency dependence of the $[P]$ matrix.

Chapter V
CONCLUSIONS

The propagation of a transient current along a multi-conductor structure above an earth has been examined. The problem was formulated in the frequency domain, where an exact solution for the fields in integral form is given. Difficulties involved in the accurate evaluation of the integral solution were discussed and a numerical technique was presented as a method of calculating the structure's characteristics. A comparison with the published results of other researchers was made to demonstrate the validity of the problem formulation.

A solution to the problem of determining the propagation of a transient current along a transmission line structure was formulated in terms of the modes which propagate on the structure. The transient current at any point, z , along the line was determined through the system impulse response as

$$[I(z,t)] = [S(z,t)] * [I^S(0,t)] \quad (5.1)$$

where

$$[S(z,t)] = \mathcal{F}^{-1} [P(\omega)] [D(z,\omega)] [P(\omega)]^{-1} \cdot \quad (5.2)$$

The formulation was derived for an infinite structure in the positive z direction and, thus, reflections from the terminating end of the transmission line were not incorporated. In the general case, the matrix $[D]$ will not be diagonal since the reflections due to each individual mode will excite all other modes at the terminating end.

The characteristics of the transmission line structure, the mode propagation constants k_z^m and the transformation matrix $[P]$, were extracted from the system of linear equations describing the structure as

$$[Z_{mn}^{\text{int}} - Z_{mn}^{\text{ext}}][I_n] = 0 \quad (5.3)$$

Elements of the impedance matrix $[Z]$ were formulated using the solution to the fields from a single wire above an earth. The field solution, which has received much attention in the literature, was derived by solving Maxwell's equations and satisfying all boundary conditions. It is an exact solution given in integral form.

Difficulty was shown to be in the exact solution of the two complex integrals $J(\bar{p}_{mn}^*)$ and $G(\bar{p}_{mn}^*)$ which are involved in the calculation of the elements of the impedance matrix. Previous solution techniques have evaluated the integrals under various restricting assumptions. A solution for the J integral was derived in terms of Struve functions following the work of other researchers. In the thesis an exact formulation is incorporated for the J integral. Next, the

accurate evaluation of the G integral was shown to pose an even greater problem since its integrand incorporates a singularity. An asymptotic expression for the G integral valid in its small argument range was derived. Also, the contribution of the singularity was calculated and was shown to be negligible except at extremely high frequencies.

The calculation of the elements of the impedance matrix (5.3), describing the transmission line structure, involves the evaluation of transcendental functions as well as the complex integrals J and G. The propagation constants k_z^m were calculated from the eigenvalues of the impedance matrix and the transformation matrix [P] was formed from the corresponding eigenvectors of the system. A numerical method of extracting the transmission line characteristics was developed.

A computer program has been written which yields k_z^m and [P] for a specified transmission line structure consisting of an arbitrary number of conductors. The solution technique utilizes the numerical method developed in the thesis and is restricted only to the extent that non-magnetic media must be used to represent the air and earth. The only major debateable assumption made in its evaluation is in the calculation of the G integral for which an asymptotic expression is incorporated.

Comparison with the results of other researchers [5,7] demonstrates the validity of the evaluation technique used

in the thesis to extract the transmission line characteristics. A study of the effect of the G integral indicated that its effect is proportional to frequency and becomes significant for high frequencies ($>10\%$ when $f > 1\text{MHz}$ for the case examined).

Further comparison with the work of other researchers [11,35] for the higher frequency range where the accurate evaluation of the G integral becomes important has shown appreciable discrepancies in the results. The evaluation method incorporated in the thesis used an asymptotic expression for the G integral whereas the other workers have considered only the singularity contribution in its evaluation. A comparison with the results produced by the EMTP, a commonly used program for power system applications, indicates that the error in the calculation of the propagation constants of the structure become appreciable at high frequencies ($>1\text{MHz}$). The EMTP uses Carson's formulation as its solution basis and was derived in the thesis from the exact formulation using the low frequency approximation. Also, a brief study of the frequency dependence of the transformation matrix [P] was made and for the two cases examined, situations exist where the [P] matrix varies drastically with frequency.

In the thesis, an exact solution for the electromagnetic fields in integral form for a transmission line structure has been given. Concentration was in the accurate solution

of this integral form for the lower portion of the frequency spectrum since limitations are encountered in the evaluation of the G integral at extremely high frequencies. Thus, further research must be done to extend the evaluation of the G integral to be accurate over the whole spectrum so that the extremely high frequency behavior of the structure can also be examined. The effect of the singularity must be studied and the possible existence of an added degenerate mode which propagates on the structure must be verified. If verified, then a method to incorporate it into the system transfer function must be developed. Finally, to make the formulation feasible for use in power system applications, the effect of a periodically grounded wire must be studied and an accurate fast Fourier transform must be developed.

REFERENCES

- [1] Carson, J. R., "Wave Propagation in Overhead Wires with Ground Return," Bell System Technical Journal, pp. 539-554, 1926.
- [2] Wait, J. R., "Theory of Wave Propagation Along a Thin Wire Parallel to an Interface," Radio Science, vol. 7, pp. 675-679, 1972.
- [3] Wise, W. H., "Propagation of High-Frequency Currents in Ground Return Curcuits," Proc. Institute of Radio Engineers, vol. 22, pp. 522-527, 1934.
- [4] Sunde, E., Earth Conduction Effects in Transmission Systems, Dover, New York, 1968.
- [5] Perel'man, L. S., "Details of the Theory of Wave Propagation Along Multi-Conductor Transmission Lines in Connection with some Engineering Problems," Izvestiya Nauchno-Issledovatel'skii Institut Postoyannogo toka, Leningrad, No. 10, pp. 103-120, 1963; translated by Kuester, E. F., Sci. Rep. No. 27, Electromagnetics Laboratory, Dept. of Elect. Eng., Univ. of Colorado, 1977.
- [6] Pistol'kors, A. A., "On the Theory of a Wire Parallel to the Plane Interface Between Two Media," Radiotekhnika, Moscow, vol. 8, pp. 8-18, 1953; translated by Kuester, E. F., Sci. Rep. No. 27, Electromagnetics Laboratory, Dept. of Elect. Eng., Univ. of Colorado, 1977.
- [7] Grinberg, G. A. and Bonshtedt, B. E., "Foundations of an Exact Theory of Transmission Line Fields," Zhurnal Tekhnicheskoi Fiziki, vol. 24, pp. 67-95, 1954; translated by Kuester, E. F., Sci. Rep. No. 27, Electromagnetics Laboratory, Dept. of Elect. Eng., Univ. of Colorado, 1977.
- [8] Wait, J. R., "On the Impedance of a Long Wire Suspended Over the Ground," Proc. Institute of Radio Engineers, vol. 49, p. 1576, 1961.
- [9] Bannister, P. R., "Electric and Magnetic Fields Near a Long Horizontal Line Source Above the Ground," Radio Science, vol. 3, pp. 203-204, 1968.

- [10] Kikuchi, H., "Wave Propagation Along an Infinite Wire Above Ground at High Frequencies," *Electrotech. Journal of Japan*, vol. 2, pp. 73-78, 1956.
- [11] Olsen, R. G. and Chang, D. C., "New Modal Representation of Electromagnetic Waves Supported by a Horizontal Wire Above a Dissipative Earth," *Electronics Letters*, pp. 92-94, 1974.
- [12] Chang, D. C. and Olsen, R. G., "Excitation of an Infinite Antenna Above a Dissipative Earth," *Radio Science*, vol. 10, pp. 823-831, 1975.
- [13] Carpentier, M. P. and dos Santos, A. F., "New Representation for the Current in a Horizontal Wire Above Ground," *Electronic Letters*, pp. 554-556, 1979.
- [14] Courbet, G. and Degauge, P., "Contribution of the Discrete Modes to the Current Propagating Along a Wire Parallel to a Moderate Conducting Earth," *Electronics Letters*, pp. 174-175, 1979.
- [15] Wait, J. R., "Reply to Professor R. W. P. King on His Comments on the Exponential Current Modes on an Infinitely Long Wire Over the Earth," *Proc. IEEE*, vol. 67, p. 1062, 1977.
- [16] Degauge, P., Courbet, G. and Heddebaut, M., "Propagation Along a Line Parallel to the Ground Surface: Comparison Between the Exact Solution and the Quasi-TEM Approximation," *IEEE Trans. Electromagnetic Compatibility*, vol. EMC-25, pp. 422-427, 1983.
- [17] Aboul-Atta, O., Shafai, L. and Tarnawecy, M. Z., "On the Theory of Infinite Line Above Ground," Technical Report TR81-7, Dept. of Electrical Engineering, University of Manitoba, 1981.
- [18] Bridges, G. and Aboul-Atta, O., "Accuracy of the Electromagnetic Transient in Overhead Transmission Lines," *Electronics Letters*, pp. 5-7, 1984.
- [19] Electrical Power Research Institute, Transmission Line Reference book 345Kv and Above, EPRI: Palo Alto, CA 94304, pp. 186-187, 1975.
- [20] Stratton, J. A., Electromagnetic Theory, McGraw-Hill, New York, 1941.
- [21] Abramowitz, M. and Stegun, I., Handbook of Mathematical Functions, National Bureau of Standards, 1964.

- [22] Sommerfeld, A., "Uber die Ausbreitung der Wellen in der drahtlosen Telegraphie," Ann. Phys., vol. 28, pp. 665-736, 1909.
- [23] Wedepohl, L. M. and Efthymiadis, A. E., "Wave Propagation in Transmission Lines Over Lossy Ground: A New Complete Field Solution," Proc. Institute of Electrical Engineers (London), vol. 125, pp. 505-517, 1978.
- [24] Aboul-Atta, O., "Investigation of Necessary and Sufficient Conditions for Uniqueness of a Class of Electromagnetic Problems," Ph.D. Thesis, University of Pennsylvania, 1965.
- [25] Westley, G. W. and Watts, J. A., The Computing Technology Center Numerical Analysis Library, Computing Technology Center, Union Carbide Corporation, Oak Ridge, Tennessee, pp. 135-143, 1970.
- [26] Gourlay, A. R. and Watson, G. A., Computational Methods for Matrix Eigenproblems, John Wiley and Sons, New York, Ch. 8, 1973.
- [27] Aaby, P. R., Introduction to Optimization Methods, Chapman and Hall, London, pp. 42-73, 1974.
- [28] Olsen, R. G., Kuester, E. F. and Chang, D. C., "Modal Theory of Long Horizontal Wire Structures Above the Earth, 2, Properties of Discrete Modes," Radio Science, vol. 13, pp. 615-623, 1978.
- [29] Morse, P. M. and Feshbach, H., Methods of Theoretical Physics, McGraw-Hill, New York, p. 462, 1953.
- [30] Kuester, E. F., Chang, D. C. and Olsen, R. G., "Modal Theory of Long Horizontal Wire Structures Above the Earth, 1, Excitation," Radio Science, vol. 13, pp. 605-613, 1978.
- [31] Sorbello, R. M. and King, R. W. P., "The Horizontal-Wire Antenna Over a Dissipative Half-Space: Generalized Formula and Measurements," IEEE Trans. Antennas and Propagation, vol. AP-25, pp. 850-854, 1977.
- [32] Olsen, R. G. and Pankaskie, T. A., "On the Exact, Carson and Image Theories for Wires at or Above The Earth's Interface," IEEE Trans. Power Apparatus and Systems, vol. PAS-102, pp. 769-778, 1983.

- [33] The University of British Columbia, "Overhead Line Parameters Program for the Frequency-Dependent Version of UBC's EMTP," Dept. of Electrical Engineering, University of British Columbia, 1982.
- [34] Marti, J. R., "Accurate Modelling of Frequency-Dependent Transmission Lines in Electromagnetic Transient Simulations," IEEE Trans. Power Apparatus and Systems, vol. PAS-101, pp. 147-157, 1982.
- [35] Olsen, R. G. and Chang, D. C., "Propagation of Modes on a Pair of Infinite Wires Above a Conducting Earth," Proc. IEEE Int'l. Symp., Antennas and Propagation Soc., University of Illinois, pp. 427-430, 1975.
- [36] Magnusson, P. C., "Travelling Waves on Multi-Conductor Open-Wire Lines- A Numerical Survey of the Effects of Frequency Dependence of Modal Composition," IEEE Trans. Power Apparatus and Systems, vol. PAS-92, pp. 999-1008, 1973.

Appendix A
POLYNOMIAL COEFFICIENT FORMULATION

In section 4.1.1 of the thesis, the determinant (4.8) is evaluated in terms of the polynomial form

$$a_N X^N + a_{N-1} X^{N-1} + \dots + a_1 X^1 + a_0 = 0 \quad (\text{A.1})$$

where the complex coefficients a_j were derived from the constant impedance matrices $A(X_m^{j-1})$ using (4.14) and $B(X_m^{j-1})$ using (4.15). Let the matrices A and B be defined by the elements a_{mn} and b_{mn} , respectively. Then, for the case $N=3$, the coefficients of (A.1) are given as:

$$\text{for } j = 0 : M_0 = 1 ,$$

$$a_0 = |A_1^0| = \begin{vmatrix} a_{11} & a_{12} & a_{13} \\ a_{21} & a_{22} & a_{23} \\ a_{31} & a_{32} & a_{33} \end{vmatrix}$$

$$\text{for } j = 1 : M_1 = 3 ,$$

$$\begin{aligned} a_1 &= |A_1^1| + |A_2^1| + |A_3^1| \\ &= \begin{vmatrix} b_{11} & a_{12} & a_{13} \\ b_{21} & a_{22} & a_{23} \\ b_{31} & a_{32} & a_{33} \end{vmatrix} + \begin{vmatrix} a_{11} & b_{12} & a_{13} \\ a_{21} & b_{22} & a_{23} \\ a_{31} & b_{32} & a_{33} \end{vmatrix} + \begin{vmatrix} a_{11} & a_{12} & b_{13} \\ a_{21} & a_{22} & b_{23} \\ a_{31} & a_{32} & b_{33} \end{vmatrix} \end{aligned}$$

$$\text{for } j = 2 : M_2 = 3 ,$$

$$\begin{aligned} a_2 &= |A_1^2| + |A_2^2| + |A_3^2| \\ &= \begin{vmatrix} b_{11} & b_{12} & a_{13} \\ b_{21} & b_{22} & a_{23} \\ b_{31} & b_{32} & a_{33} \end{vmatrix} + \begin{vmatrix} b_{11} & a_{12} & b_{13} \\ b_{21} & a_{22} & b_{23} \\ b_{31} & a_{32} & b_{33} \end{vmatrix} + \begin{vmatrix} a_{11} & b_{12} & b_{13} \\ a_{21} & b_{22} & b_{23} \\ a_{31} & b_{32} & b_{33} \end{vmatrix} \end{aligned}$$

for $j = 3$: $M_3 = 1$,

$$a_3 = |A_1^3| = \begin{vmatrix} b_{11} & b_{12} & b_{13} \\ b_{21} & b_{22} & b_{23} \\ b_{31} & b_{32} & b_{33} \end{vmatrix}$$

Appendix B

MULTI-CONDUCTOR CHARACTERISTIC EXTRACTION
COMPUTER PROGRAM


```

C      1.0D0    1.0D0    1.0D-2
C      2
C      1.0D0    0.0D0    57.0D6    1.0D-2    0.0D0    10.0D0
C      1.0D0    0.0D0    57.0D6    1.0D-2    10.0D0    10.0D0
C      END
C      //GO.FT11FOO1 DD DSN=GBRIDGE.TEST.DATA2,DISP=SHR
C      //GO.FT12FOO1 DD DSN=GBRIDGE.TEST.DATA3,DISP=SHR
C
C
C      PI=3.141592653589793D0
C      UO=4.0D0*PI*1.0D-7
C      EPSO=1.0D0/(UO*8.988004D16)
C      URO=1.0D0
C      CF1=(1.0D0,0.0D0)
C      CF2=(0.0D0,1.0D0)
C
C      SET UP FOR MULTIPLE EXECUTION
C
C      READ (5,*) NOUT,NPLOT
C      IF (NPLOT.GT.0) WRITE (11,2001) NPLOT
800 READ (5,3001) (ICASE (J),J=1,60)
C      IF (NPLOT.GT.0) WRITE (11,3001) (ICASE (J),J=1,60)
C      IF (ICASE (1) .EQ. IT1 .AND. ICASE (2) .EQ. IT2 .AND. ICASE (3) .EQ. IT3)
C      >GO TO 810
C      READ (5,*) NRUN,NVARST
C      READ (5,*) NOCT,NPTS,FREQST,DFREQ
C      NUMCAL=NOCT*NPTS
C      IF (NOCT.EQ.0) NUMCAL=NPTS
C      FDIV=(10.0D0)**(1.0D0/DFLOAT (NPTS))
C      FREQ=FREQST/FDIV
C      NVAR=0
C      IF (NOUT.LT.6) WRITE (6,3002) (ICASE (J),J=1,60)
C
C      SETUP VARIABLES FOR THE RUN
C
C      CALL INPUT (NDIM,NVAR,AMOUNT)
C      IF (NOUT.EQ.7) WRITE (12,4001) NDIM,NOCT,NPTS,FREQST,DFREQ
C      IF (NPLOT.GT.0) WRITE (11,2003) NUMCAL,NDIM,NOCT,NPTS,FREQST,DFREQ
C
C      DO 888 NSET=1,NUMCAL
C      FREQ=FREQ*FDIV
C      IF (NOCT.EQ.0) FREQ=FREQST+(NSET-1)*DFREQ
C      FREQRM (NSET) =FREQ
C      WRAD=FREQ*2.0D0*PI
C      CALL CKCAL (NDIM,WRAD)
C
C      FOR THE FIRST APPROX. CTE=0.0
C
C      CALL BEGIN (CTE,NDIM)
C
C      CALCULATE THE VALUE OF CKZ USING THE FIRST APPROX FOR CTE
C
C      EPS=1.0D-6
C      CALL FIND (NDIM,EPS)

```

```

C
C   CALCULATE THE RELETIVE PROP. CONST. MATRIX KZ/KE
C
DO 420 J=1,NDIM
NST=NITT(J)
DO 430 K=1,NST
CKZREL(K)=CDSQRT(CKZRM2(J,K))/CKE
430 CONTINUE
CKZRML(J,NSET)=CKZREL(NST)
IF(NOUT.LT.5) WRITE(6,1003) (J,CKZREL(K),K=1,NST)
420 CONTINUE

C
C   CALCULATE THE TRANSFORMATION MATRICES
C
IF(NOUT.EQ.7) WRITE(12,4000) (CKZRM2(J,NITT(J)),J=1,NDIM)

C
CALL EIGEN(CPT,CPIT,NDIM,RO)
IF(NOUT.EQ.7) WRITE(12,4002) ((CPT(N1,N2),N2=1,NDIM),N1=1,NDIM)
IF(NOUT.GT.5) GO TO 960
WRITE(6,1011) FREQ
DO 970 N1=1,NDIM
970 WRITE(6,1012) (CPT(N1,N2),N2=1,NDIM)
960 IF(NPLOT.EQ.3) WRITE(11,2004) ((CPT(N1,N2),N2=1,NDIM),N1=1,NDIM)

C
TLEG=100000.0DO
DO 910 J=1,NDIM
NST=NITT(J)
DO 910 K=1,NDIM
CDIAG(J,K)=(0.0DO,0.0DO)
IF(J.EQ.K) CDIAG(J,K)=CDEXP(CF2*TLEG*CDSQRT(CKZRM2(J,NST)))
910 CONTINUE
CALL MATM1(CDIAG,CPIT,NDIM,CFK1)
CALL MATM1(CPT,CFK1,NDIM,CSYST)
WRITE(6,*) ((CDIAG(N1,N2),N2=1,NDIM),N1=1,NDIM)
WRITE(6,*) ((CSYST(N1,N2),N2=1,NDIM),N1=1,NDIM)

C
C   THIS SECTION OUTPUTS INTERMEDIATE KZ/KE RESULTS IF REQUIRED
C
IF(NOUT.GT.3) GO TO 888
NUP=NDIM+1
C
WRITE(12,2001) INDEX,NUP
DO 300 K=1,INDEX
C
WRITE(12,2002) (CTERM(K,J),J=1,NUP)
300 WRITE(6,1001) (CTERM(K,J),J=1,NUP)
C
888 CONTINUE

C
C   OUTPUT RELETIVE VELOCITIES
C
IF(NOUT.GT.5) GO TO 510
WRITE(6,3002) (ICASE(J),J=1,60)
WRITE(6,1005) (SST(J),J=1,6)
WRITE(6,1006)
WRITE(6,1007) (J,(WST(J,K),K=1,6),J=1,NDIM)

```

```

510 CONTINUE
    IF (NOUT.LT.6) WRITE (6,1009)
    DO 530 J=1,NUMCAL
    IF (NPLLOT.EQ.1.OR.NPLOT.EQ.2) WRITE (11,2002) (CKZRML (K,J),K=1,NDIM)
    IF (NOUT.LT.6) WRITE (6,1008) FREQRM (J),CKZRML (1,J)
    IF (NDIM.EQ.1) GO TO 530
    IF (NOUT.LT.6) WRITE (6,1010) (K,CKZRML (K,J),K=2,NDIM)
530 CONTINUE
    IF (NOUT.LT.6.AND.NUMCAL.GT.1)
    >CALL GRAPH (CKZRML,FREQRM,1,NDIM,1,NUMCAL)
    GO TO 800
810 WRITE (6,1002)

```

C

C FORMAT CODES

C

```

1001 FORMAT ('0', ' ROOTS FOR CTE=',2E16.8,5 (/1X,2E16.8,4X,2E16.8))
1002 FORMAT ('1')
1003 FORMAT (' ',8X,'REL. PROP. CONST.',/3X,'MODE',12X,'CKZ/CKE',
    >10 (/3X,13,2F15.12))
1005 FORMAT ('0',10X,'AIR DATA',/9X,' UE EPSE ROE',
    >/6X,2F8.3,D11.4, //11X,'GROUND DATA',/9X,
    >' UG EPSG ROG',/6X,2F8.3,D11.4)
1006 FORMAT ('0',10X,'WIRE DATA',/6X,' NO. UN EPSN RON',
    >7X,'RADIUS X-POSITION Y-POSITION')
1007 FORMAT (' ',5X,13,2X,2F8.3,4D11.4)
1008 FORMAT (2X,D11.5,' ',1',2F16.12)
1009 FORMAT (/9X,'FINAL PROP. CONST.',
    >/3X,'FREQUENCY MODE',12X,'CKZ/CKE')
1010 FORMAT (' ',12X,14,2F16.12)
1011 FORMAT (' ',/3X,'[P] MATRIX FOR FREQUENCY=',F12.2)
1012 FORMAT (' ',3X,5 (2X,2F9.5))
2001 FORMAT (3I5)
2002 FORMAT (2F12.8)
2003 FORMAT (4I5,2E14.7)
2004 FORMAT (4E14.7)
3001 FORMAT (60A1)
3002 FORMAT ('1',60A1)
4000 FORMAT (4D17.10)
4001 FORMAT (3I6,2E12.6)
4002 FORMAT (4D17.10)
    STOP
    END

```

C

C

C THIS SUBROUTINE READS THE INPUT DATA AND CALCULATES THE
C NECESSARY GEOMETRICAL CONSTANTS TO BEGIN EXECUTION.
C IF INCR=0 THEN DATA IS INITIALLY READ FROM INPUT CARDS.
C IF INCR>0 THEN ONE VARIABLE IN WST OR SST IS GIVEN THE
C VALUE AS SPECIFIED BY AMOUNT.
C INCR= OX -MEDIUM CHANGE FOR SST (X)
C INCR= NX -CONDUCTOR CHANGE FOR CONDUCTOR N WST (N,X)
C X DESCRIPTIONS ARE AS BELOW.

C

SUBROUTINE INPUT (N, INCR, AMOUNT)

```

      IMPLICIT COMPLEX*16 (C) , REAL*8 (A,B,D-H,O-Z)
      COMMON /INP1/RO,ROR,THETA
      COMMON /INP3/WST,SST
      COMMON /PASS2/NOUT
      DIMENSION RO (10,10),ROR (10,10),THETA (10,10)
      DIMENSION WST (10,6),SST (6)

C
      PI=3.141592653589793D0
      CF1=(1.0D0,0.0D0)
      CF2=(0.0D0,1.0D0)

C
      IF (INCR.NE.0) GO TO 110

C
C
      READ INPUT DATA FROM CARDS
C
      READ (5,*) SST (1),SST (2),SST (3)
      READ (5,*) SST (4),SST (5),SST (6)
      READ (5,*) N
      DO 50 J=1,N
50  READ (5,*) (WST (J,K),K=1,6)
      GO TO 100

C
C
      CHANGE A GEOMETRY OR MEDIUM VALUE
C
      110 NSUB1=INCR-INCR/10*10
         NSUB2=INCR/10
         IF (NSUB2.GT.0) GO TO 120
         SST (NSUB1)=AMOUNT
         GO TO 100
      120 WST (NSUB2,NSUB1)=AMOUNT

C
C
      INITIALIZE GEOMETRY
C
      100 DO 10 I=1,N
         RO (I,1)=WST (I,4)
         ROR (I,1)=2.0D0*WST (I,6)
         THETA (I,1)=90.0D0
         IF (I.EQ.N) GO TO 10
         NST=I+1
         DO 20 J=NST,N
            F1=DABS (WST (I,5)-WST (J,5))
            F2=F1*F1
            F3=DABS ((WST (I,6)-WST (J,6))*(WST (I,6)-WST (J,6)))
            F4=DABS ((WST (I,6)+WST (J,6))*(WST (I,6)+WST (J,6)))
            RO (I,J)=DSQRT (F2+F3)
            RO (J,I)=RO (I,J)
            ROR (I,J)=DSQRT (F2+F4)
            ROR (J,I)=ROR (I,J)
            THETA (I,J)=DABS (DARCOS (F1/ROR (I,J))*180.0D0/PI)
            THETA (J,I)=THETA (I,J)
20  CONTINUE
10  CONTINUE

C
      IF (NOUT.GT.3.AND.INCR.NE.0.OR.NOUT.GT.4) GO TO 999

```

```

WRITE (6,1000) N, INCR
1000 FORMAT ('-',5X, 'INPUT DATA   N=',13, '   VARIABLE=',14,
>/6X, 'ARRAYS RO , ROR , THETA ',/1X)
DO 500 J=1,N
500 WRITE (6,1001) (RO (J,K) ,K=1,N)
DO 501 J=1,N
501 WRITE (6,1001) (ROR (J,K) ,K=1,N)
DO 502 J=1,N
502 WRITE (6,1001) (THETA (J,K) ,K=1,N)
1001 FORMAT (' ',10E12.5)
999 RETURN
END

```

C
C
C
C
C

THIS SUBROUTINE PRODUCES A GRAPH OF THE CKZ/CKE DATA THAT IS
A FUNCTION OF FREQUENCY.

```

SUBROUTINE GRAPH (CKZ, FREQ, NFIR, NLAS, NSTR, NFIN)
COMPLEX*16 CKZ (10,100)
REAL*8 FREQ (100) , X (10,100) , TMAX, DAIMAG
INTEGER NREM (10)
INTEGER*4 FORM (10) /'1', '2', '3', '4', '5', '6', '7', '8', '9', '0'/
INTEGER*4 DT1 /'>', DT2 /'<', DT3 /' ', DT4 /'0'/
INTEGER*4 NLINE (101)
DATA NLINE /'0', 100* ' '/
REAL*8 DIV (10)
REAL*8 OFCHAN (10)

```

C

```

DO 100 J=1, NLAS
OFCHAN (J) =0.0DO
TMAX=0.0DO
DO 110 K=1, NFIN
X (J,K) =DAIMAG (CKZ (J,K))
110 IF (X (J,K) .GT. TMAX) TMAX=X (J,K)
100 DIV (J) =TMAX/100.0DO
WRITE (6,1000)
1000 FORMAT ('1',1X, 'FREQUENCY LOG10 (F) ', '0', 100 ('+'))

```

C

```

DO 10 K=NSTR, NFIN
DO 30 L=NFIR, NLAS
NSET=X (L,K) /DIV (L) +OFCHAN (L) +1.5
IF (NSET.LE.101) GO TO 20
NREM (L) =101
NLINE (101) =DT1
GO TO 30
20 IF (NSET.GE.1) GO TO 40
NREM (L) =1
NLINE (1) =DT2
GO TO 30
40 NLINE (NSET) =FORM (L)
NREM (L) =NSET
30 CONTINUE
F=DLOG10 (FREQ (K))
WRITE (6,2000) FREQ (K) , F, (NLINE (I) , I=1, 101)

```

```

2000 FORMAT (' ',D11.5,F9.4,1X,101A1)
DO 50 L=NFIR,NLAS
50 NLINE (NREM(L))=DT3
NLINE (1)=DT4
10 CONTINUE
RETURN
END

```

C
C
C
C
C

THIS SUBROUTINE CALCULATES THE NESSECARY VALUES OF CKE, CKG
AND CK FOR A SPECIFIC FREQUENCY AND MEDIUM DATA.

```

SUBROUTINE CKCAL (N,WRAD)
IMPLICIT COMPLEX*16 (C) , REAL*8 (A,B,D-H,O-Z)
COMMON /INP2/CKE2,CKG2,CK2,CKE,CKG,CK,URE,UR
COMMON /INP3/WST,SST
COMMON /PASS2/NOUT
DIMENSION CK2 (10) ,CK (10) ,UR (10)
DIMENSION WST (10,6) ,SST (6)

```

C

```

PI=3.141592653589793D0
UO=4.0D0*PI*1.0D-7
EPSO=1.0D0/(UO*8.988004D16)
CF1=(1.0D0,0.0D0)
CF2=(0.0D0,1.0D0)

```

C

```

URE=SST (1)
CZ1=CF1*WRAD*WRAD*EPSO*UO
CZ2=CF2*WRAD*UO
CKE2=CZ1*SST (1) *SST (2) +CZ2*SST (1) *SST (3)
CKG2=CZ1*SST (4) *SST (5) +CZ2*SST (4) *SST (6)
CKE=CDSQRT (CKE2)
CKG=CDSQRT (CKG2)
DO 30 I=1,N
UR (I) =WST (I, 1)
CK2 (I) =CZ1*WST (I, 1) *WST (I, 2) +CZ2*WST (I, 1) *WST (I, 3)
CK (I) =CDSQRT (CK2 (I))

```

```

30 CONTINUE

```

C

```

IF (NOUT.GT.3) GO TO 999
WRITE (6,1000) N,WRAD
1000 FORMAT ('-',5X,'CK DATA N=',13,' WRAD=',E12.5,
>/6X,'ARRAYS CKE , CKG , CK',/1X)
WRITE (6,1002) CKE
WRITE (6,1002) CKG
WRITE (6,1002) (CK (J) ,J=1,N)
1002 FORMAT (' ',5 (2X,2E12.5))
999 RETURN
END

```

C
C
C
C
C

THIS SUBROUTINE DETERMINES THE STRATEGY FOR FINDING THE ROOTS
OF THE SYSTEM TO AN ACCURACY OF EPS.

```

SUBROUTINE FIND (NDIM, EPS)
IMPLICIT COMPLEX*16 (C) , REAL*8 (A, B, D-H, O-Z)
REAL*8 CDABS
COMMON /INP2/CKE2, CKG2, CK2, CKE, CKG, CK, URE, UR
COMMON /PASS1/CTERM, CKZRM2, NITT, INDEX
COMMON /PASS2/NOUT
COMMON /PASS3/CZIMP, CSPHI
DIMENSION UR (10), CK2 (10), CK (10), CT (10)
DIMENSION CA (10, 10), CB (10, 10), CPF (11), CROOT (10)
DIMENSION CTERM (200, 11), CKZRM2 (10, 20), NITT (10)
DIMENSION CZIMP (10, 10, 10), CSPHI (10)
DIMENSION RATIO (10)

```

C

```

IF (NDIM.GT.1) GO TO 100
CTE=CTERM (1, 2)
CALL ITERAT (CTE, 1, NDIM, EPS)
IF (NOUT.LT.3) WRITE (6, 1000)
RETURN

```

C

```

100 TEST=1.2D0
DO 110 J=2, NDIM
110 RATIO (J-1)=DREAL (CTERM (1, J)) /DREAL (CTERM (1, J+1))
KROOT=1
200 NSET=1
IF (KROOT.EQ.NDIM) GO TO 90
IF (RATIO (KROOT) .GT.TEST) GO TO 90

```

C

```

NSTR=KROOT
NFAK=NDIM-1
DO 20 NSTP=KROOT, NFAK
20 IF (RATIO (NSTP) .GT.TEST) GO TO 30
30 IF (NSTP.EQ.NFAK) NSTP=NDIM
CAVE= (0.0D0, 0.0D0)
DO 40 K=NSTR, NSTP
40 CAVE=CAVE+CTERM (1, K+1)
CTE=CAVE / (NSTP-NSTR+1)
CKZ2=CTE*CTE+CKE2
CTG=CDSQRT (CKZ2-CKG2)
DO 50 K=1, NDIM
50 CT (K)=CDSQRT (CKZ2-CK2 (K))
CALL MATCAL (CA, CB, NDIM, CTE, CTG, CT)
CALL POLY (CA, CB, NDIM, CPF)
CALL ROOTS (CPF, NDIM, CROOT)
CALL SORT (CROOT, NDIM, 10)
INDEX=INDEX+1
CTERM (INDEX, 1)=CTE
DO 60 K=1, NDIM
CTE2=CKE2*CROOT (K)
60 CTERM (INDEX, K+1)=CDSQRT (CTE2)
NSET=INDEX
DO 70 J=NSTR, NSTP
CTE=CTERM (NSET, J+1)
NITT (J)=NITT (J)+1
CKZRM2 (J, NITT (J))=CTE*CTE+CKE2

```

```

VAL=CDABS (CTE-CTERM (NSET, 1))
IF (VAL.LT.EPS) GO TO 120
CALL ITERAT (CTE, J, NDIM, EPS)
GO TO 70
120 CSPHI (J) =CROOT (J)
DO 130 K1=1, NDIM
DO 130 K2=1, NDIM
130 CZIMP (J, K1, K2) =CSPHI (J) *CA (K1, K2) +CB (K1, K2)
70 CONTINUE
KROOT=NSTP
GO TO 80
C
90 CTE=CTERM (NSET, KROOT+1)
CALL ITERAT (CTE, KROOT, NDIM, EPS)
80 KROOT=KROOT+1
IF (KROOT.LE.NDIM) GO TO 200
IF (NOUT.LT.3) WRITE (6, 1000)
1000 FORMAT (' ', 5X, 'ROUTINE FIND EXECUTED')
RETURN
END
C
C
C THIS SUBROUTINE INITIALIZES THE STORAGE ARRAYS CTERM AND
C CKZRM2 WHICH STORE THE CALCULATED VALUES OF CTE AND CKZ.
C THIS SUBROUTINE MUST BE USED FIRST SINCE IT ASSUMES A
C VALUE OF CTE= (0.0,0.0) . RESULTING VALUES OF CTE ROOTS
C ARE THEN CALCULATED AND STORED IN CTERM(CTE,1,2,3,...,NDIM) .
C
SUBROUTINE BEGIN (CTE, NDIM)
IMPLICIT COMPLEX*16 (C) , REAL*8 (A, B, D-H, O-Z)
COMMON /INP2/CKE2, CKG2, CK2, CKE, CKG, CK, URE, UR
COMMON /PASS1/CTERM, CKZRM2, NITT, INDEX
COMMON /PASS2/NOUT
COMMON /PASS3/CZIMP, CSPHI
DIMENSION UR (10), CK2 (10), CK (10), CT (10)
DIMENSION CA (10, 10), CB (10, 10), CPF (11), CROOT (10)
DIMENSION CTERM (200, 11), CKZRM2 (10, 20), NITT (10)
DIMENSION CZIMP (10, 10, 10), CSPHI (10)
C
CTE= (0.0D0, 0.0D0)
DO 10 J=1, NDIM
NITT (J) =2
10 CKZRM2 (J, 1) =CKE2
INDEX=1
CTERM (INDEX, 1) =CTE
C
CALL MATCAL (CA, CB, -NDIM, CTE, CTG, CT)
CALL POLY (CA, CB, NDIM, CPF)
CALL ROOTS (CPF, NDIM, CROOT)
CALL SORT (CROOT, NDIM, 10)
DO 30 J=1, NDIM
CSPHI (J) =CROOT (J)
DO 40 K1=1, NDIM
DO 40 K2=1, NDIM

```

```

40 CZIMP (J,K1,K2)=CSPHI (J)*CA (K1,K2)+CB (K1,K2)
30 CONTINUE

```

```

C
DO 20 J=1,NDIM
CTE2=CKE2*CROOT (J)
CKZ2=CTE2+CKE2
CTERM (INDEX,J+1)=CDSQRT (CTE2)
20 CKZRM2 (J,2)=CKZ2
IF (NOUT.LT.3) WRITE (6,1000)
1000 FORMAT (' ',5X,'ROUTINE BEGIN EXECUTED FOR CTE=(0.0,0.0) ')
RETURN
END

```

```

C
C
C THIS SUBROUTINE CALCULATES THE EXACT VALUE OF CTE FOR THE
C ROOT = KROOT. THE INPUT STARTING POINT IS GIVEN BY CTE
C EPS = MAXIMUM ERROR BETWEEN ITERATIONS FOR CTE OR
C NMAX = MAXIMUM ALLOWABLE ITERATIONS BEFORE EXITING NMAX<9.
C ALL VALUES OF CTE AND THE RESULTING ROOTS ARE STORED IN
C ARRAYS CTERM , CKZRM2 , NITT.
C

```

```

SUBROUTINE ITERAT (CTE,KROOT,NDIM,EPS)
IMPLICIT COMPLEX*16 (C) , REAL*8 (A,B,D-H,O-Z)
REAL*8 CDABS
COMMON /INP2/CKE2,CKG2,CK2,CKE,CKG,CK,URE,UR
COMMON /PASS1/CTERM,CKZRM2,NITT,INDEX
COMMON /PASS2/NOUT
COMMON /PASS3/CZIMP,CSPHI
DIMENSION UR (10) ,CK2 (10) ,CK (10) ,CT (10)
DIMENSION CA (10,10) ,CB (10,10) ,CPF (11) ,CROOT (10)
DIMENSION CTERM (200,11) ,CKZRM2 (10,20) ,NITT (10)
DIMENSION CZIMP (10,10,10) ,CSPHI (10)

```

```

C
NMAX=8
CKZ2=CTE*CTE+CKE2
DO 10 J=1,NMAX
CTG=CDSQRT (CKZ2-CKG2)
DO 20 K=1,NDIM
20 CT (K)=CDSQRT (CKZ2-CK2 (K))

```

```

C
CALL MATCAL (CA,CB,NDIM,CTE,CTG,CT)
CALL POLY (CA,CB,NDIM,CPF)
CALL ROOTS (CPF,NDIM,CROOT)
CALL SORT (CROOT,NDIM,10)

```

```

C
INDEX=INDEX+1
CTERM (INDEX,1)=CTE
DO 30 K=1,NDIM
CTE2=CKE2*CROOT (K)
IF (K.EQ.KROOT) CKZ2=CTE2+CKE2
30 CTERM (INDEX,K+1)=CDSQRT (CTE2)
CTE=CTERM (INDEX,KROOT+1)
NITT (KROOT)=NITT (KROOT)+1
CKZRM2 (KROOT,NITT (KROOT))=CKZ2

```

```

    VAL=CDABS (CTE-CTERM (INDEX,1))
    IF (VAL.LT.EPS) GO TO 100
  10 CONTINUE
    IF (NOUT.LT.6) WRITE (6,1000) NMAX,KROOT
  1000 FORMAT (' ', '**WARNING** NO. OF ITERATIONS >',13,
    >' FOR ROOT',13, ' ERROR>EPS')
    100 IF (NOUT.LT.3) WRITE (6,1001) KROOT,J
  1001 FORMAT (' ',5X,'ROUTINE ITERAT EXECUTED FOR ROOT=',13,
    >/6X,'NO.OF ITERATIONS REQUIRED IS',13)

```

```

C
  CSPHI (KROOT)=CROOT (KROOT)
  DO 40 K1=1,NDIM
  DO 40 K2=1,NDIM
  40 CZIMP (KROOT,K1,K2)=CSPHI (KROOT)*CA (K1,K2)+CB (K1,K2)
  RETURN
  END

```

```

C
C
C THIS SUBROUTINE CALCULATES THE ROOTS OF A GIVEN POLYNOMIAL
C OF DEGREE N WHERE THE COEFFICIENTS ARE STORED IN THE ARRAY CPF.
C  $PF(N+1)X^{*N} + PF(N)X^{*N-1} + \dots + PF(2)X + PF(1) = 0$ 
C

```

```

SUBROUTINE ROOTS (CPF,N,CROOT)
  IMPLICIT COMPLEX*16 (C) , REAL*8 (A,B,D-H,O-Z)
  COMMON /PASS2/NOUT
  REAL*8 CDABS
  DIMENSION CPF (11) ,CROOT (10)
  PI=3.141592653589793DO
  CF1=(1.0DO,0.0DO)
  CF2=(0.0DO,1.0DO)

```

```

C
C EXACT VALUES FOR THE ROOTS FOR N=1,2,3,4 ARE CAPABLE.
C ROOT 1 IS USUALLY THE GROUND MODE.

```

```

C
C N = 1

```

```

  IF (N.GT.1) GO TO 2
  CROOT (1)=-1.0DO*CPF (1) /CPF (2)
  GO TO 100

```

```

C
C N = 2

```

```

  2 IF (N.GT.2) GO TO 3
  CFK=CPF (2) *CPF (2) -4.0DO*CPF (1) *CPF (3)
  CROOT (1) = (-1.0DO*CPF (2) +CDSQRT (CFK)) / (2.0DO*CPF (3))
  CROOT (2) = (-1.0DO*CPF (2) -CDSQRT (CFK)) / (2.0DO*CPF (3))
  GO TO 100

```

```

C
C N = 3

```

```

  3 IF (N.GT.3) GO TO 4
  CP=CPF (3) /CPF (4)
  CQ=CPF (2) /CPF (4)
  CR=CPF (1) /CPF (4)

```

```

41 CONTINUE
CA=CQ-CP*CP/3.0DO
CB=CP*CP*CP/13.5DO-CP*CQ/3.0DO+CR
CFK1=CB*CB/4.0DO+CA*CA*CA/27.0DO
CFK1=CDSQRT (CFK1)
CFK2=-CB/2.0DO
CV1=CFK2+CFK1
CV2=CFK2-CFK1
DR1=DREAL (CV1)
DR2=DREAL (CV2)
DI1=DAIMAG (CV1)
DI2=DAIMAG (CV2)
R1=(DSQRT (DR1*DR1+DI1*DI1))**(1.0DO/3.0DO)
R2=(DSQRT (DR2*DR2+DI2*DI2))**(1.0DO/3.0DO)
TH1=DATAN2 (DI1,DR1)
TH2=DATAN2 (DI2,DR2)
IF (DI1.LT.0.0DO) TH1=2.0DO*PI+TH1
IF (DI2.LT.0.0DO) TH2=2.0DO*PI+TH2
THP1=TH1/3.0DO
DO 30 J=1,3
THP2=TH2/3.0DO-(J-1)*2.0DO*PI/3.0DO
CS=R1*(DCOS (THP1)+CF2*DSIN (THP1))
CT=R2*(DCOS (THP2)+CF2*DSIN (THP2))
CRT=CS+CT
CZERO=CRT*CRT*CRT+CA*CRT+CB
IF (CDABS (CZERO) .LT.1.0D-10) GO TO 31
30 CONTINUE
IF (NOUT.LT.7) WRITE (6,1001) N
1001 FORMAT (' ', '**ERROR** NO ROOTS FOUND FOR NDIM=',15)
31 CROOT (1)=CS+CT-CP/3.0DO
IF (N.EQ.4) GO TO 42
CFK1=-1.0DO*(CS+CT)/2.0DO
CFK2=(CS-CT)*CF2*DSQRT (3.0DO)/2.0DO
CROOT (2)=CFK1+CFK2-CP/3.0DO
CROOT (3)=CFK1-CFK2-CP/3.0DO
GO TO 100

C
C N = 4
C
4 IF (N.GT.4) GO TO 5
C4D=CPF (1)/CPF (5)
C4C=CPF (2)/CPF (5)
C4B=CPF (3)/CPF (5)
C4A=CPF (4)/CPF (5)
CP=-C4B
CQ=C4A*C4C-4.0DO*C4D
CR=4.0DO*C4B*C4D-C4C*C4C-C4A*C4A*C4D
GO TO 41
42 CRT=CROOT (1)
CR=CDSQRT (C4A*C4A/4.0DO-C4B+CRT)
IF (CDABS (CR) .LT.1.0D-40) GO TO 43
CFK1=3.0DO*C4A*C4A/4.0DO-CR*CR-2.0DO*C4B
CFK2=(4.0DO*C4A*C4B-8.0DO*C4C-C4A*C4A*C4A)/(4.0DO*CR)
GO TO 44

```

```

43 CFK1=3.0DO*C4A*C4A/4.0DO-2.0DO*C4B
   CFK2=2.0DO*CDSQRT (CRT*CRT-4.0DO*C4D)
44 CD=CDSQRT (CFK1+CFK2)
   CE=CDSQRT (CFK1-CFK2)
   CFK1=-C4A/4.0DO
   CFK2=CR/2.0DO
   CROOT (1)=CFK1+CFK2+CD/2.0DO
   CROOT (2)=CFK1+CFK2-CD/2.0DO
   CROOT (3)=CFK1-CFK2+CE/2.0DO
   CROOT (4)=CFK1-CFK2-CE/2.0DO
   GO TO 100

```

C
C
C

N.GT.4 THEN USE NUMERICAL ROUTINE POLSOL

```

5 CALL POLSOL (CPF,CROOT,N)
100 IF (NOUT.LT.2) WRITE (6,1000) (CROOT (J),J=1,N)
1000 FORMAT (' ',5X,'ROUTINE CROOT EXECUTED ROOTS:',10 (/8X,2E16.8))
RETURN
END

```

C
C
C
C
C
C
C
C
C
C
C
C
C
C

THIS SUBROUTINE SOLVES NUMERICALLY FOR THE ROOTS OF A POLYNOMIAL WHOSE COEFFICIENTS ARE STORED IN CPF OF DEGREE N, AND THE RETURNED ROOTS ARE IN CROOT. IT USES THE ROUTINES SHIFT, ANULUS, FUNDER, AND RCHECK EXCLUSIVLY.

AUTHOR: G.W. STEWART III, COMPUTER TECHNOLOGY CENTER,
UNION CARBIDE CORPORATION, NUCLEAR DIVISION,
OAK RIDGE, TENNESSEE.

REF: THE COMPUTER TECHNOLOGY CENTER NUMERICAL ANALYSIS
LIBRARY, NATIONAL TECHNICAL INFORMATION SERVICE,
U.S. DEPT. OF COMMERCE, SPRINGFIELD, VA 22151

```

SUBROUTINE POLSOL (AA,ZZ,NN)
COMPLEX*16 AA (11),ZZ (10),P (10),DP (10),A (11),B (11),C (11),Z,Q,ZI,
>F,FP,DZ
REAL*8 RS,R1,R2,RI,CDABS
COMPLEX*16 UNIT8 (8) / (1.0DO,0.0DO), (0.707106781186547,
>-0.707106781186547), (0.707106781186547,0.707106781186547),
>(0.0DO,-1.0DO), (0.0DO,1.0DO), (-0.707106781186547,
>-0.707106781186547), (-0.707106781186547,0.707106781186547),
>(-1.0DO,0.0DO) /
REAL*8 CONQ/1.625DO/,CONRI/0.875DO/,EPS/1.0D-12/
INTEGER*4 NEWTON/10/
10 N=IABS (NN)
   NK=N
   DO 20 I=1,N
20 A (I)=AA (I)/AA (N+1)
   A (N+1)=(1.0DO,0.0DO)
   RS=0.0DO

```

C
C
C

LOCATE AN ANNULUS ABOUT ZERO CONTAINING A ROOT

```

30 Z=(0.0DO,0.0DO)

```

```

    IF (RS.GT.0.0D0) GO TO 40
    R1=1.1D0*CDABS (A (1)) ** (1.0D0/FLOAT (NK))
    GO TO 50
40 R1=-RS
50 CALL ANULUS (A,R1,R2,NK)
    RS=R1
    IF (R1.EQ.0.0D0) GO TO 150

```

C
C
C

COVER THE ANNULUS WITH CIRCLES AND FIND ONE WITH A ROOT IN IT

```

60 Q=CONQ*R1
    IF (CDABS (Z) .EQ.0.0D0) GO TO 70
    Q=-Q*(Z/CDABS (Z))
    GO TO 80
70 IF (NK.EQ.N) GO TO 80
    IF (CDABS (ZZ (N-NK)) .NE.0.0D0) Q=Q*(DCONJG (ZZ (N-NK)) /
    >CDABS (ZZ (N-NK)))
80 R1=CONR1*R1
    DO 90 I=1,8
    ZI=Z+Q*UNIT8 (I)
    CALL SHIFT (A,B,ZI,NK)
    CALL RCHECK (B,KKK,R1,NK)
    GO TO (100,90),KKK
90 CONTINUE
    R1=2.0D0*R2
    LLL=2
    GO TO 110
100 LLL=1
    R1=R1
    Z=ZI

```

C
C
C

ITERATE FOR THE ROOT

```

110 ZI=Z+R1*(0.0D0,0.01D0)
    DO 120 I=1,NEWTON
    CALL FUNDER (A,B,ZI,F,FP,NK)
    DZ=-F/FP
    ZI=ZI+DZ
    IF (CDABS (ZI-Z) .GT.R1) GO TO (140,150),LLL
    IF (CDABS (DZ/ZI) .LT.EPS) GO TO 130
120 CONTINUE
    GO TO (140,130),LLL
130 Z=ZI
    GO TO 150
140 CALL SHIFT (A,B,Z,NK)
    CALL ANULUS (B,R1,R2,NK)
    IF (R1.EQ.0.0D0) GO TO 150
    GO TO 60

```

C
C
C

DEFLATE THE POLYNOMIAL AND TEST TO SEE IF ALL ROOTS HAVE BEEN FOUND

```

150 CALL FUNDER (A,B,Z,F,FP,NK)
160 ZZ (N-NK+1)=Z
    DO 170 I=1,NK

```

```

170 A(I)=B(I)
    NK=NK-1
    IF(NK.NE.1) GO TO 30
    ZZ(N)=-A(I)
C
C   PURIFY THE ROOTS IN THE ORIGINAL POLYNOMIAL
C
180 IF(NN.LT.0) GO TO 210
    DO 200 K=1,N
    DO 190 I=1,5
    CALL FUNDER(AA,B,ZZ(K),P(K),DP(K),N)
    DZ=-P(K)/DP(K)
    IF(CDABS(DZ/ZZ(K)).LT.EPS) GO TO 200
190 ZZ(K)=ZZ(K)+DZ
200 CONTINUE
    RETURN
210 DO 220 I=1,N
220 CALL FUNDER(AA,B,ZZ(I),P(I),DP(I),N)
    RETURN
    END

```

```

C
C   THIS SUBROUTINE IS USED WITH POLSOL AND EVALUATES THE N-TH
C   DEGREE POLYNOMIAL WITH COEFFICIENTS IN A AND ITS DERIVATIVE
C   AT Z. THE VALUE IS RETURNED IN F AND ITS DERIVATIVE IN
C   FP. THE COEFFICIENTS OF THE DEFLATED POLYNOMIAL ARE IN B.
C

```

```

SUBROUTINE FUNDER(A,B,Z,F,FP,N)
COMPLEX*16 A(11),B(11),Z,F,FP
F=A(N+1)
FP=(0.0D0,0.0D0)
DO 10 I=1,N
    I1=N-I+1
    B(I1)=F
    F=A(I1)+Z*F
10 FP=B(I1)+Z*FP
RETURN
END

```

```

C
C   THIS SUBROUTINE IS USED BY POLSOL AND SHIFTS THE ROOTS OF A
C   POLYNOMIAL. GIVEN COEFFICIENTS IN A THE ROUTINE RETURNS IN B THE
C   COEFFICIENTS OF A POLYNOMIAL WHOSE ROOTS HAVE BEEN SHIFTED BY -Z.
C

```

```

SUBROUTINE SHIFT(A,B,Z,N)
COMPLEX*16 A(11),B(11),Z
N1=N+1
DO 10 I=1,N1
10 B(I)=A(I)
DO 20 I=1,N
DO 20 J=1,N
    JJ=N-J+1
20 B(JJ)=B(JJ)+Z*B(JJ+1)
RETURN

```

END

C
C
C
C
C
C
C
C
C

THIS SUBROUTINE IS USED BY POLSOL AND IT FINDS AN ANNULUS IN WHICH THE POLYNOMIAL WITH COEFFICIENTS IN A HAS AT LEAST ONE ROOT. UPON ENTRY R1 MUST CONTAIN A STARTING RADIUS. IF R1 IS POSITIVE IT IS ASSUMED THE ROOT IS IN THE CIRCLE $Z.LE.R1$. UPON RETURN R1 AND R2 CONTAIN THE INNER AND OUTER RADII OF THE ANNULUS. IF A ROOT IS AT $Z=0$ THEN $R1=R2=0$.

```
SUBROUTINE ANULUS (A,R1,R2,N)
COMPLEX*16 A(11),B(11)
REAL*8 R1,R2,FAC/2.0DO/
IF (CDABS(A(1)).NE.0.0DO) GO TO 10
R1=0.0DO
R2=0.0DO
RETURN
10 IF (R1.GT.0.0DO) GO TO 30
R1=-R1
20 R2=R1
CALL RCHECK(A,KKK,R1,N)
GO TO (30,40),KKK
30 R2=R1
R1=R1/FAC
CALL RCHECK(A,KKK,R1,N)
GO TO (30,50),KKK
40 R1=R2
R2=FAC*R1
CALL RCHECK(A,KKK,R2,N)
GO TO (50,40),KKK
50 RETURN
END
```

C
C
C
C
C
C

THIS SUBROUTINE IS USED BY POLSOL TO DETERMINE IF THE POLYNOMIAL WITH COEFFICIENTS IN AA HAS A ROOT IN THE UNIT CIRCLE. IT RETURNS WITH $KKK=1$ IF YES AND $KKK=2$ IF NO.

```
SUBROUTINE RCHECK(A,KKK,R,N)
COMPLEX*16 A(11),AA(11),B(11),MULT,TEMP
REAL*8 R,RR,MAX,AN,AO,BIG/1.0D60/
N1=N+1
MAX=0.0DO
DO 10 I=1,N1
10 MAX=DMAX1(MAX,CDABS(A(I)))
RR=BIG/MAX
IF (R.GT.1.0DO) GO TO 30
DO 20 I=1,N1
AA(I)=RR*A(I)
20 RR=R*RR
GO TO 100
30 DO 40 I=1,N1
II=N1-I+1
AA(II)=RR*A(II)
```



```

PI=3.141592653589793D0
CF1=(1.0D0,0.0D0)
CF2=(0.0D0,1.0D0)
TRANS=6.0D0

C
DO 200 I=1,10
DO 200 J=1,10
CA(I,J)=(0.0D0,0.0D0)
CB(I,J)=(0.0D0,0.0D0)
200 CONTINUE
N=1ABS(NDIM)
IF(NDIM.LT.0) GO TO 100
DO 10 I=1,N
NSTP=1
DO 20 J=1,NSTP
CZ1=CTE*RO(I,J)
CZ2=CTE*ROR(I,J)
CALL MFBSL(CZ1,C110,C111,C1K0,C1K1,C1K2)
CALL MFBSL(CZ2,C210,C211,C2K0,C2K1,C2K2)
CALL CJCAL(TRANS,CTE,CTG,ROR(I,J),THETA(I,J),CJ)
CALL CGCAL(CTE,ROR(I,J),CJ,CG)
CA(I,J)=C1K0-C2K0+CG
CB(I,J)=CG-CJ
IF(J.NE.NSTP) GO TO 20
CZ3=CT(I)*RO(I,J)
IF(DREAL(CZ3).LT.160.0D0) GO TO 50
IF(NOUT.LT.4) WRITE(6,1000)
1000 FORMAT(' ','**NOTE** APPROX- CZ3 IN MATCAL > 160.0 IN MFBSL')
C310=(1.0D0,0.0D0)
C311=(1.0D0,0.0D0)
CMULT=(1.0D0,0.0D0)
DO 60 L=1,5
CMULT=CMULT*CZ3
C310=C310+VO(L)/CMULT
C311=C311-V1(L)/CMULT
60 CONTINUE
GO TO 55
50 CALL MFBSL(CZ3,C310,C311,C3K0,C3K1,C3K2)
55 CCMM=(C310/C311)*UR(I)*CT(I)*CT(I)*CZ1*C1K1/(URE*CK2(I)*CZ3)
CB(I,J)=CB(I,J)+CCMM
20 CONTINUE
10 CONTINUE
DO 30 I=1,N
DO 30 J=1,N
CA(I,J)=CA(J,I)
30 CB(I,J)=CB(J,I)
RETURN

C
C CALCULATION FOR CTE=(0.0,0.0)
C
100 CTE=(0.0D0,0.0D0)
CTG=CDSQRT(CKE2-CKG2)
DO 110 I=1,N
CT2F=CKE2-CK2(I)

```

```

CT(1)=CDSQRT(CT2F)
NSTP=1
DO 120 J=1,NSTP
CALL CJCAL(TRANS,CTE,CTG,ROR(1,J),THETA(1,J),CJ)
CG=(0.0DO,0.0DO)
CA(1,J)=CF1*DLOG(ROR(1,J)/RO(1,J))+CG
CB(1,J)=CG-CJ
IF(J.NE.NSTP) GO TO 120
CZ3=CT(1)*RO(1,J)
IF(DREAL(CZ3).LT.160.0DO) GO TO 150
IF(NOUT.LT.4) WRITE(6,1000)
C310=(1.0DO,0.0DO)
C311=(1.0DO,0.0DO)
CMULT=(1.0DO,0.0DO)
DO 160 L=1,5
CMULT=CMULT*CZ3
C310=C310+VO(L)/CMULT
C311=C311-V1(L)/CMULT
160 CONTINUE
GO TO 155
150 CALL MFBSL(CZ3,C310,C311,C3K0,C3K1,C3K2)
155 CCMM=(C310/C311)*UR(1)*CT2F/(URE*CK2(1)*CZ3)
CB(1,J)=CB(1,J)+CCMM
120 CONTINUE
110 CONTINUE
DO 130 I=1,N
DO 130 J=1,N
CA(I,J)=CA(J,I)
130 CB(I,J)=CB(J,I)
RETURN
END

```

C
C
C
C
C
C
C
C
C

THIS SUBROUTINE CREATES THE POLYNOMIAL DERIVED FROM THE EIGENMATRIX SYSTEM $\text{DET}(A \cdot X + B) = 0$ IN THE FORM GIVEN AS $\text{PF}(N+1)X^{*N} + \text{PF}(N)X^{*N-1} + \dots + \text{PF}(2)X + \text{PF}(1) = 0$

NOTE: MATRICES A, B ARE CONSIDERED TO BE SYMMETRIC.

```

SUBROUTINE POLY(CA,CB,N,CPF)
IMPLICIT COMPLEX*16 (C)
COMMON /PASS2/NOUT
INTEGER*4 FORM(9) / (' /', '1', ' /', '1X', '1', '1', ' (2X', '1', '2F12',
>' .7)', '))' /
INTEGER*4 NVAL(10) / '1', '2', '3', '4', '5', '6', '7', '8', '9', '10' /
DIMENSION CA(10,10),CB(10,10),CPF(11),CDA(10,10),CDB(10,10)
FORM(2)=NVAL(N/6+1)
FORM(5)=NVAL(N-N/6*5)
IF(NOUT.LT.2) WRITE(6,1001)
1001 FORMAT(' ',5X,'ROUTINE POLY EXECUTING DETERMINANTS:')
C
C CALCULATION FOR N=1
C
IF(N.GT.1) GO TO 100

```

```
CPF (1) =CB (1, 1)
CPF (2) =CA (1, 1)
GO TO 999
```

```
C
C CALCULATION FOR N=2
C
```

```
100 IF (N.GT.2) GO TO 200
CPF (1) =CB (1, 1) *CB (2, 2) -CB (2, 1) *CB (2, 1)
CPF (2) =CA (1, 1) *CB (2, 2) +CA (2, 2) *CB (1, 1) -2.ODO*CA (2, 1) *CB (2, 1)
CPF (3) =CA (1, 1) *CA (2, 2) -CA (2, 1) *CA (2, 1)
GO TO 999
```

```
C
C CALCULATION FOR N GT 2
C
```

```
200 NST=N+1
DO 10 J=1,NST
10 CPF (J) = (0.ODO, 0.ODO)
DO 11 I=1,N
DO 11 J=1,N
CDA (I, J) =CA (I, J)
11 CDB (I, J) =CB (I, J)
```

```
C
IF (NOUT.LT.2) WRITE (6, 1000) N
1000 FORMAT (' ', 5X, 6I5)
IF (NOUT.LT.2) WRITE (6, FORM) ((CDA (NN, MM), MM=1, N), NN=1, N)
IF (NOUT.LT.2) WRITE (6, FORM) ((CDB (NN, MM), MM=1, N), NN=1, N)
CPF (1) =CDET (CDB, N)
CPF (N+1) =CDET (CDA, N)
```

```
C
DO 110 I1=1, N
IF (N.EQ.2.AND.I1.GT.1) GO TO 110
DO 41 J=1, N
CDA (I1, J) =CB (I1, J)
41 CDB (I1, J) =CA (I1, J)
IF (NOUT.LT.2) WRITE (6, 1000) N, I1
IF (NOUT.LT.2) WRITE (6, FORM) ((CDA (NN, MM), MM=1, N), NN=1, N)
IF (NOUT.LT.2) WRITE (6, FORM) ((CDB (NN, MM), MM=1, N), NN=1, N)
CPF (2) =CPF (2) +CDET (CDB, N)
CPF (N) =CPF (N) +CDET (CDA, N)
NST2=I1+1
IF (NST2.GT.N.OR.N.LT.4) GO TO 21
```

```
C
DO 120 I2=NST2, N
IF (N.EQ.4.AND.I1.GT.1) GO TO 120
DO 42 J=1, N
CDA (I2, J) =CB (I2, J)
42 CDB (I2, J) =CA (I2, J)
IF (NOUT.LT.2) WRITE (6, 1000) N, I1, I2
IF (NOUT.LT.2) WRITE (6, FORM) ((CDA (NN, MM), MM=1, N), NN=1, N)
IF (NOUT.LT.2) WRITE (6, FORM) ((CDB (NN, MM), MM=1, N), NN=1, N)
CPF (3) =CPF (3) +CDET (CDB, N)
CPF (N-1) =CPF (N-1) +CDET (CDA, N)
NST3=I2+1
IF (NST3.GT.N.OR.N.LT.6) GO TO 22
```

C

```
DO 130 I3=NST3,N
IF (N.EQ.6.AND.I1.GT.1) GO TO 130
DO 43 J=1,N
CDA (13,J)=CB (13,J)
43 CDB (13,J)=CA (13,J)
IF (NOUT.LT.2) WRITE (6,1000) N,11,12,13
IF (NOUT.LT.2) WRITE (6,FORM) ((CDA (NN,MM),MM=1,N),NN=1,N)
IF (NOUT.LT.2) WRITE (6,FORM) ((CDB (NN,MM),MM=1,N),NN=1,N)
CPF (4)=CPF (4)+CDET (CDB,N)
CPF (N-2)=CPF (N-2)+CDET (CDA,N)
NST4=I3+1
IF (NST4.GT.N.OR.N.LT.8) GO TO 23
```

C

```
DO 140 I4=NST4,N
IF (N.EQ.8.AND.I1.GT.1) GO TO 140
DO 44 J=1,N
CDA (14,J)=CB (14,J)
44 CDB (14,J)=CA (14,J)
IF (NOUT.LT.2) WRITE (6,1000) N,11,12,13,14
IF (NOUT.LT.2) WRITE (6,FORM) ((CDA (NN,MM),MM=1,N),NN=1,N)
IF (NOUT.LT.2) WRITE (6,FORM) ((CDB (NN,MM),MM=1,N),NN=1,N)
CPF (5)=CPF (5)+CDET (CDB,N)
CPF (N-3)=CPF (N-3)+CDET (CDA,N)
NST5=I4+1
IF (NST5.GT.N.OR.N.LT.10) GO TO 24
```

C

```
DO 150 I5=NST5,N
IF (N.EQ.10.AND.I1.GT.1) GO TO 150
DO 45 J=1,N
CDA (15,J)=CB (15,J)
45 CDB (15,J)=CA (15,J)
IF (NOUT.LT.2) WRITE (6,1000) N,11,12,13,14,15
IF (NOUT.LT.2) WRITE (6,FORM) ((CDA (NN,MM),MM=1,N),NN=1,N)
IF (NOUT.LT.2) WRITE (6,FORM) ((CDB (NN,MM),MM=1,N),NN=1,N)
CPF (6)=CPF (6)+CDET (CDB,N)
CPF (N-4)=CPF (N-4)+CDET (CDA,N)
```

C

```
DO 35 J=1,N
CDA (15,J)=CA (15,J)
35 CDB (15,J)=CB (15,J)
150 CONTINUE
24 DO 34 J=1,N
CDA (14,J)=CA (14,J)
34 CDB (14,J)=CB (14,J)
140 CONTINUE
23 DO 33 J=1,N
CDA (13,J)=CA (13,J)
33 CDB (13,J)=CB (13,J)
130 CONTINUE
22 DO 32 J=1,N
CDA (12,J)=CA (12,J)
32 CDB (12,J)=CB (12,J)
120 CONTINUE
```

```

21 DO 31 J=1,N
   CDA(11,J)=CA(11,J)
31 CDB(11,J)=CB(11,J)
110 CONTINUE
999 NST=N+1
   IF(NOUT.LT.2) WRITE(6,1002) (CPF(J),J=1,NST)
1002 FORMAT(' ',5X,'RESULTING POLYNOMIAL:',10(/8X,2E16.8))
   RETURN
   END

```

C
C
C
C
C
C

THIS SUBROUTINE DETERMINES THE TRANSFORM MATRICES [P] AND [P]-1 FROM THE IMPEDENCE MATRIX CZIMP. THE RETURNED VECTORS ARE THE NORMALIZED (MAG AND PHASE) EIGENVECTORS OF THE SYSTEM.

```

SUBROUTINE EIGEN(CP,CPI,NDIM,RO)
  IMPLICIT COMPLEX*16 (C) , REAL*8 (A,B,D-H,O-Z)
  REAL*8 CDABS
  COMMON /INP2/CKE2,CKG2,CK2,CKE,CKG,CK,URE,UR
  COMMON /PASS2/NOUT
  COMMON /PASS3/CZIMP,CSPHI
  DIMENSION UR(10),CK2(10),CK(10),CT(10)
  DIMENSION CZIMP(10,10,10),CSPHI(10)
  DIMENSION CP(10,10),CPI(10,10),RO(10,10),CD(10,10),CIFACT(10)
  CF1=(1.0D0,0.0D0)
  CF2=(0.0D0,1.0D0)

```

C

```

  IF(NDIM.GT.1) GO TO 2
  CP(1,1)=CF1
  CPI(1,1)=CF1
  RETURN

```

C

```

2 DO 10 J=1,NDIM
  CTE=CDSQRT(CSPHI(J)*CKE2)
  CZ1=CTE*RO(J,J)
  CALL MFBSL(CZ1,C110,C111,C1K0,C1K1,C1K2)
10 CIFACT(J)=CZ1*C1K1
  IF(NDIM.GT.2) GO TO 3
  DO 20 J=1,2
  CP(1,J)=CZIMP(J,2,2)*CIFACT(1)
20 CP(2,J)=-CZIMP(J,2,1)*CIFACT(2)
  GO TO 200

```

C

```

3 DO 100 NDX=1,NDIM
  DO 110 J=2,NDIM
  DO 110 K=2,NDIM
110 CD(J-1,K-1)=CZIMP(NDX,J,K)
  NSIZE=NDIM-1
  CP(1,NDX)=CDET(CD,NSIZE)*CIFACT(1)
  NSGN=1
  DO 120 K=2,NDIM
  DO 130 J=2,NDIM
130 CD(J-1,K-1)=CZIMP(NDX,J,K-1)
  NSGN=NSGN*(-1)

```

```

      CP (K, NDX) = NSGN * CDET (CD, NSIZE) * CFACT (K)
120 CONTINUE
100 CONTINUE

```

```

C
C  NORMALIZE THE PHASE AND MAGNITUDE OF THE VECTORS
C

```

```

200 DO 230 J=1,NDIM
      CDIV=CP (1,J)
      DO 230 K=1,NDIM
230  CP (K, J) = CP (K, J) / CDIV
      DO 205 J=1,NDIM
          DSUM=0.000
          DO 210 K=1,NDIM
210   DSUM=DSUM+CDABS (CP (K, J)) * CDABS (CP (K, J))
          DSUM=DSQRT (DSUM)
          DO 220 K=1,NDIM
220   CP (K, J) = CP (K, J) / DSUM
205 CONTINUE

```

```

C
      CALL MATINV (CP, NDIM, CPI)
      RETURN
      END

```

```

C
C
C
C

```

THIS FUNCTION CALCULATES THE VALUE OF THE G REFLECTION FUNCTION.

```

SUBROUTINE CGCAL (CTE, RO, CJ, CG)
  IMPLICIT COMPLEX*16 (C) , REAL*8 (A, B, D-H, O-Z)
  COMMON /INP2/CKE2,CKG2,CK2,CKE,CKG,CK,URE,UR
  DIMENSION UR (10),CK2 (10),CK (10)
  PI=3.14159265358979300
  CF1=(1.000,0.000)
  CF2=(0.000,1.000)

```

```

C
      CZ1=RO*CTE
      CALL MFBSL (CZ1, C110, C111, C1K0, C1K1, C1K2)
      CFK1=2.000*CKE2 / (CKG2+CKE2)
      CFK2=(CKG2-CKE2) / (CKG2+CKE2)
      CG=CFK1*(CFK2*C1K0+CFK1*CJ)
      RETURN
      END

```

```

C
C
C
C
C

```

THIS SUBROUTINE SORTS THE COMPLEX ARRAY CARRY IN INCREASING ORDER OF ITS REAL VALUE, WHERE NSIZE IS THE ARRAY DIMENSION.

```

SUBROUTINE SORT (CARRY, N, NSIZE)
  IMPLICIT COMPLEX*16 (C) , REAL*8 (A, B, D-H, O-Z)
  REAL*8 CDABS
  DIMENSION CARRY (NSIZE)
  IF (N.LE.1) RETURN
  IUP=N-1
  DO 30 I=1, IUP
    JH=I

```

```

HI=DREAL (CARRY (I))
JL=I+1
DO 20 J=JL,N
VAL=DREAL (CARRY (J))
IF (VAL.LE.HI) GO TO 20
HI=VAL
JH=J
20 CONTINUE
IF (JH.EQ.I) GO TO 30
CT=CARRY (JH)
CARRY (JH)=CARRY (I)
CARRY (I)=CT
30 CONTINUE
RETURN
END

```

C
C
C
C

THIS SUBROUTINE INVERTS A COMPLEX MATRIX

```

SUBROUTINE MATINV (CIN,N,COU)
IMPLICIT COMPLEX*16 (C) , REAL*8 (A,B,D-H,O-Z)
DIMENSION CIN (10,10) , COU (10,10)
DO 100 J=1,N
DO 100 K=1,N
100 COU (J,K)=CIN (J,K)
DO 10 I=1,N
DO 20 J=1,N
IF (I.EQ.J) GO TO 20
COU (I,J)=COU (I,J)/COU (I,I)
20 CONTINUE
COU (I,I)=1.0D0/COU (I,I)
DO 30 K=1,N
IF (K.EQ.I) GO TO 30
DO 40 L=1,N
IF (L.EQ.I) GO TO 40
COU (K,L)=COU (K,L)-COU (I,L)*COU (K,I)
40 CONTINUE
30 CONTINUE
DO 50 M=1,N
IF (M.EQ.I) GO TO 50
COU (M,I)=-1.0D0*COU (M,I)*COU (I,I)
50 CONTINUE
10 CONTINUE
RETURN
END

```

C
C
C
C
C

THIS SUBROUTINE MULTIPLIES MATRICES IN THE FORM
CIN1 (10,10)*CIN2 (10,10)=COU (10,10)

```

SUBROUTINE MATM1 (CIN1,CIN2,NDIM,COU)
IMPLICIT COMPLEX*16 (C) , REAL*8 (A,B,D-H,O-Z)
DIMENSION CIN1 (10,10) , CIN2 (10,10) , COU (10,10)
DO 10 J=1,NDIM

```

```

DO 10 K=1,NDIM
COU(J,K)=(0.000,0.000)
DO 20 L=1,NDIM
20 COU(J,K)=COU(J,K)+CIN1(J,L)*CIN2(L,K)
10 CONTINUE
RETURN
END

```

C
C
C
C
C

THIS SUBROUTINE MULTIPLIES MATRICES IN THE FORM
CIN1(10,10)*CIN2(10)=COU(10)

```

SUBROUTINE MATM2(CIN1,CIN2,NDIM,COU)
IMPLICIT COMPLEX*16 (C) , REAL*8 (A,B,D-H,O-Z)
DIMENSION CIN1(10,10),CIN2(10),COU(10)
DO 10 J=1,NDIM
COU(J)=(0.000,0.000)
DO 10 K=1,NDIM
10 COU(J)=COU(J)+CIN1(J,K)*CIN2(K)
RETURN
END

```

C
C
C
C
C

THIS FUNCTION CALCULATES THE DETERMINANT OF THE COMPLEX
MATRIX CDIN OF DIMENSION IS N. CDIN IS NOT DESTROYED.

```

FUNCTION CDET(CDIN,N)
IMPLICIT COMPLEX*16 (C) , REAL*8 (A,B,D-H,O-Z)
REAL*8 CDABS
COMMON /PASS2/NOU
DIMENSION CD(10,10),CDIN(10,10)
IF(N.EQ.1) GO TO 70
NM1=N-1
CDET=(1.000,0.000)
DO 100 I=1,N
DO 100 J=1,N
100 CD(I,J)=CDIN(I,J)
DO 50 I=1,NM1

```

C
C
C

THIS SECTION PERFORMS PARTIAL PIVOTING

```

S=0.000
DO 10 J=1,N
R=CDABS(CD(J,1))
IF(R.LT.S) GO TO 10
S=R
L=J
10 CONTINUE
IF(L.EQ.1) GO TO 30
DO 20 J=1,N
CT=CD(I,J)
CD(I,J)=CD(L,J)
CD(L,J)=CT
20 CONTINUE

```

```

      CDET=-CDET
C
C   THIS SECTION CALCULATES THE DET BY COLUMN REDUCTION
C
30  IF (CDABS (CD (1,1)) .EQ.0.0D0) GO TO 80
      IP1=I+1
      DO 50 J=IP1,N
      CT=CD (J,1)/CD (1,1)
      DO 40 K=IP1,N
      CFK=(0.0D0,0.0D0)
      CCK=CD (1,K)*CT
      RCK=DREAL (CCK)
      ACK=DAIMAG (CCK)
      RCD=DREAL (CD (J,K))
      ACD=DAIMAG (CD (J,K))
      DCK=1.0D-60
      IF (RCD.EQ.RCK.AND.ACD.EQ.ACK) GO TO 40
      CFK=CD (J,K)-CCK
40  CD (J,K)=CFK
50  CONTINUE
      DO 60 I=1,N
60  CDET=CDET*CD (I,1)
      GO TO 200
70  CDET=CDIN (1,1)
      GO TO 200
80  CDET=(0.0D0,0.0D0)
200 IF (NOUT.LT.2) WRITE (6,1000) CDET
1000 FORMAT (' ',5X,'DETERMINANT=',2E16.8)
      RETURN
      END

```